DEVELOPMENT OF EFFECTIVE ANTI-CANCER AGENTS TARGETING DRUG-RESISTANT MALIGNANCIES

A DISSERTATION

SUBMITTED TO THE FACULTY OF THE GRADUATE SCHOOL

OF THE UNIVERSITY OF MINNESOTA

BY

SONIA GOUTAM KUMAR DAS

IN PARTIAL FULFILLMENT OF THE REQUIREMENTS

FOR THE DEGREE OF

DOCTOR OF PHILOSOPHY

Dr. CHENGGUO XING, ADVISER

SEPTEMBER 2011

ACKNOWLEDGEMENTS

"No one who achieves success does so without the help of others.
The wise and confident acknowledge this help with gratitude. "
-Alfred North Whitehead

In this part of my thesis I will try my best to thank all the people who made it possible for me to stand where I am now.

First and foremost, I would like to thank my family. My mother is my biggest pillar of strength, she has showered me with love and always supported me to pursue my dreams. Without her, I would not have had the courage to come halfway across the world to an unfamiliar place to pursue my PhD. She has believed in me and provided me with the confidence I needed to go on, in the hardest of times. I shall forever be in her debt. I thank my father, for being the best teacher I ever had and for providing me with pertinent advice whenever I needed it. He has taught me to be the best in whatever I do, to be an independent thinker, to approach a problem rationally and not emotionally and to stand for what I believe. I am fortunate to have a sister who has always loved and protected me like a second mother. Since my childhood, I have looked up to my sister for her brilliance, hard work and singular focus to achieve her goals. She has contributed to my growth in many ways and she will forever be my role model. Finally, I would like to thank my fiancé Ajay Yekkirala for being my closest friend, teacher and love. Without his unconditional love and support I could not have pulled this through. I look forward to our journey together and the wonderful times that are yet to come.

My advisor, mentor and a friend, Dr. Chengguo Xing or Chris, is the next person to whom I owe my sincere gratitude. I still remember the first time I met Chris, I mistook him to be a post-doc or a student in the department. Indeed, we have come a long way since then. After Chris took me under his wing in my first year, he has guided and supported me in every way. I was like a child learning to walk and he held my hand and patiently taught me the do's and don'ts of research. To say I have learnt a lot from him is an understatement. He has imbibed in me, his hardworking ethic, his passion for research, his strive for perfection, and his tenacity. Most important of all, he gave me the freedom

to explore and test new waters. He has been my biggest support when I went for my internship at Novartis or when I decided to move from the field of medicinal chemistry to molecular biology for my post-doc. I thank him for always being there for me.

My Journey in the Xing lab is incomplete without the mention of my friends and colleagues in the lab that I worked with, and who made every day fun and a learning experience. Jignesh Doshi, David Hermanson, Defeng Tian, Liangyou Wang, Sadiya Addo, Balasubramanian Srinivasan, Ahmad Shaik, Nicholas Bleeker, Bo Zhou, Jinling Zhang and Aridoss Gopalakrishnan. Thank you all. Special thanks to David Hermanson, for pulling pranks at everyone in the lab and cheering me up when I was feeling down.

During my PhD, I have been fortunate to have many great mentors. Dr. Wagner is the first one who comes to mind. He was the first professor I was in touch with in the Department of Medicinal Chemistry. From guiding me through my first year as I was settling down in my new life as a graduate student to writing reference letters for me when I was looking for post-doctoral positions, Dr. Wagner has always supported me and I sincerely thank him for everything. Dr. Sturla has been another role model since the day I met her. Her zeal and enthusiasm for everything in life has caught me in awe. She has provided me with valuable advice in many instances and I will always try to emulate her. I would also like to thank the entire faculty of the Department of Medicinal Chemistry for providing me with knowledge and experience that will go a long way in my pursuit of a career.

I would also like to extend my sincere gratitude to my committee members Dr. Johnson, Dr. Remmel and Dr. Taton for providing me with valuable feedback for my research. I would like to convey my special thanks to Dr. Johnson for helping in my search for post-doctoral positions and writing reference letters for me.

During my PhD, I was also fortunate to work as an NMR assistant. It was during this time that I had the opportunity to meet Dr. Beverly Ostrowski. Bev is a wonderful person, who taught me everything I know about NMR today. She has been a great friend and mentor and I will miss her when I leave Minneapolis. I would also like to mention

Todd Rappe and Eric Perkins who were wonderful colleagues and I will always remember the fun times we shared.

When I arrived at Minneapolis on 17th August 2006, this place was a stranger to me, and a lot of people have helped me make this my home. So much so that I feel sad when I think of leaving. I would like to thank them all for making this journey a special experience and for always being there for me. I will begin with thanking my friends in the department, Sadiya Addo, Sanaa Bardaweel, Jolanna Norton, Leila Datoo, Swapna Bhagwanth, Erick Leggans, Amber Onorato, Theresa Aliwarga, Erin Michaelson, Lei Meng, Rahul Lad, Katie Pietsch, Jin Zhou, Todd Geders, Narsi, Abbas and Kathy Liu. A special thanks to Sadiya for not only providing me with professional advice but also helping me in my personal life like an elder sister.

I would next like to thank my friends outside the department, Vandana Phadke, Radhika Venkatasubramanian, Bodhisatwa Sadhu, Mukund Srinivasan, Kalyani Mallela, Vijay Tadipatri, Madhura Joglekar, Harini Ramanujam and Anja Lesaja for making me a part of their family and sharing with me the important moments of their lives. They truly had a huge role to play in making my PhD, and my stay in Minneapolis, memorable.

Finally, I would like to thank Joyce Reha who has been like another mother to me. I would also like to thank Caitlin Boley for being a good friend and for helping me out with printing my thesis.

I have been truly blessed to meet such wonderful people in my life and I thank God for giving me this wonderful opportunity. I will forever cherish the memories and bonds that I have made during my journey as a graduate student. Thank you, one and all!

DEDICATION

To

My Family

Maa, Bapi and Didi

Without their love and support I could have never done this

ABSTRACT

Sonia G. Das

350 Words

Rapid development of multidrug resistance (MDR) against current therapies is a major barrier in the treatment of cancer. Over-expression of anti-apoptotic Bcl-2 proteins has been implicated in development of cancer and drug resistance. Hence, our research has focused on developing anti-apoptotic Bcl-2 inhibitors that can eliminate drug-resistant cancer cells. HA 14-1 was the first small-molecule reported to inhibit anti-apoptotic Bcl-2 proteins and selectively eliminated cancer cells over-expressing anti-apoptotic Bcl-2 proteins. However, previous work in our lab revealed that HA 14-1 is unstable and decomposes within 15 min in cell culture medium at 37°C. Therefore, the main aim of this thesis was to develop a stable, more potent analog of HA 14-1, which would retain its beneficial properties.

In the current work we were able to design a stable analog of HA 14-1 (sHA 14-1) by removing the cyano group from HA 14-1. Although sHA 14-1 had beneficial properties like HA 14-1, it was 2-fold less potent in activity. Further SAR studies carried out to improve the activity of sHA 14-1 led to the discovery of CXL017, which was ~27 fold more potent than sHA 14-1 and ~12 fold more potent than HA 14-1. Biological studies on CXL017 revealed that CXL017 causes cell death via apoptosis characterized by caspase-3/7 activation and PARP cleavage. Furthermore, CXL017 selectively eliminated drug-resistant cancer cells both *in vitro* and *in vivo.*

These interesting results, prompted us to investigate the effects of long-term exposure to CXL017 in drug-resistant cancer cells. Our results show that drug-resistant cells do not develop stable resistance to CXL017 upon prolonged exposure for 6 months. In addition, drug-resistant cells exposed to CXL017 for 4 months develop collateral sensitivity towards a variety of standard therapies. Mechanistic investigations suggests that the re-sensitization observed in drug-resistant cells exposed to CXL017 is caused due to the down-regulation of Mcl-1 and a decrease in ER calcium content in these cell lines. Taken together, the results demonstrated in this work show that CXL017 is a more potent stable analog of HA 14-1, which merits further investigation for its potential as a drug candidate for the treatment of MDR cancers.

TABLE OF CONTENTS

LIST OF FIGURES

LIST OF TABLES

LIST OF SCHEMES

ABBREVIATIONS

ABC	ATP-binding cassette
ACN	Acetonitrile
AML	Acute myeloid leukemia
Apaf-1	Apoptosis activating factor-1
Bcl-2	B-cell lymphoma-2
BH	Bcl-2 homology
BBr_3	Boron tribromide
$CDCl_3$	Deuterated chloroform
CH_2Cl_2	Dichloromethane
CH_3CN	Acetonitrile
DMSO	Dimethylsulfoxide
DMSO-d_6	Deuterated dimethylsulfoxide DTT dithiothreitol
CHOP	cyclophosphamide-hydroxyldaunorubicin-oncovin-prednisone
CLLs	Chronic lymphocytic leukemias
DISC	Death induced signaling complexes
DLCLs	Diffuse large cell lymphomas
DMA	*N, N*-Dimethylacetamide
DR	Death receptor
DTT	Dithiothreitol
EDTA	Ethylene diamine tetraacetic acid
EGTA	Ethylene glycol tetraacetic acid

ER	Endoplasmic reticulum
Et_3N	Triethylamine
FADD	Fas Associated protein with Death Domain
HCl	Hydrochloric acid
HEPES	4-(2-hydroxyethyl)-1-piperazineethanesulfonic acid
EtOH	Ethanol
EtOAc	Ethyl actetate
FASL	Fas ligand
FDA	Food and Drug Administration
HPLC	High performance liquid chromatography
HRMS	High resolution mass spectrometry
H_2O	Water
H_2SO_4	Sulfuric acid
H_2DCFDA	2',7'-dichlorodihydrofluorescein diacetate
IR	Infra red spectroscopy
IPTG	Isopropyl-beta-D-thiogalactopyranoside
IP_3Rs	Inositol triphosphate receptors
K_2CO_3	Potassium carbonate KOH potassium hydroxide
MDR	multidrug resistance
$MgCl_2$	Magnesium chloride
$MgSO_4$	Magnesium sulfate
MOMP	Mitochondria outer membrane permeabilization

MP	Melting point
NaCl	Sodium chloride
$NaHCO_3$	Sodium bicarbonate
NaOH	Sodium hydroxide
NaOEt	Sodium ethoxide
NaOiPr	Sodium isopropoxide
NMR	Nuclear magnetic resonance
NHLs	Non-Hodgkin lymphomas
P-gp	P-glycoprotein
PBS	Phosphate buffered saline
$Pd(OAc)_2$	Palladium(II) acetate
$POCl_3$	Phosphorus oxychloride
PVDF	Polyvinylene difluoride
P_2O_5	Phosphorous pentoxide
Rf	Retention factor
RPMI	Rosewell park memorial institute
SDS-PAGE	Sodium dodecyl sulfate polyacrylamide gel electrophoresis
ROS	Reactive oxygen species
SAHBs	stabilized α-helix of Bcl-2 domains
SAR	Structure-activity relationship
SCLC	Small cell lung cancer
SERCA	Sarco-endoplasmic reticulum calcium ATPase

SMI	Small molecule inhibitor
TG	Thapsigargin
TNF-α	Tumor necrosis factor-alpha
TPP	Triphenylphosphine

CHAPTER 1

1. Targeting anti-apoptotic Bcl-2 family proteins to treat drug resistant malignancies

1.1. Cancer and Drug resistance

Cancer is a disease in which mutated and damaged cells continue to survive and proliferate beyond their normal life span. Extensive research has led to the development of a plethora of chemotherapeutic agents to help manage this disease; however, none of these agents are capable of completely curing cancer. Drug resistance, especially acquired drug resistance, is a prime cause contributing to the current inadequacy of chemotherapy and poses a major challenge to the treatment of cancer. Moreover, acquired drug resistance among cancer patients often leads to cross-resistance to a broad spectrum of anticancer agents with varied mechanism of action. Because most anticancer agents in use have a low therapeutic index, increasing dosage to overcome drug resistance is not feasible. Consequently, there is a vital need to develop new therapeutic entities to overcome drug resistance to chemotherapy.

To develop novel therapies for the treatment of drug resistance, an in-depth understanding of the mechanisms responsible for the development of drug resistance in cancer cells is essential. Cancer cells utilize multiple mechanisms in the development of drug resistance. The main cellular mechanisms known thus far are alterations in drug transport, protein targets or cellular repair mechanisms. Cancer cells alter drug transport by over-expressing a family of proteins known as ATP-binding cassette (ABC) transporters.[1, 2] The ABC transporter proteins help shuttle small molecules out of the cell.

ABCB1 or P-glycoprotein (P-gp), the most prominent and well-characterized member of the ABC family, is responsible for multidrug resistance (MDR) to a variety of structurally unrelated drugs.[3] Over-expressed P-gp in cancer cells acts as a drug efflux pump, thereby lowering the intracellular concentrations of the drug and leading to resistance.

Besides altering drug transport, cancer cells also develop resistance by modifying cellular repair mechanisms. One such process involves changing a programmed cell death pathway known as apoptosis. Apoptosis is a tightly regulated multi-step pathway that removes cells in an orderly manner without triggering inflammation.[4] This process is characterized by cell shrinkage, plasma membrane blebbing without loss of integrity, nuclear fragmentation, and chromatin condensation.[5] Apoptosis is activated via two main pathways: the intrinsic pathway and the extrinsic pathway.[6, 7] The intrinsic pathway, also termed the mitochondrial pathway, is tightly controlled by the B-cell lymphoma-2 (Bcl-2) family proteins. A variety of insults (stress signals) to our body can trigger the intrinsic apoptotic pathway such as DNA damage, hypoxia, and survival factor deprivation, etc. Following the reception of stress signals, pro-apoptotic Bcl-2 family proteins are activated and are recruited to the mitochondrial membrane. On the mitochondrial membrane, these pro-apoptotic proteins undergo oligomerization leading to pore formation and mitochondrial outer membrane permeabilization (MOMP). MOMP leads to cytochrome c release from the mitochondria. Once cytochrome c is released, it binds with apoptotic protease activating factor - 1 (Apaf-1) and ATP, which then bind to pro-caspase-9 to create a protein complex known as an apoptosome. The apoptosome cleaves

the pro-caspase-9 to its active form, which in turn activates the effector caspase-3, leading to apoptosis.[8]

The extrinsic pathway, on the other hand, operates through the cell surface receptors such as the death receptors (DR).[9-11] Cytokines such as FAS ligand (FASL) and Tumor Necrosis Factor-α (TNFα) initiate this pathway by binding to death receptor family members, leading to the formation of death-induced signaling complexes (DISC). The DISC recruit and activate caspase-8, which can cleave and activate downstream caspases leading to cell death.

Most, if not all, classical chemotherapeutic agents eliminate cancerous cells via induction of apoptosis. Therefore, alterations leading to evasion of apoptosis is another major mechanism by which cancer cells develop drug resistance.

1.2. Detailed functions and mechanisms of Bcl-2 family proteins in apoptosis and drug resistance

Bcl-2 was the first protein member of the Bcl-2 family to be molecularly characterized. The *BCL2* gene was first discovered in 1985 because of its participation in the t(14;18) chromosomal translocations observed in non-Hodgkins lymphomas.[12] Since then altered Bcl-2 expression has been observed in a variety of tumors and additional members have been identified.[13] In mammals, there are at least 25 Bcl-2 family proteins. These proteins can be classified into two different groups (pro-apoptotic and anti-apoptotic) based on their function.[14]

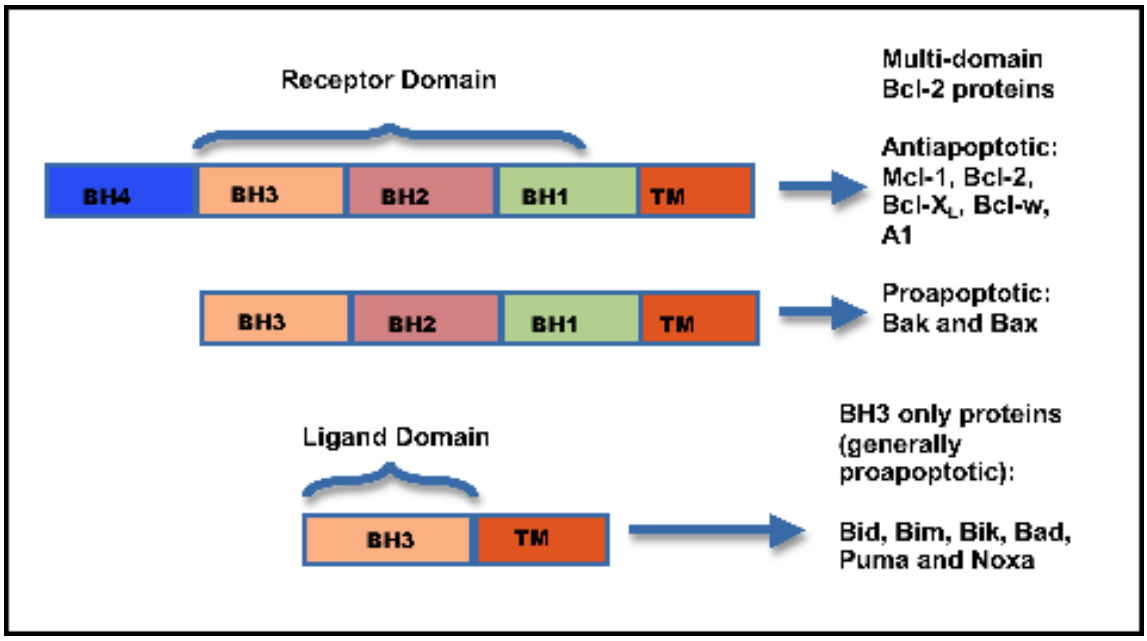

Figure 1.1. Bcl-2 Family Proteins

As the name suggests, the anti-apoptotic Bcl-2 family proteins prevent apoptosis. They consist of five main proteins - Mcl-1, Bcl-2, Bcl-X_L, Bcl-w and A1. Structurally, the anti-apoptotic proteins have four conserved Bcl-2 homology (BH) domains (BH1-BH4) and a transmembrane domain (Figure 1.1). The pro-apoptotic Bcl-2 family proteins that promote apoptosis are further divided into two groups (multi-domain and BH3-only) based on the number of BH domains present. The multi-domain proteins like Bax and Bak have three BH domains, BH1-BH3, while the BH3-only proteins (Bid, Bad, Bik, Puma, Noxa etc.) as their name suggests, have only the BH3 domain (Figure 1.1). The BH domains play an important role in the function of these proteins; the BH1, BH2, and BH3 domains of the anti-apoptotic proteins form a long hydrophobic cleft that is proposed to physically interact with and functionally antagonize the pro-apoptotic

proteins. The transmembrane domain, common to both pro-apoptotic and anti-apoptotic proteins help them anchor to membranes in an organelle-specific manner. Thus far the Bcl-2 family proteins have been characterized to localize on the mitochondria, endoplasmic reticulum (ER) and the nuclear envelope. The pro-apoptotic and anti-apoptotic proteins together interact with each other to tightly control the process of apoptosis.[15, 16] In a normal cell there is a balance between pro-apoptotic and anti-apoptotic proteins, which maintains cell survival and death. However, when there is an over-expression of anti-apoptotic proteins, this balance is disturbed preventing apoptosis, leading to the development of cancer and drug resistance (Figure 1.2).[17, 18]

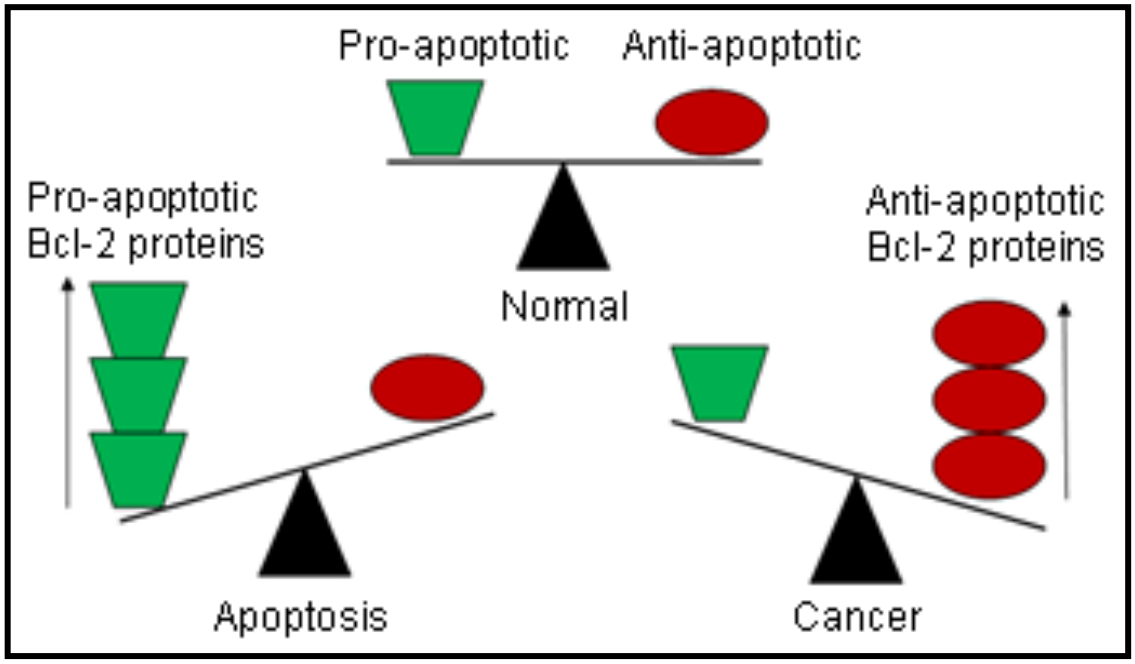

Figure 1.2. Role of Bcl-2 Family Proteins in Cancer

There are three speculative models explaining how BH3-only proteins can interact with other Bcl-2 family proteins to induce apoptosis. The ‘‘direct activation model’’

suggested by Letai *et al.* divides BH3-only domain proteins into two groups, ‘‘sensitizers’’ and ‘‘activators’’.[19] The activator BH3-only molecules (Bim, Bid) directly bind to and cause oligomerization of Bax/Bak, leading to the release of cytochrome c. The sensitizers, such as Bad, Bik, and Noxa, cannot directly activate Bax/Bak, but they inhibit anti-apoptotic Bcl-2 proteins from engaging with, and thereby sequestering, Bax/Bak. In the second model (indirect activation model), Bax and Bak do not require activation by BH3-only molecules like Bim or Bid, but are rather intrinsically activated, and must thus be always bound and sequestered by anti-apoptotic Bcl-2 (or related anti-apoptotic) proteins to maintain survival. The BH3-only proteins in this model have no activator function, but rather act only as antagonists of the anti-apoptotic proteins like Bcl-2 and displace pro-apoptotic Bax or Bak proteins from the hydrophobic cleft.[20] The engagement of BH3-only proteins with anti-apoptotic Bcl-2 members is common between the two models. In the third and final model known as the “embedded together” model, the anti-apoptotic proteins are able to sequester both active Bax/Bak and BH3-only activators. BH3-only sensitizers displace Bax/Bak and BH3-only activators from the anti-apoptotic proteins. The ‘freed’ Bax/Bak can oligomerize whereas the BH3-only activators can bind and recruit additional Bax/Bak, which also oligomerizes, resulting in pore formation and MOMP. These important interactions occur within the mitochondrial outer membrane, where all three classes of Bcl-2 family members undergo specific conformational changes.[20]

Recently the role Bcl-2 family proteins localized on the ER have been of interest. Several studies suggest that Bcl-2 proteins found on the ER exert an equally important regulatory effect on apoptotic induction as their mitochondrial counterparts. On the ER, Bcl-2 proteins are thought to regulate the calcium signaling to control apoptosis.[21] Pro-apoptotic proteins Bax and Bak, enhance calcium levels in the ER and its release and also its uptake by the mitochondria, committing the cells to apoptosis route.[22] On the other hand Bcl-2 proteins dampen the release of calcium from the ER by reducing the total releasable calcium from the store.[23] This hampers the death signal transduction. The general consensus is that Bcl-2 modulates apoptosis via the Ca^{2+} route, however the exact mechanism by which Bcl-2 achieves such modulation is under intense investigation.[21, 24] Some recent studies have shed light to the mechanism of Bcl-2 proteins on the ER. These studies suggest that Bcl-2 proteins might be regulating calcium on the ER by interacting with various ER calcium transporters. For instance, Bcl-X_L and Bax can interact with and regulate the inositol triphosphate receptors (IP_3Rs), which release ER Ca^{2+} into the cytosol.[25, 26] Some reports also suggest that Bcl-2 interacts with and regulates the function of sarco-endoplasmic reticulum ATPase (SERCA) pumps, which pump cytosolic Ca^{2+} into the ER.[27-29] Given that the over-expression of the anti-apoptotic Bcl-2 family proteins and dysregulation of the calcium channels have both been reported to be responsible for MDR in cancer, simultaneously regulating both pathways is possible and may provide an effective strategy to overcome drug resistance in cancer therapies.

Since the original observations showing that anti-apoptotic Bcl-2 expression can induce cell survival,[30, 31] over-expression of anti-apoptotic Bcl-2 family proteins have been implicated in cancer development and drug resistance. For example, elevated levels in Bcl-2 protein as a result of t(14;18) translocations involving the *BCL2* gene occurs in 80% to 90% of low-grade follicular non-Hodgkin lymphomas (NHLs).[32, 33] Approximately one third of diffuse large cell lymphomas (DLCLs) have pathologically elevated Bcl-2 (often in association with t(14;18) translocations or gene amplification), correlating with shorter patient survival when treated with combination chemotherapy.[34, 35] Most chronic lymphocytic leukemias (CLLs) contain elevated Bcl-2, associated with hypomethylation of the *BCL2* gene.[36, 37] Furthermore, over-expression of Bcl-2 has been shown to be the underlying cause for resistance to a wide range of cancer therapies, such as cisplatin,[38] glucocorticoids,[39] adriamycin,[40] docetaxel,[41]daunorubicin,[42] thapsigargin,[43] and imatinib.[44] Elevated Mcl-1 protein expression, which is associated in some cases with mutations in the promoter of the *MCL1* gene, has also been correlated with failure to achieve complete remission after treatment with chemotherapy.[45-47] In addition, increased Mcl-1 levels in cancer cells have been demonstrated to prevent apoptosis induced by ABT-737 (an inhibitor of Bcl-2 and Bcl-X_L proteins), and Lapatinib (a tyrosine kinase inhibitor).[48, 49] Likewise over-expression of Bcl-X_L has been associated with resistance to apoptosis induced by a variety of chemotherapeutic agents.[50-53] Taken together these studies demonstrate that apart from its widespread role in development of cancer, anti-apoptotic Bcl-2 proteins also play a very important role in development of drug resistance to chemotherapy.

As one of the key clinical problems in oncology is dealing with drug resistant tumors, antagonizing anti-apoptotic Bcl-2 family proteins provides a promising strategy for overcoming drug resistance.[54, 55] Over the years, tremendous progress has been made in designing ways to inhibit the anti-apoptotic Bcl-2 family proteins.[56-59] The different approaches used to target anti-apoptotic Bcl-2 family proteins will be discussed in the following sections.

1.3. Early approaches used to target anti-apoptotic Bcl-2 family proteins

In 1990, Reed and colleagues, using antisense methods, made the first demonstration that knocking down Bcl-2 expression induces leukemia cell death and inhibits leukemic growth *in vivo*.[60, 61] In 1991, *BCL2* gene knockout mice were generated by Sentman et al,[62] revealing a requirement for Bcl-2 for postnatal survival of lymphocytes and melanocytes. These seminal reports geared the thought process of using gene silencing or down regulation of protein expression as an approach towards targeting anti-apoptotic Bcl-2 family proteins.

Genasense (G3139, Oblimersen sodium)

Antisense oligonucleotides are about 20 nucleotides in length and act via hybridizing mRNA, resulting in a substrate for ribonuclease H (RNase H). This enzyme specifically degrades the RNA strand of the RNA-DNA duplex.[63] Genasense, also known as Oblimersen sodium, was the first agent targeting Bcl-2 proteins that entered the clinical trials. Genasense is an 18-mer phosphorothioate antisense oligonucleotide that targets Bcl-2 mRNA and alters Bcl-2 expression levels.[64, 65] The apoptotic effect of

Genasense antisense occurs via an increase in Bax and PARP, releasing cytochrome c, activating caspases, and ultimately releasing Smac/DIABLO to antagonize proteins that are inhibitors of apoptosis or releasing apoptosis-inducing factors from mitochondria to induce DNA fragmentation.[58]

Genasense has been clinically tested in combination with other anticancer chemotherapeutic agents in a variety of cancers. However Genasense therapy was only moderately successful against low-grade lymphoid malignancies, where it had been anticipated to be most active,[66-68] and did not obtain US Food and Drug Administration (FDA) approval after failing to result in survival differences in a pivotal melanoma trial.[69] Potential explanations for these disappointing outcomes include suboptimal penetration in cancer cells, a long half-life of the Bcl-2 protein and the narrow specificity of the target. Furthermore, antisense oligonucleotides have a short half-life and are prone to rapid enzymatic degradation and turnover, which provides a hindrance in the use of antisense agents for cancer therapy.

Other early approaches

Another attractive approach to block the activity of Bcl-2 is via the use of antibodies directed against Bcl-2. An intracellular anti-Bcl-2 single-chain antibody has been shown to increase drug-induced cytotoxicity in the MCF-7 breast cancer cell lines as well as other cancers.[70] Other approaches include the use of a ribozyme against Bcl-2. The recombinant anti-Bcl-2 ribozymes were designed to have two independent catalytic domains which would cleave Bcl-2 mRNA at two different sites.[71] However, none of these approaches have been proven to be effective in clinic.

1.4. Current approaches to target anti-apoptotic Bcl-2 proteins

Due to the shortcomings of early approaches, a second approach via direct antagonism of the over-expressed anti-apoptotic Bcl-2 proteins was explored. The anti-apoptotic function of Bcl-2 proteins, at least in part, is attributed to their ability to heterodimerize with the BH3 domain of pro-apoptotic proteins like Bim and Bid. Therefore it was hypothesized that molecules that bind to the hydrophobic groove of the anti-apoptotic proteins could inhibit their function, thereby tilting the balance towards apoptosis in cancer cells. The crystal structure of Bcl-X_L bound to a Bak BH3 peptide revealed that the BH1-3 domains of Bcl-X_L formed a hydrophobic groove, where the α-helix of the BH3 domain of the pro-apoptotic protein binds.[72, 73] This discovery helped set the stage for subsequent drug discovery and provided an impetus in the design of BH3-mimetics.

1.4.1. Peptides and Peptidomimetic approach

Peptides containing the BH3 domains of several Bcl-2 family members such as Bax, Bak, Bik, Bid, and Bad have been demonstrated to bind to the anti-apoptotic Bcl-2 family members, such as Bcl- X_L.[73] Cell permeable forms of these BH3 domain peptides also have the capability of triggering intracellular apoptosis.[74] One such example is CPM-1285, which binds to Bcl-2 with an IC_{50} of 130 nM in a competition assay against a fluorescently-tagged Bak BH3 peptide. In HL-60 cells, CPM-1285 induced caspase-3 activation and triggered DNA fragmentation and PARP cleavage, which are characteristics of apoptosis.[75] The limitations of peptides as drugs has been alleviated by

developing either α-helix constrained BH3 peptides or unnatural amino acid-based peptides.[76-78] For e.g., the stapled peptides, also known as the 'stabilized α-helix of Bcl-2 domains' (SAHBs), unlike normal peptides, demonstrate increased cell-membrane permeability and extended half-life in the presence of serum, which offers the possibility of *in vivo* efficacy. SAHBs also demonstrate increased binding affinity towards multi-domain Bcl-2 member pockets.[79] Furthermore, synthetic stapled Bid-BH3 peptides synthesized have also shown to have better apoptotic potential in leukemia cells, in comparison with the parent peptides alone. These compounds have shown activity in animal models and are currently in preclinical testing. Peptidomimetic approaches used to improve the pharmacological properties of peptides have only been reasonably successful. For e.g. peptidomimetic approaches using a terphenyl scaffold as an α-helix mimic afforded an antagonist of Bcl-X_L with a Ki of 114 nM.[80] However no cellular activity has been reported to date.

1.4.2. Small molecule inhibitors (SMI)

SMIs are organic molecules of low molecular mass (usually < 750 Daltons). Their small size makes their *in vivo* use more practical, and possibly more cost-efficient, compared to oligonucleotides or other small peptides. Over the past twelve years, several small molecules have been reported to interact with the anti-apoptotic Bcl-2 proteins and function as antagonists against these proteins (Table 1.1). These small molecules were identified from natural products, by library screening, or via molecular design (Table 1.1). The small molecule inhibitors currently in clinical trials shown in Figure 1.3 will be described below:

Table 1.1. Small molecule inhibitors of anti-apoptotic Bcl-2 proteins

Compound	Companies	Use	Clinical Trials	No of Trials	Molecular Targets
Gossypol (BL-193, AT-101)	Ascenta Therapeutics	Head and Neck tumors, malignant gliomas, prostate cancer, leukemia and lymphoma	Phase II/III	20	Mcl-1, Bcl-2, Bcl-X_L (Highest to lowest affinity)
ABT-737	Abbott laboratories	Myeloma, AML, NSCLC, lymphoma	Phase I	NA	Bcl-2 and Bcl-$X_{L,}$
ABT-263 (Nacitoclax)	Abbott laboratories	Myeloma, CLL, NSCLC, Lymphoma, Solid tumor	Phase I/ IIa	17	Bcl-2, Bcl-$X_{L,}$ Bcl-w, Bcl-B
Obatoclax	Gemin X	Solid tumor malignancies, advanced CLL, refractory leukemia, myelodysplasia	Phase I/ II	16	Mcl-1, Bcl-2, Bcl-$X_{L,}$ Bcl-w
TW-37	University of Michigan	Non-Hodgkin lymphoma. Pancreatic and lung cancer	Preclinical studies	NA	Mcl-1, Bcl-2, Bcl-$X_{L,}$ Bcl-w, A1
Apogossypolone	Ascenta Therapeutics	Non-Hodgkin lymphoma	Preclinical studies	NA	Mcl-1, Bcl-2, Bcl-X_L
HA 14-1	Thomas Jeffereson University	Leukemia and others	Preclinical studies	NA	Bcl-2 and Bcl-$X_{L,}$
Antimycin A	Fred Hutchinson Cancer Research Center	Various types of cancer	Preclinical studies	NA	Bcl-2 and Bcl-X_L
BH3I-1 /BH3I-2[81]	Harvard University	Various types of cancer	Preclinical	NA	Bcl-2
Terphenyl derivative	Yale University	Various types of cancer	Preclinical	NA	Bcl-2
Apogossypol /Theaflavin	The Burnham Institute	Various types of cancer	Preclinical	NA	Bcl-2

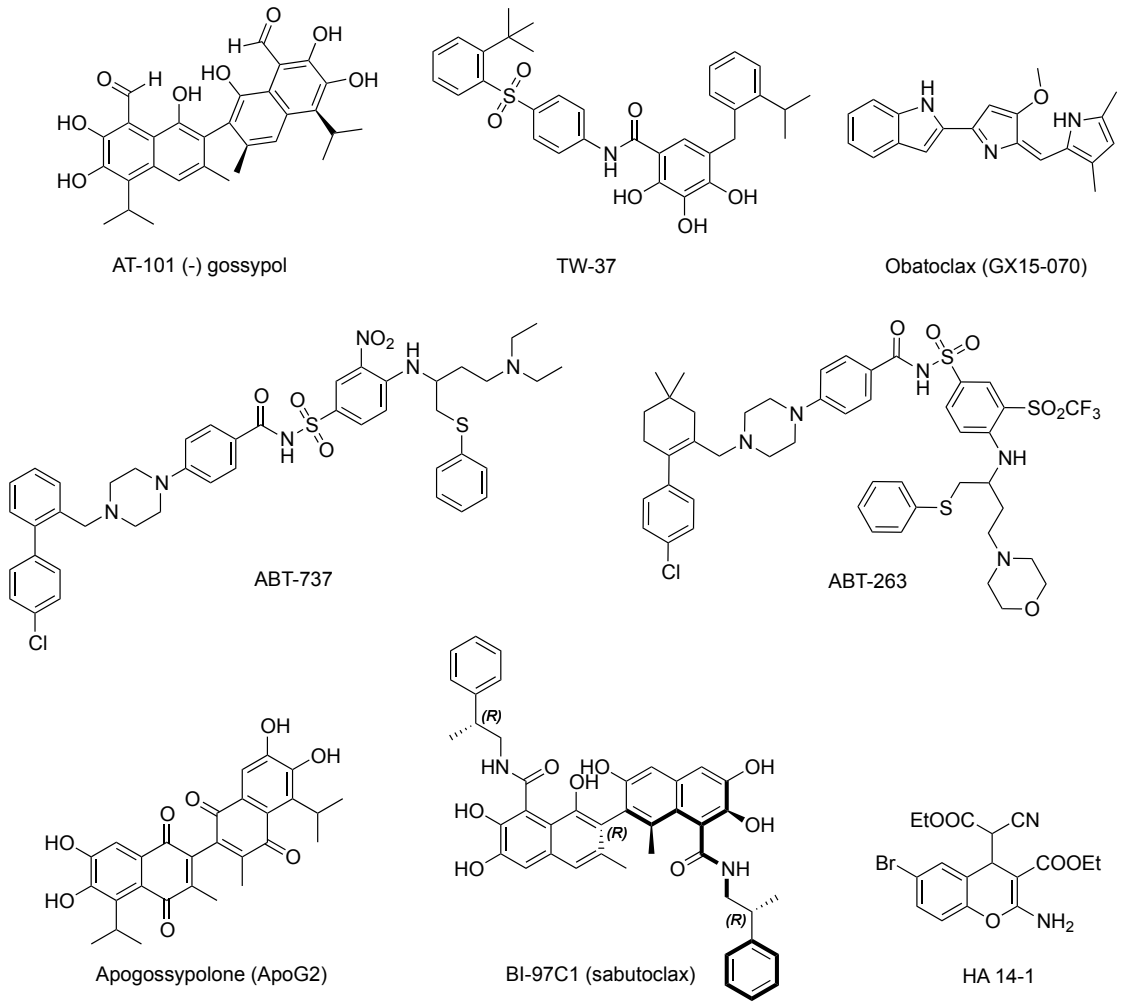

Figure 1.3. Small molecule inhibitors currently in clinical trial

(-) Gossypol (AT-101)

Gossypol is an orally available natural product of the cotton plant (Gossypium sp.). Around 20 years ago, racemic gossypol was shown to inhibit growth of cancer cells but the mechanism of action was unknown. Recently, Pellechia *et al.,* showed that gossypol disrupts Bcl-2– and Bcl-X_L–ligand interactions by blocking the BH3-binding site, exhibiting submicromolar binding affinity for Bcl-2 and Mcl-1.[81] Subsequently,

Pellechia and others showed that the two enantiomers in the racemic gossypol had different efficacies,[82] with the negative enantiomer having ten fold greater antiproliferative capacity, and potentially a separate primary mechanism of action, compared to the positive enantiomer.[83, 84] The negative enantiomer, ((−)-gossypol) has since been developed as an anticancer compound under the name AT-101 (Ascenta Therapeutics Inc., Malvern, PA) (Figure 1.3).

AT-101 has been extensively examined in preclinical studies in a variety of cancers.[85-93] To date about 20 Phase I/II/III clinical trials of AT-101, as a single agent or in combination with other chemotherapeutic agents have been initiated (clinicaltrials.gov), with some of these trials are still ongoing. A single agent Phase I/II study with AT-101 showed that clinically 30 mg/p.o./q.d. AT-101 for 21 days was well tolerated in treatment of castrate-resistant prostate cancer with modest clinical response.[94] AT-101 is the only Bcl-2 inhibitor that has reached Phase III clinical trials.

Synthetic derivatives of gossypol

TW-37

TW-37 (Figure 1.3) is a benzenesulfonyl derivative of AT-101.[95] It is a pan-Bcl-2 inhibitor that is able to inhibit all major members of the anti-apoptotic Bcl-2 family including Bcl-2, Bcl-X_L, and Mcl-1. It has both pro-apoptotic and anti-angiogenic activity. Although derived from AT-101, it has a distinctly different structure and a lower binding efficacy for Bcl-X_L (IC_{50} = 1.1 μM, TW-37 vs. 0.48 μM, AT-101) while maintaining similar binding capacity for Bcl-2 and Mcl-1, both in the low nanomolar range. TW-37 was well tolerated *in vivo* with maximum tolerated doses in severe combined immunodeficient mice of up to 40 mg/kg/day for 20 days as single agent (5

days on, 1 day off) and 20 mg/ kg/day for 3 days in conjunction with traditional chemotherapy such as cyclophosphamide-hydroxyldaunorubicin (doxorubicin)-oncovin (vincristine)-prednisone (CHOP) regimen.[96] In addition, TW-37 has shown *in vitro* and *in vivo* efficacy against a variety of cancer cell lines, which include head and neck, melanoma, pancreatic and lymphocytic cancers.[97-100] The *in vivo* efficacy of TW-37 was relatively modest as a single agent; however, a significant tumor inhibition is observed in combination.[96] TW-37 is currently under preclinical studies.

Apogossypolone (ApoG2)

ApoG2 (Figure 1.3) is also synthetically derived from gossypol similar to TW-37. It was designed by Ascenta Therapeutics to reduce the non-specific reactivity and toxicity observed with gossypol. The structural changes involved the removal of the two reactive aldehyde groups on the polyphenolic rings of gossypol.[101, 102] Similar to TW-37, ApoG2 is a pan–Bcl-2 inhibitor and demonstrates potent inhibition towards Mcl-1 unlike ABT-737. ApoG2 is also currently in preclinical studies.[103, 104]

BI-97C1 (sabutoclax)

BI-97C1 (Figure 1.3) is an optically pure apogossypol derivative. It is a pan Bcl-2 inhibitor with binding affinities towards Bcl-X_L, Bcl-2, Mcl-1, and Bfl-1 in the micro molar range.[105] It shows efficacy in prostate, lung and lympoma cancer cell lines *in vitro* and in prostate cancer *in vivo*.[106, 107] BI-97C1 holds promise in combination therapy and is currently under preclinical investigation.

The ABT series of Bcl-2 inhibitors

ABT-737

Abbott laboratories used a high-throughput NMR-based screening method called 'SAR by NMR' to identify small molecules that bind to the hydrophobic BH3 binding domain of Bcl-X_L. In this approach proximal fragments are linked to achieve high-affinity binding.[108] ABT-737 (Figure 1.3) was the lead compound obtained after screening and optimization. ABT-737 mimicked the BH3 domain of BAD and bound with high affinity to Bcl-2, Bcl-X_L and Bcl-W with dissociation constant (K_D) in the nano molar range. However, ABT-737 had poor affinity to Mcl-1 and Bfl-1 with a K_D in the micro molar range. ABT-737 is effective in a variety of cancers *in vitro* and *in vivo*.[109-112] The first major limitation of ABT-737 is that it is not orally active, thereby making it difficult for use in clinical trials. The second limitation with ABT-737 is that it is not effective in cancers over-expressing Mcl-1 protein.[48, 113-115] Due to these limitations, currently there are no clinical trials ongoing with ABT-737. To overcome the first limitation of ABT-737, Abbott laboratories developed an orally available derivative of ABT-737 known as ABT-263.[116]

ABT-263 (Navitoclax)

ABT-263 is an orally available derivative of ABT-737, which has entered 17 clinical trials to date, including efficacy studies in chronic lymphocytic leukemia, lymphoma, small-cell lung cancer (SCLC), and other solid tumors. A phase I clinical study with ABT-263 in SCLC conducted to determine its safety, pharmacokinetics, and preliminary efficacy in patients with solid tumors showed that ABT-263 is safe and well tolerated, with dose-dependent thrombocytopenia as the major adverse effect.

Preliminary efficacy data were encouraging in SCLC, with one patient having a confirmed partial response lasting longer than 2 years, and eight patients with SCLC or carcinoid having a stable disease.[117] Another phase I study conducted to test its efficacy in lymphoid malignancies was also successful. Ten of 46 patients with assessable disease had a partial response, and these responders had median progression-free survival of 455 days.[118] Phase II studies in both SCLC and lymphoid malignancies are currently ongoing. One of the major limitations of ABT-263, like its predecessor-ABT-737, is its weak binding affinity towards Mcl-1, which makes ABT-263 ineffective in malignancies over-expressing Mcl-1,[119] limiting its therapeutic potential.

Obatoclax (GX15-070)

Obatoclax (Figure 1.3) was developed by Gemin X Biotechnologies from derivatives of the bacterially-derived natural product streptorubin B. Obatoclax (GX15-070) is a small-molecule pan-Bcl-2 family inhibitor that binds and blocks the function of Bcl-X_L, Mcl-1, Bcl-w, A1, and Bcl-b.[120] Unlike ABT-737, obatoclax can antagonize Mcl-1 and overcome the resistance observed through Mcl-1.[120] Obatoclax showed modest activity in a phase I clinical trial in heavily pretreated CLL patients.[121] One of 26 patients (4%) achieved a partial response, and notably this was in the least heavily-pretreated patient in the trial. Activity was also observed in a Phase I clinical trial in patients with refractory leukemia and myelodysplasia.[122] Furthermore, a patient with a refractory AML, who harbored a MLL t(9;11) translocation achieved complete response with one course of obatoclax and had a sustained remission for 8 months. Obatoclax is currently

under Phase II clinical trials. To date about 18 phase I/II clinical trials of obatoclax have been registered. (clinicaltrials.gov). Unfortunately, this compound may need to be redesigned for pharmacokinetic reasons; a recent study showed the treatment of mice with bolus injection of GX-015–070 failed to reach pharmacologically effective levels in the blood; and dose escalation was limited by significant neurologic toxicity.[123]

1.5. HA 14-1 as a lead small molecule antagonist against anti-apoptotic Bcl-2 proteins

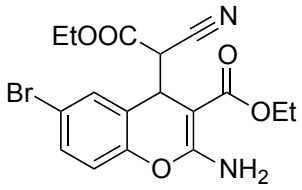

HA 14-1

Figure 1.4. Structure of HA 14-1

HA 14-1 (Figure 1.4) was one of the first small-molecule antagonists against anti-apoptotic Bcl-2 family proteins identified by Huang *et al.* in 2000 via a virtual screen.[124] It was subsequently demonstrated to selectively induce apoptosis in malignant cells that over-express Bcl-2.[125-127] In a study by Dai *et al.,* leukemia cells developed resistance to imatinib via over-expression of Bcl-2.[44] Interestingly, HA 14-1 selectively eliminated the resistant cells while sparing the parent leukemia cells, underscoring the potential of HA 14-1 to selectively eliminate drug-resistant tumors that over-express Bcl-2 proteins. Furthermore, two *in vivo* studies also demonstrated the tumor suppressing activity for HA 14-1.[127, 128] Lastly, another interesting feature of HA 14-1 is its ability to sensitize different types of cancer cells with varying levels of Bcl-2 proteins to a wide range of

cancer therapies.[126, 129-136] Taken together these studies emphasize the potential of HA 14-1 for combination therapy and to overcome drug resistance in cancers.[125]

Since HA 14-1 was discovered as a single lead through virtual screening, little information about the pharmacophore of HA 14-1 was available, and, since its discovery in 2000, no effort had been reported to modify HA 14-1 to improve its bioactivity. The relatively low *in vitro* cytotoxicity (GI_{50}: ~20 μM) and the poorly defined binding affinity of HA 14-1 to Bcl-2 protein (only IC_{50} was reported), encouraged us to initiate SAR studies to search for more potent candidates and to define the pharmacophore of HA 14-1.

In spite of its interesting biological activities, studies on HA 14-1 have revealed that it is unstable under standard tissue culture conditions with a half-life of 15 min.[137] Moreover, decomposition of HA 14-1 leads to reactive oxygen species (ROS) generation, which might be responsible for its observed activity instead of its ability to antagonize Bcl-2 proteins.[133, 137, 138] The short half-life of HA 14-1 in cell culture media limits any potential clinical use. Therefore, the ***first objective*** of my research is to develop potent and stable analogs of HA 14-1 and assess their anti-cancer activity.

CHAPTER 2*

2. Synthesis and structure-activity relationship of stable analogs of HA 14-1

2.1. Introduction

As discussed in the previous chapter our studies revealed that HA 14-1 was unstable in cell culture media and decomposed with a half life of < 15 min.[137] Therefore, there was a need to develop a stable analog of HA 14-1, which would retain its beneficial properties and have a longer half-life in cell culture media. In order to develop a stable analog of HA 14-1 an understanding of decomposition pathway of HA 14-1 was required. Based on previous studies in our lab, the decomposition of HA 14-1 was proposed to occur via the rapid elimination of a stable ethyl cyanoacetate anion leading to the formation of an imine intermediate (**1**), which rapidly hydrolysed to form the lactone ester (**2**) followed by further hydrolysis to the lactone acid (**3**) (Scheme 2.1).[137] Since the first step in the decomposition of HA 14-1 was the elimination of the stable ethyl cyanoacetate anion, we hypothesized that destabilizing the anion by removing the cyano group present on HA 14-1 would lead to a stable analog.

---

*Parts of this chapter have been reproduced with permission from {Das, S. G. et al. Structure-activity relationship and molecular mechanisms of ethyl 2-amino-4-(2-ethoxy-2-oxoethyl)-6-phenyl-4h-chromene-3-carboxylate (sHA 14-1) and its analogues. J Med Chem 2009, 52, 5937-49}. Copyright {2009} American Chemical Society.

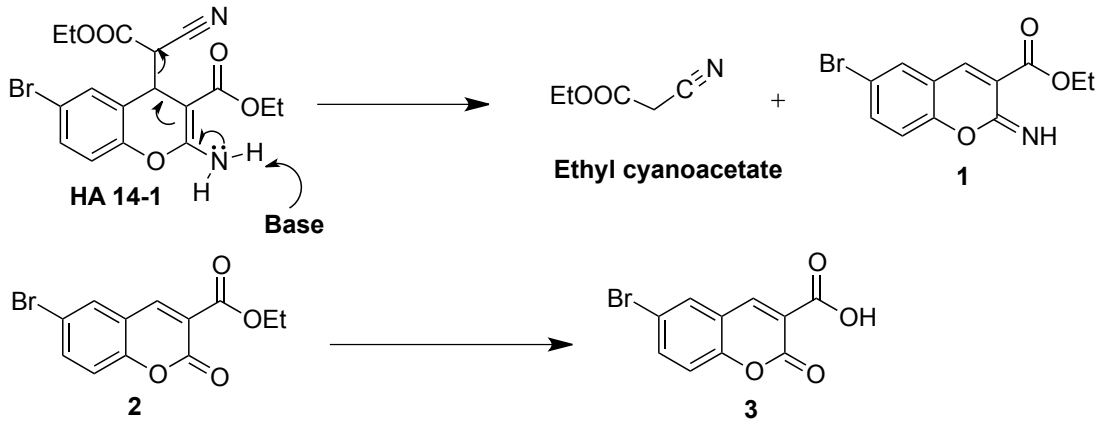

Scheme 2.1. Proposed decomposition pathway of HA 14-1

2.2. Results and discussion

2.2.1. Design and synthesis of a stable analog of HA 14-1 (sHA 14-1)

To test the hypothesis mentioned above, we removed the cyano group from a potent analog of HA 14-1 (**4,** IC_{50} ~ 3.9 μM) previously synthesized in our lab (Figure 2.1),[139] which was about 3-fold more potent than HA 14-1 (IC_{50} ~ 11μM) in Jurkat cells (T-cell leukemia cell line).[139]

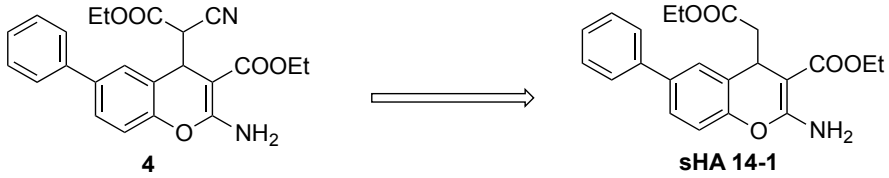

Figure 2.1. Structure of a potent analog of HA 14-1 and the proposed stable analog sHA 14-1

The first step towards the synthesis of sHA 14-1 involved the ortho-formylation of 4-phenyl phenol using paraformaldehyde, anhydrous magnesium chloride and

triethylamine in ACN to yield 5-phenyl salicylaldehyde. The 5-phenyl salicylaldehyde was then treated with *N,N*-dimethylacetamide and phosphorus oxychloride, followed by acidic workup to yield 6-phenylcoumarin. This was then subjected to a base-promoted rearrangement and Michael addition with ethyl cyanoacetate to furnish sHA 14-1 (Scheme 2.2).

Scheme 2.2. Synthetic scheme for the preparation of sHA 14-1

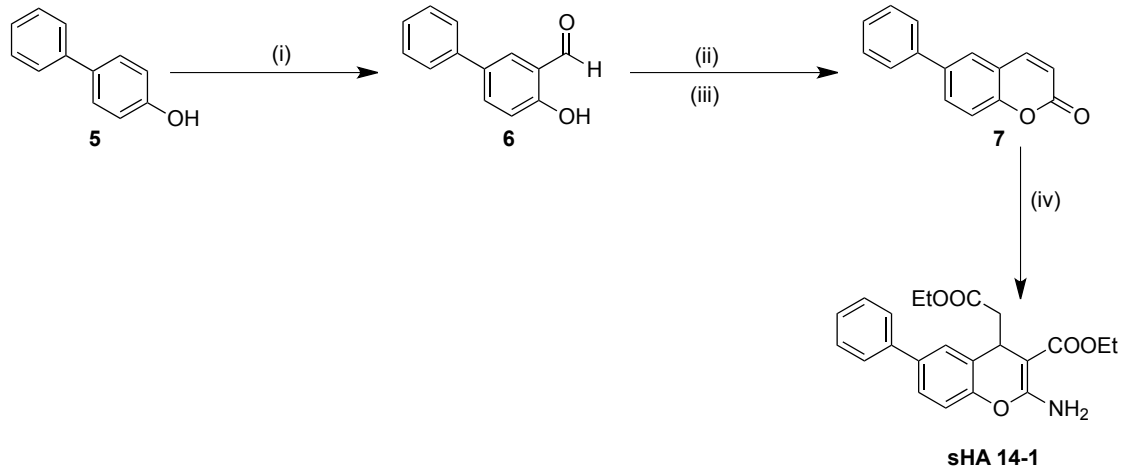

5 6 7 sHA 14-1

Reagents and conditions: (i) $MgCl_2$, Et_3N, paraformaldehyde, anhydrous CH_3CN, reflux; (ii) DMA, $POCl_3$ 60 ºC, 4-8 h; (iii) $NaHCO_3$, 60 ºC, 0.5 h; (iv) ethyl cyanoacetate, EtOH, NaOEt, room temp, 2 h.

2.2.2. Evaluation of stability of sHA 14-1

With sHA 14-1 in hand, we first evaluated its *in vitro* stability under physiological conditions to determine if it demonstrated improved stability over HA 14-1. In brief, sHA 14-1 was incubated in cell culture media at 37 °C for 24 h and the *in vitro* cytotoxicity was determined. HA 14-1 was run in parallel for comparison. As shown in Figure 2.2, a 24 h incubation in cell culture media resulted in ~ 58-fold loss in activity of HA 14-1 when compared to freshly prepared HA 14-1 solutions. sHA 14-1 on the other hand

exhibited only 1.7-fold loss in activity, indicating that sHA 14-1 is more stable than HA 14-1 under experimental conditions.

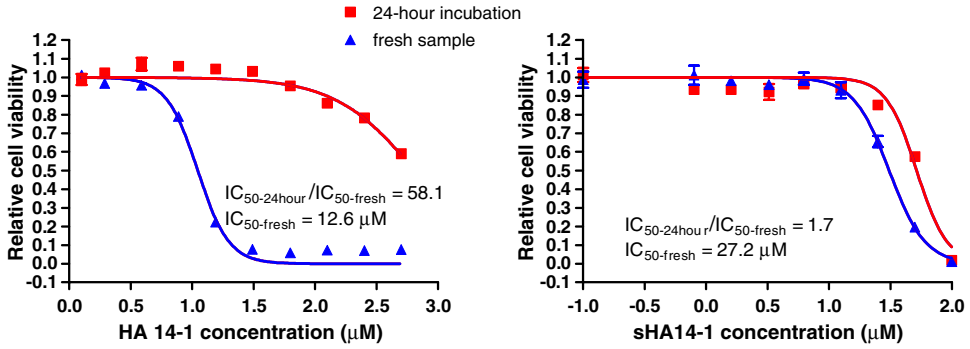

Figure 2.2. Cytotoxicity of HA 14-1 and sHA 14-1 using freshly prepared and 24-hour old samples in Jurkat cells

2.2.3. Fluorescent polarization (FP) assay to determine the binding affinity of sHA 14-1 to anti-apoptotic Bcl-2 proteins

We next explored the binding affinity of sHA 14-1 with anti-apoptotic Bcl-2 proteins, including Bcl-2, Bcl-X_L and Mcl-1. Briefly, a series of 3-fold dilutions of sHA 14-1 were prepared in DMSO and incubated with a premixed solution of 50 nM Flu-Bak peptide and the anti-apoptotic Bcl-2 protein at 23 °C for one hour. Subsequently, the fluorescence polarization (in mP unit) was measured using the Tecan plate reader. The controls in this experiment included dose-response measurements in the absence of proteins to assess for any interactions between the compounds and the Flu-Bak peptide. Inhibitory constants (Ki) were determined by fitting the FP values to the concentrations of sHA 14-1 using a single-site competition model for fluorescence polarization based competition assay established in this laboratory in GraphPad (San Diego, CA).

Based on our results, sHA 14-1 demonstrates increased potency to disrupt the binding interaction of the Bak peptide with Bcl-X_L proteins in comparison to HA 14-1. However, the Ki value of sHA 14-1 is in the high micromolar range while ABT-737 is in the nanomolar range (Table 2.1). These results suggests that although sHA 14-1 is better than HA 14-1, it has weak binding interaction with the anti-apoptotic Bcl-2 family proteins in the FP assay. Nonetheless, it is important to keep in mind that the FP assay described above uses recombinant Bcl-2 proteins that lack the transmembrane domain in the native protein. Therefore, although this assay is widely used to determine the binding affinity of various Bcl-2 inhibitors, this assay may not fully mimic the naturally membrane-bound proteins. In the light of this, the results based on this assay cannot completely rule out the possibility of sHA 14-1 as an antagonist against anti-apoptotic Bcl-2 family proteins.

Table 2.1. The binding interactions of HA 14-1, sHA 14-1 and ABT-737 with Bcl-X_L recombinant protein

Antiapoptotic Bcl-2 proteins	HA 14-1	sHA 14-1 Ki (μM)	ABT-737
Bcl-X_L	848.1	442.1	0.1224

2.2.4. Ability of sHA 14-1 to induce Caspase-3/7 activation in NALM-6 cells

As Bcl-2 family proteins play key role in the regulation of apoptosis. We were intrigued to determine if sHA 14-1 induced cell death via apoptosis. In order to do this, we examined the ability of sHA 14-1 to induce caspase-3/7 activation in cancer cells.

Caspase-3/7 are downstream caspases that are activated in the apoptotic pathway and are widely used as a marker for apoptosis. Briefly, NALM-6 (Pre B-Acute lymphoid leukemia) cells were treated with varying concentrations of sHA 14-1 for 24 h. After 24 h, the caspase-3/7 activation was measured using the Apo-ONE® Homogeneous Caspase-3/7 Assay kit. Our results show that sHA 14-1 induced caspase-3/7 activation in a dose-dependent manner in NALM-6 cells (Figure 2.3 A). We also performed a time dependent study for caspase-3/7 activation by sHA 14-1 and the results demonstrate that sHA 14-1 induces caspase activation in less than 1 h after treatment in NALM-6 cells (Figure 2.3 B). Taken together these results show that sHA 14-1 induces cell death via apoptosis as indicated by the dose-dependent and time-dependent caspase-3/7 activation.

A B

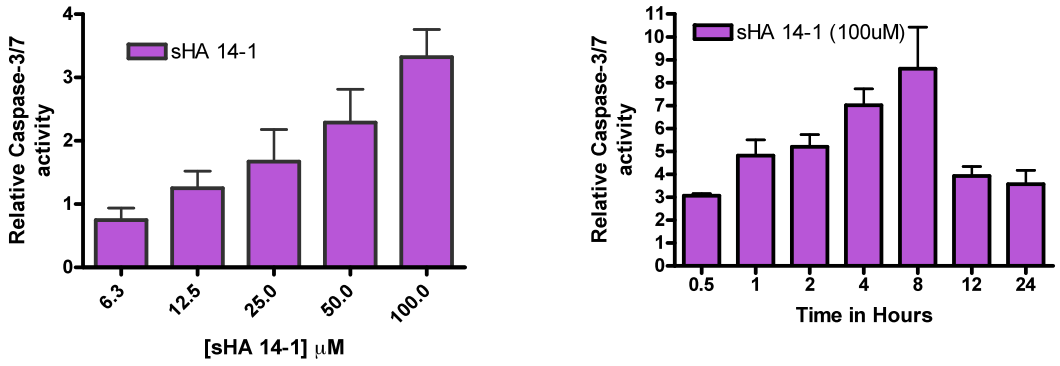

Figure 2.3. Caspase-3/7 activation induced upon sHA 14-1 treatment in NALM-6 cells

2.2.5. Activity in Jurkat cells over expressing anti-apoptotic Bcl-2 proteins

Having established that sHA 14-1 induces cell death via apoptosis, sHA 14-1 was further studied for its capability to overcome drug resistance induced by the over-expression of anti-apoptotic Bcl-2 family proteins. Specifically, the activity of sHA 14-1 was evaluated in Jurkat cells stably over-expressing Bcl-2 and Bcl-X_L proteins. Briefly, we treated the different cell lines with varying concentration of sHA 14-1 for a period of 48 h and evaluated the cell viability using the CellTiter-Blue assay. HA 14-1 was also evaluated for comparison. Results obtained from this experiment show that cells over-expressing Bcl-2 proteins are slightly more sensitive to the treatment of sHA 14-1 in comparison with the control Jurkat Neo cells (No transfection) (Table 2.2). Jurkat cells overexpressing Bcl-X_L also show no difference in activity when compared to the control cells. HA 14-1 on the other hand showed similar activity in cells over-expressing Bcl-2 and Bcl-X_L proteins, which is in accordance with previous studies in our lab.[139] These results further indicate that like HA 14-1, cells over-expressing anti-apoptotic Bcl-2 proteins fail to induce resistance to sHA 14-1.

Table 2.2. IC_{50} values of sHA 14-1 and HA 14-1 in Jurkat cells over-expressing anti-apoptotic Bcl-2 family proteins

Cell lines	HA 14-1	sHA 14-1
	IC_{50} (μM) ± SEM	
Neo	11.94 ± 3	19.4 ± 3
Bcl-2-WT	13.95 ± 4	11.71 ± 0.01
Bcl-X_L	14.8 ± 4	19.3 ± 1.9

2.2.6. Ability of sHA 14-1 to target drug resistant cancer cells (performed by David Hermanson)

Given that Jurkat cells exogenously over-expressing Bcl-2 and Bcl-X_L do not show any resistance towards sHA 14-1, we were eager to determine if similar effects will be observed in drug-resistant cancer cells endogenously over-expressing Bcl-2 proteins. In order to evaluate the potential of sHA 14-1 to selectively target drug-resistant cancer cells, we obtained both parental (non-resistant cancer cells) (HL60, CCRF-CEM) and drug-resistant (resistant to known chemotherapeutic agents) [HL60/MX2 – resistant to mitoxantrone (MX), CCRF-CEM/CT – resistant to camptothecin (CT)] cell lines. The resistant cells demonstrate cross-resistance to many known first-line anti-cancer drugs and over-express anti-apoptotic Bcl-2 proteins, making them the ideal cell lines for our study.[140] The drug resistant cell lines were treated with a series of dilutions of varying concentrations of sHA 14-1 for a period of 48 h in a 96-well plate. After which the cell viability was measured using the CellTiter-Blue assay. The results of this study show that sHA 14-1 demonstrates selectivity towards both the drug-resistant cell lines (CCRF-CEM/CT and HL60/MX2), with greater selectivity observed towards HL60/MX2 cells (Figure 2.4).

A

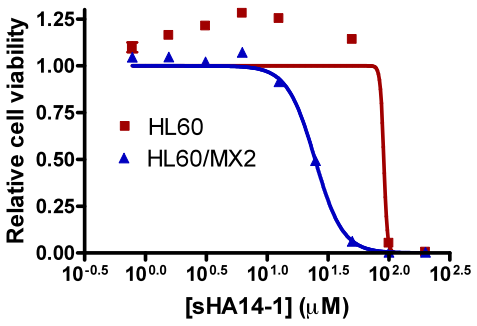

	HL60	HL60/MX2
IC_{50} (μM)	91.0 ± 0.3	23.2 ± 1.5

B

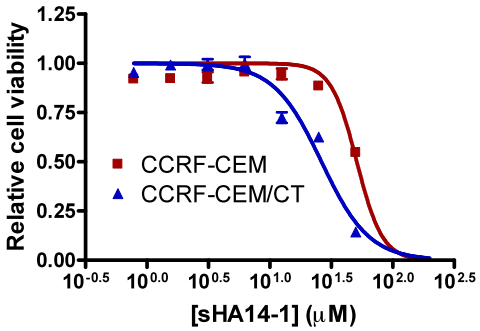

	CCRF-CEM	CCRF-CEM/CT
IC_{50} (μM)	51	26.3

Figure 2.4. Sensitivity of A) mitoxantrone resistant HL-60 cells to sHA 14-1 and B) camptothecin resistant CCRF-CEM cells to sHA 14-1

2.2.7. Synergism of sHA 14-1 (Performed by Dr. Jignesh Doshi)

As mentioned in the introduction, apart from overcoming drug resistance, another attractive feature of HA 14-1 was its ability to synergize numerous cancer therapies in a host of cancer cell types. So we also examined the ability of sHA 14-1 to synergize with other anticancer agents. Studies performed in our lab on the mechanism of sHA 14-1 have suggested that sHA 14-1 can induce apoptotic stress through intrinsic and extrinsic apoptotic pathways.[141] It was thus speculated that sHA 14-1 might be able to synergize the anti-cancer activity of both intrinsic apoptotic and extrinsic apoptotic stimuli. Therefore, the synergistic potential of sHA 14-1 towards several different stimuli: dexamethasone, doxorubicin, taxol, and vincristine (intrinsic apoptotic pathway) and Fas ligand (extrinsic apoptotic pathway) was evaluated. As demonstrated in Table 2.3, the

combination indices of sHA 14-1 with dexamethasone, Fas ligand, taxol, and vinscristine indicate that sHA 14-1 synergizes the anti-cancer activity of all these agents. Doxorubicin, on the other hand exhibits antagonistic interactions with sHA 14-1 (Table 2.3).

Table 2.3. The combination index values (CI) for each anticancer drug combined with sHA 14-1 in Jurkat cells

Treatment	Dose	Combination index (CI)
Dexamethasone	GI_{50}	0.78 ± 0.03
	0.75 GI_{50}	0.71 ± 0.02
	0.5 GI_{50}	0.89 ± 0.04
Doxorubicin	GI_{50}	1.50 ± 0.06
	0.75 GI_{50}	1.40 ± 0.09
	0.5 GI_{50}	1.21 ± 0.14
Fas ligand	GI_{50}	0.05 ± 0.02
	0.75 GI_{50}	0.24 ± 0.1
	0.5 GI_{50}	0.44 ± 0.13
Taxol	GI_{50}	0.84 ± 0.10
	0.5 GI_{50}	0.56 ± 0.07
	0.25 GI_{50}	0.61 ± 0.12
Vincristine	GI_{50}	0.58 ± 0.07
	0.5 GI_{50}	0.54 ± 0.05
	0.25 GI_{50}	0.58 ± 0.12

Three individual experiments were performed to obtain the CI values and the SD. The CI (combination index) was calculated by the combination index equation of Chou and Talalay. CI < 1, CI = 1, and CI > 1 indicate synergism, additive effect, and antagonism, respectively.

2.2.8. Structure-activity relationship studies of sHA 14-1

Although sHA 14-1 is a more stable analog of HA 14-1 and retains its beneficial properties, sHA 14-1 is 2 fold less potent than HA 14-1. Therefore, we moved on to perform a thorough SAR study of sHA 14-1 with an aim to improve its potency. The design of sHA 14-1 analogs began with substitutions at the 6-position of the chromene nucleus with various small to bulky groups of different lipophilicity. Specifically, hydrogen, bromo, *n*-propyl, and t-butyl phenyl substituents were explored at the 6-position affording analogs CXL002, CXL003, CXL004 and CXL005 respectively (Table 2.4). These analogs were synthesized from their corresponding salicylaldehydes as depicted in Scheme 2.3.

Scheme 2.3. Synthesis of analogs CXL002-CXL008

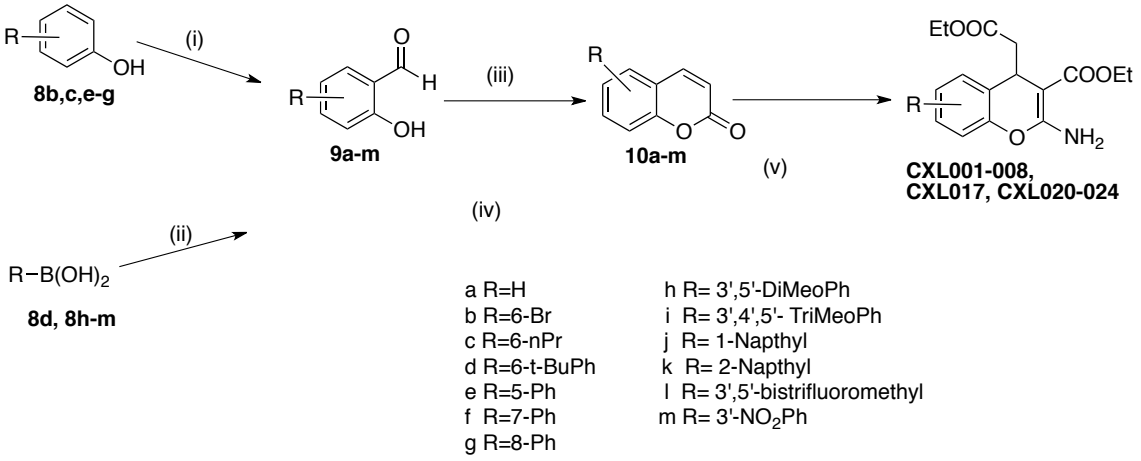

Reagents and condition: (i) $MgCl_2$, Et_3N, paraformaldehyde, anhydrous CH_3CN, reflux; (ii) 5-bromosalicylaldehyde, $Pd(OAc)_2$, K_2CO_3, H_2O, room temp; (ii) DMA, $POCl_3$ 60 ºC, 4-8 h; (iv) $NaHCO_3$, 60 ºC, 0.5 h; (v) ethyl cyanoacetate, EtOH, NaOEt, room temp.

A preliminary *in vitro* cytotoxicity evaluation indicated that the cytotoxicity of these analogs increased with increasing lipophilicity. However, the highly lipophilic and steric *t*-butyl phenyl analog (CXL005), was slightly less active compared to sHA 14-1 (Table 2.4). A possible reason for this observation could be unfavorable steric interactions with the binding site or decreased solubility. As the modifications at the 6-position did not improve the activity of sHA 14-1, we next explored the effect of varying the position of the phenyl ring on the chromene core (5, 7, and 8), providing analogs CXL006, CXL007, and CXL008 respectively (Table 2.4). These analogs were synthesized from their corresponding salicylaldehydes as depicted in Scheme 2.3. *In vitro* cytotoxicity evaluations showed that the phenyl substituent at position 5, 7, or 8 resulted in decreased cytotoxicity compared to sHA 14-1. Hence, the phenyl substituent at the 6-position was retained for further studies.

Table 2.4. IC_{50} values (μM) of sHA14-1 analogs with substitution at positions 5, 6, 7, and 8

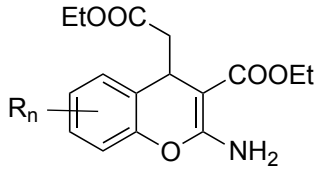

Compound	R_5	R_6	R_7	R_8	$IC_{50} \pm SEM$[a]	*CLogP*[b]
sHA 14-1 (CXL001)	H	Ph	H	H	27.2± 3.4	5.8
CXL002	H	H	H	H	91.43 ±	2.8
CXL003	H	Br	H	H	57.29 ±	4.9
CXL004	H	n-Pr	H	H	57.27 ±	5.5
CXL005	H	*t*-BuPh	H	H	35.51 ±	7.6
CXL006	Ph	H	H	H	44.3 ± 3.2	5.8
CXL007	H	H	Ph	H	51.6 ± 2.8	5.8
CXL008	H	H	H	Ph	49.8 ± 3.0	5.8

[a] Results are given as the mean of three independent experiments with triplicate in each experiment.
[b] The ClogP values mentioned in this table were calculated using the ChemBiodraw Ultra software.

The effect of altering functional groups on the other positions (namely 2, 3, and 4) on the chromene nucleus was next examined. The role of the 2-amino group was first explored by synthesis and evaluation of the monoacetylated and diacetylated analogs CXL009 and CXL010 respectively (Table 2.5). These analogs were synthesized from sHA 14-1 as depicted in Scheme 2.4. Replacement of one or both hydrogen atoms on the amino group led to a decrease in cytotoxicity compared to parent compound sHA 14-1.

Scheme 2.4. Synthesis of analogs CXL009 and CXL010

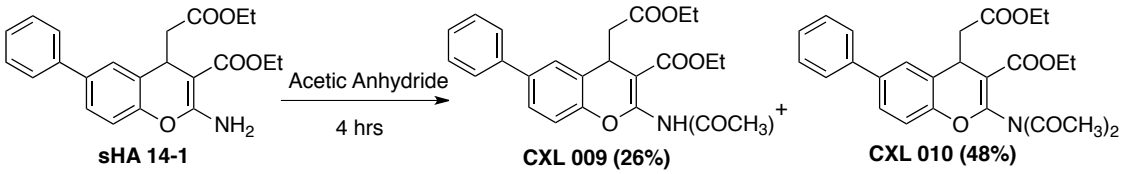

Subsequently, the effect of various electron withdrawing groups (EWG) at the 3-position was evaluated. This was done by first replacing the ethyl ester with a cyano functional group leading to analog CXL011 (Table 2.5). This analog was synthesized from the corresponding coumarin as depicted in Scheme 2.5. Biological evaluation indicated that CXL011 was less active than parent sHA 14-1. Replacement of the ethyl ester with an isopropyl ester at the 3 and 4-position also resulted in a slight decrease in cytotoxicity, demonstrated by analog CXL012 (Table 2.5). This analog was synthesized as depicted in Scheme 2.6. Further exploration of the influence of the ester functionality at the 4-position led to the synthesis of various amides such as piperidinyl, morpholinyl, piperazinyl, and diethylamino analogs (CXL013-016) (Table 2.5). These analogs were synthesized from their corresponding salicylaldehydes as depicted in Scheme 2.6. Unfortunately, all amide analogs exhibit decreased cytotoxicity compared to the parent sHA 14-1.

Scheme 2.5. Synthesis of CXL011

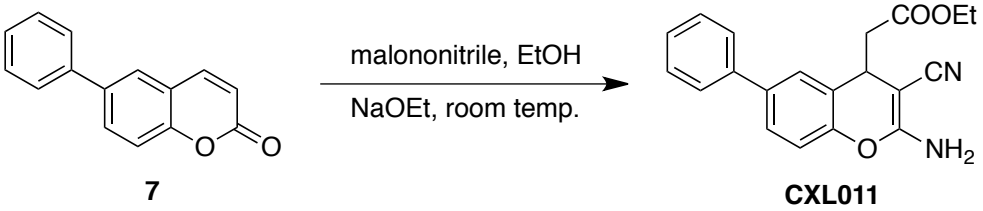

Table 2.5. IC_{50} values (μM) for analogs of sHA 14-1 with modification at position 3 and 4

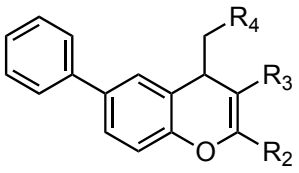

Compound	R_2	R_3	R_4	$IC_{50} \pm SEM$[a]
CXL009	$NH(COCH_3)$	H	H	67.7± 1.5
CXL010	$NH(COCH_3)_2$	H	H	70.6± 5.2
CXL011	NH_2	CN	OEt	52.5 ± 0.9
CXL012	NH_2	COOiPr	COOiPr	38.7 ± 4.1
CXL013	NH_2	COOEt	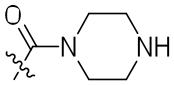	53.7 ± 1.1
CXL014	NH_2	COOEt	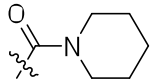	58.5 ± 2.6
CXL015	NH_2	COOEt	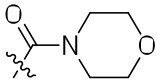	> 100
CXL016	NH_2	COOEt	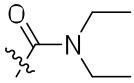	49.6 ± 0.3

[a] Results are given as the mean of three independent experiments with triplicate in each experiment.

Scheme 2.6. Synthesis of analogs (CXL012-CXL016)

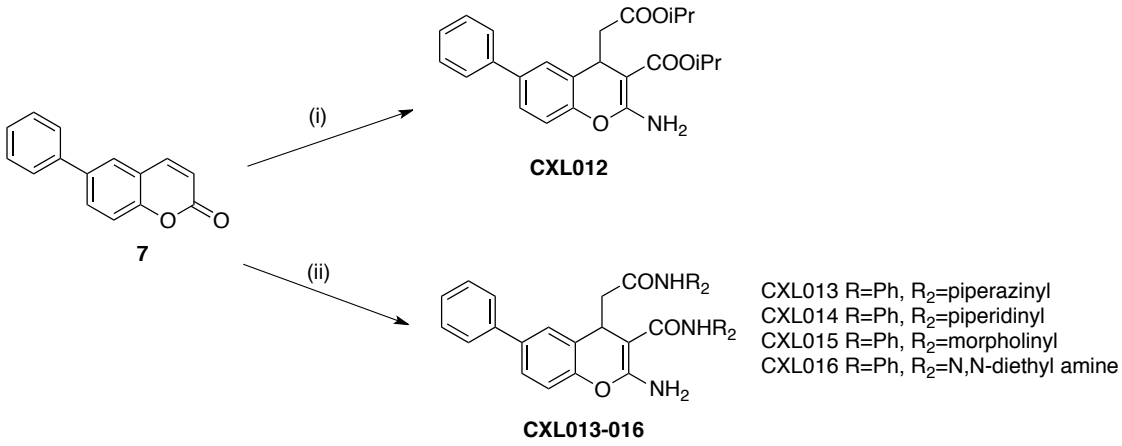

Reagents and conditions: (i) ethyl cyanoacetate, isopropanol, NaOiPr, room temp; (ii) ethyl cyanoacetate, benzene (C_6H_6)/dry ethanol, R_2H (base), room temp.

Having studied the various modifications on the chromene core structure with no improvement in activity of sHA 14-1, we sought to explore the SAR on the 6-phenyl ring. We started by substituting the 6-phenyl ring with 3′, 5′-dimethoxy substituent. This modification led to the development of (CXL017), which has low micromolar activity, ~27 times more cytotoxic than sHA 14-1 (Table 2.6). Demethylation of CXL017 to determine the effect of decreased hydrophobicity led to the synthesis of CXL018-019. These analogs were synthesized from CXL017 as depicted in Scheme 2.7. Conversion of a single methoxy group to hydroxyl group led to 4-fold decrease in cytotoxicity and replacing both methoxy groups with hydroxyl groups led to 16-fold decrease in cytotoxicity (Table 2.6). Subsequently, the 3′, 4′, 5′-trimethoxy analog was synthesized (CXL020). CXL020 showed a 14-fold decrease in activity compared CXL017 (Table 2.6), suggesting that the 4′-position of the 6-phenyl ring does not tolerate additional steric hindrance. To further confirm the effect of sterics at the 4-position of the phenyl ring, we

synthesized the 1-naphthyl and 2-naphthyl analogs CXL021 and CXL022 respectively. Biological evaluation of these compounds showed that CXL021 is 3-fold more cytotoxic than CXL022, supporting the notion that substitution at the 4-position of the 6-phenyl ring would result in decreased cytotoxicity, possibly due to steric effect, consistent with *t*-butylphenyl substitution in CXL005.

Finally, to determine the effect of electron withdrawing (EWG) substituent on the phenyl ring, we designed CXL023 with a trifluoromethyl group at the 3′ and the 5′ positions and CXL024 with a nitro group at the 3′position. Interestingly both CXL023 and CXL024 show a 4 to 7-fold decrease in activity in comparison to CXL017 suggesting that EWG on the phenyl ring lead to loss in activity. Analogs CXL017 and CXL020-024 were synthesized as shown in Scheme 2.3.

Scheme 2.7. Synthesis of analogs CXL018 and CXL019

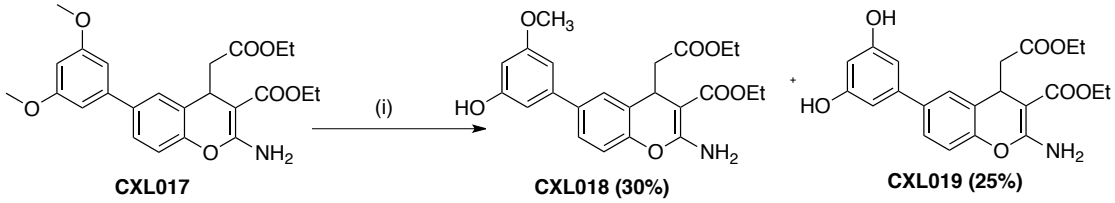

CXL017 CXL018 (30%) CXL019 (25%)

Reagent and conditions: (i) BBr_3 5eq, Dry CH_2Cl_2, 3Å molecular sieves, -78 °C-0 °C, 4 h.

Table 2.6. IC_{50} values of sHA 14-1 analogs with modification on the 6-phenyl ring

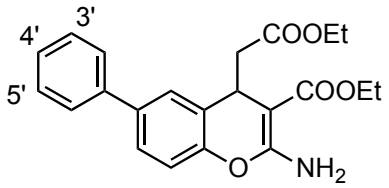

Compound	$R_{2'}$	$R_{3'}$	$R_{4'}$	$R_{5'}$	IC_{50} ± SEM[a]
CXL017	H	OCH_3	H	OCH_3	1.2 ± 0.1
CXL018	H	OH	H	OCH_3	4.2 ± 0.7
CXL019	H	OH	H	OH	18.3 ± 2.7
CXL020	H	OCH_3	OCH_3	OCH_3	13.6 ± 0.1
CXL021			H	H	5.83 ± 0.02
CXL022	H			H	18.7 ± 3.2
CXL023	H	CF_3	CF_3	H	7.1 ± 1.5
CXL024	H	NO_2	H	H	4.2 ± 1.1

[a] Results are given as the mean of three independent experiments with triplicate in each experiment.

2.3. Conclusion

HA 14-1, a small-molecule putative antagonist against anti-apoptotic Bcl-2 proteins, has been demonstrated to have great potential for cancer treatment. However, due to its instability in cell culture medium and decomposition-associated generation of ROS, it is not an appropriate candidate for future therapeutic evaluation and biological application. The current work describes the development of a stable analog of HA 14-1 –

sHA 14-1, its SAR, and mechanism of actions. In summary the current study demonstrated that sHA 14-1 is a stable analog of HA 14-1, as it is stable in cell culture medium for more than 24 h and does not generate ROS.[141] In addition, sHA 14-1 demonstrated selectivity towards drug resistant cancer cells endogenously or exogenously over expressing anti-apoptotic Bcl-2 family proteins. Finally sHA 14-1 could synergize with chemotherapeutic agents with varied mechanism of action.[141] These results taken together demonstrate that sHA 14-1 is a stable analog of HA 14-1 with beneficial properties similar to HA 14-1 and thus holds potential as a lead candidate for further optimization. Since, sHA 14-1 is 2-fold less potent than HA 14-1 in activity, we also performed SAR studies of sHA 14-1 to improve potency. SAR studies led to the discovery of CXL017, which is the most potent analog of this series with ~27 fold increased potency compared to sHA 14-1 and ~ 12-fold more than HA 14-1 in Jurkat cells. Thus, we have been able to develop a more potent stable analog of HA 14-1.

2.4. Experimental procedures

Chemistry: All commercial reagents and anhydrous solvents were purchased from vendors and were used without further purification or distillation, unless otherwise stated. Analytical thin layer chromatography was performed on Whatman® silica gel 60 Å with fluorescent indicator (partisil® K6F). Compounds were visualized by UV light and/or stained with potassium permanganate solution followed by heating. Flash column chromatography was performed on Whatman® silica gel 60 Å (230-400 mesh). NMR (^{1}H), (^{13}C) spectra were recorded on a Varian 300/400MHz or a Bruker 400MHz

spectrometer and calibrated using an internal reference. Electrospray ionization (ESI) mode mass spectra were recorded on a Bruker BiotofII mass spectrometer. All compounds synthesized are racemic mixtures and are more than 95% pure, analyzed using elemental analyses or HPLC. M-H-W Laboratories, Phoenix, AZ., performed the elemental analyses.

2.4.1. General procedure for the synthesis of the salicylaldehydes (6,9b,c,e-g)

The syntheses of the salicylaldehydes **(6,9b,c,e-g)** were carried out by formylation of the corresponding phenols using a procedure similar to that reported by Skattebol et al.[142] In brief, the 4-substituted phenol (1.6 mmol), anhydrous magnesium dichloride (2.4 mmol), dry triethylamine (6.1 mmol) were taken in dry acetonitrile (4 mL). To this dry paraformaldehyde (dried over P_2O_5) (11 mmol) was added and the reaction mixture was heated under reflux for 5-8 h. The reaction was monitored by TLC and upon consumption of the phenol, it was cooled and quenched by the addition of water. The reaction mass was then acidified using HCl (5.5 N) and extracted using ethyl acetate (3 x 30 mL). The extracts were combined, dried (anhydrous $MgSO_4$), and the solvent removed under reduced pressure to furnish an oil, which upon purification by flash chromatography afforded the pure salicylaldehyde (**6, 9b,c,e,-g,** 70-82%). Salicylaldehydes **(6,9b,c,e-g)** are known compounds with no characterization reported herein.

2.4.2. General procedure for the synthesis of salicylaldehydes (9d, 9h-m)

5-bromosalicylaldehyde (1 g, 4.97 mmol), K_2CO_3 (2.061 g, 14.91 mmol), boronic acid (0.9954 g, 5.47mmol), triphenylphosphine (TPP) (1 mol%) and $Pd(OAc)_2$ (1 mol%) were dissolved in DME:water (1:1) (12 ml). The mixture was stirred at room temperature

under an atmosphere of nitrogen for 24 h. The reaction mixture was acidified using HCl (1N) on an ice bath, followed by extraction with ethyl acetate. The organic extracts were combined, dried ($MgSO_4$), and the solvent was removed under vacuum. The crude solid was purified by flash chromatography (hexane:ethylacetate) to isolate the desired salicylaldehyde.

2.4.3. 2-hydroxy-5-(3', 5'-dimethoxyphenyl)benzaldehyde (9h)

Yield: (45%); ^{1}H NMR ($CDCl_3$): 11.01 (1H, s, OH), 9.98 (1H, s, CHO), 7.77-7.74 (2H, m, Ar Hs), 7.08 (1H, d, *J* = 9 Hz, Ar H), 6.67 (2H, d, *J* = 3 Hz, 2', 6'-H), 6.48-6.46 (1H, m, 4'-H), 3.86 (6H, s, 3', 5'-OCH_3). ^{13}C NMR (100 MHz, $CDCl_3$): 196.63, 161.27 161.15, 135.74, 133.23, 131.91, 120.62, 118.05, 105.01, 99.14, 55.45.

2.4.4. 2-hydroxy-5-(3', 4', 5'-trimethoxyphenyl)benzaldehyde (9i)

Yield: (38%); ^{1}H NMR ($CDCl_3$): δ 11.01 (1H, s, OH), 9.98 (1H, s, CHO), 7.74-7.70 (2H, m, Ar Hs), 7.08 (1H, d, *J* = 8.4 Hz, Ar H), 6.72 (2H, s, 2',6'-H), 3.94 (6H, s, 3',5'-OCH_3), 3.89 (3H, s, 4'-OCH_3). ^{13}C NMR (75 MHz, $CDCl_3$): 196.58, 160.95, 153.65, 137.77, 135.70, 135.36, 133.49, 131.73, 120.62, 118.11, 104.64, 104.05, 60.98, 56.27.

2.4.5. 2-hydroxy-5-(napthalen-1-yl)benzaldehyde (9j)

Yield: (40%); ^{1}H NMR ($CDCl_3$): δ 11.01 (1H, s, OH), 9.87 (1H, s, CHO), 8.2 (1H, d, *J* = 1.6Hz, 6H), 8.1- 8.02 (5H, m, Ar), 7.86 (1H, dd, *J* = 1.6, 8.4 Hz, 4H), 7.6 (2H, m, Ar), 7.14 (1H, d, *J* = 8.4 Hz, 3-H). ^{13}C NMR (100 MHz, $CDCl_3$): 196.63, 160.95, 138.69, 136.7, 135.2, 134.73, 133.86, 132.59, 128.48, 128.07, 127.02, 126.37, 125.99, 125.99, 125.40, 120.50, 117.65.

2.4.6. 2-hydroxy-5-(napthalen-2-yl)benzaldehyde (9k)

Yield: (52%); ^{1}H NMR ($CDCl_3$): δ 11.05 (1H, s, OH), 10.03 (1H, s, CHO), 8.0 (1H, d, *J* = 1.6 Hz, 6-H), 7.94-7.86 (5H, m, Ar), 7.71 (1H, dd, *J* = 1.6, 8.4 Hz, 4-H), 7.55-7.48 (2H, m, Ar), 7.13 (1H, d, *J* = 8.4 Hz, 3-H). ^{13}C NMR (100 MHz, $CDCl_3$): 196.73, 160.82, 136.61, 136, 133.64, 133.24, 132.54, 132.14, 128.76, 128.07, 127.69, 126.57, 126.13, 125.23, 124.88, 120.77, 118.27. ESI-MS (positive) m/z 271.28 $(M+Na)^+$

2.4.7. 4-hydroxy-3', 5'-bis(trifluoromethyl)biphenyl-3-carbaldehyde (9l)

Yield: 60 %. ^{1}H NMR ($CDCl_3$): δ 11.13 (1H, s), 10.03 (1H, s), 7.98 (2H, s), 7.87 (1H, s), 7.82-7.79 (2H, m), 7.16 (1H, d, *J*=8.4 Hz). ^{13}C NMR (75 MHz, $CDCl_3$): δ 196.28, 162.09, 141.46, 135.47, 132.59, 132.26, 132.14, 130.18, 126.64, 126.6, 124.6, 121.88, 121.05, 120.96, 120.86, 118.96.

2.4.8. 4-Hydroxy-3'-nitro-[1,1'-biphenyl]-3-carbaldehyde (9m)

Yield: 51 %. ^{1}H NMR ($CDCl_3$): δ 11.11 (1H, s), 10.02 (1H, s), 8.434-8.425 (1H, m), 8.23-8.20 (1H, m), 7.90-7.88 (1H, m), 7.84-7.80 (2H, m), 7.64 (1H, m) 7.15 (1H, d, *J*=8.4 Hz). ^{13}C NMR (75 MHz, $CDCl_3$): δ 196.34, 162.16, 147.08, 140.64, 135.64, 132.35, 130.73, 127.32, 127.19, 124.38, 124.22, 120.84, 118.83.

2.4.9. General procedure for the synthesis of coumarin

To *N*,*N*-dimethylacetamide (1.98 mmol) stirred at 0 °C, phosphorus oxychloride (1.98 mmol) was added slowly. The reaction mixture was allowed to stir at 0 °C for 30 min followed by addition of the corresponding salicylaldehyde (0.99 mmol). The reaction mass was then heated at 68-70 °C for 3 h. Following this, the reaction mass was cooled to room temperature and saturated $NaHCO_3$ solution (10 mL) was added to it. The reaction mass was heated at 68-70 °C for another 30 min, cooled, and acidified (1 N HCl)

followed by extraction with methylene chloride. The extracts were combined, dried (anhydrous $MgSO_4$) and concentrated under reduced pressure to afford a residue, which upon column chromatography afforded the desired coumarin.

2.4.10. 6-phenyl-2*H*-chromen-2-one (7)

Synthesized from 5-phenyl salicylaldehyde. Yield (62 %) TLC (ethyl acetate/hexane = 1:4), Rf 0.38. MP: 120-122 °C, 118 °C (literature). ^{1}H NMR (300 MHz, $CDCl_3$): δ 7.77 (1H, d, *J* = 9.6 Hz), 7.76 (1H, dd, *J* = 2.1, 9.0 Hz), 7.67 (1H, d, *J* = 2.4 Hz), 7.58 (2H, m), 7.45 (4H, m), 6.43 (1H, d, *J* = 9.6 Hz, C=CHCO). ^{13}C NMR (75 MHz, $CDCl_3$): δ 160.94, 153.67, 143.72, 139.64, 138.08, 131.01, 129.27, 128.04, 127.29, 126.30, 119.28, 117.53, 117.30.

2.4.11. 2*H*-chromen-2-one (10a)

Synthesized from salicylaldehyde. Yield: (58%). TLC (ethyl acetate/hexane = 1:4), Rf 0.39. MP: 68-70 °C (observed). 68-69 °C (literature). ^{1}H NMR (300 MHz, $CDCl_3$): δ 7.63 (3H, m), 7.23 (1H, d, *J* = 9.0 Hz), 6.47 (1H, d, *J* = 9.9 Hz, C=CHCO). ^{13}C NMR (75 MHz, $CDCl_3$): δ 160.21 (C=O), 153.16, 142.34, 134.84, 130.41, 120.56, 118.89, 118.11, 117.23.

2.4.12. 6-Bromo-2*H*-chromen-2-one (10b)

Synthesized from 5-bromosalicylaldehyde. Yield (56 %). TLC (ethyl acetate/hexane = 1:4), Rf 0.56. MP: 160-162 °C (observed), 161-163 °C (literature). ^{1}H NMR (300 MHz, $CDCl_3$): δ 7.63 (3H, m), 7.22 (1H, d, *J* = 9.6 Hz, 8- H), 6.89 (1H, d, *J* = 9.6 Hz, C=CHCO). ^{13}C NMR (75 MHz, $CDCl_3$): δ 160.16, 153.16, 142.31, 134.82, 130.40, 120.56, 118.87, 118.11, 117.21.

2.4.13. 6-n-propyl-2*H*-chromen-2-one (10c)

Synthesized from 5-n-propyl salicylaldehyde. Yield: (54%) TLC (ethyl acetate/hexane = 1:4), Rf 0.35. ^{1}H NMR (300 MHz, $CDCl_3$): 7.68 (1H, d, *J* = 9.3 Hz, CH=CH), 7.35 (1H, dd, *J* = 2.1, 8.5 Hz), 7.25 (2H, m), 6.41 (1H, d, *J* = 9.3 Hz, C=CHCO), 2.64 (2H, t, *J* = 7.3 Hz, $CH_2CH_2CH_3$), 1.67 (2H, m, $CH_2CH_2CH_3$), 0.96 (3H, t, *J* = 7.3 Hz, $CH_2CH_2CH_3$).

2.4.14. 6-t-butylphenyl-2*H*-chromen-2-one (10d)

Synthesized from 5-t-butylphenyl salicylaldehyde. Yield (57 %). TLC (ethyl acetate/hexane = 1:4), Rf 0.38. MP: 148-150 °C. ^{1}H NMR (300 MHz $CDCl_3$): δ 7.63 (3H, m), 7.23 (1H, d, *J* = 9.0 Hz), 6.47 (1H, d, *J* = 9.9 Hz, C=CHCO). ^{13}C NMR (75 MHz, $CDCl_3$): δ 161.03, 153.51, 151.19, 143.80, 137.92, 136.70, 130.89, 126.93, 126.23, 126.06, 119.26, 117.46, 117.20, 34.84, 31.56.

2.4.15. 5-phenyl-2*H*-chromen-2-one (10e)

Synthesized from 6-phenyl. Yield (64 %). TLC (ethyl acetate/hexane = 1:2), Rf 0.47. ^{1}H NMR (300 MHz, $CDCl_3$): δ 7.76 (2H, m), 7.68 (1H, s, *J* = 2.1 Hz), 7.59 (2H, m), 7.48 (2H, m), 7.41 (2H, m), 6.48 (1H, d, *J* = 9.3 Hz, C=CHCO). ^{13}C NMR (75 MHz, $CDCl_3$): δ 160.98, 153.66, 143.74, 139.63, 139.08, 131.01, 129.27, 128.04, 127.29, 126.30, 119.28, 117.52, 117.29.

2.4.16. 7-phenyl-2*H*-chromen-2-one (10f)

Synthesized from 4-phenyl salicylaldehyde. Yield (62 %). TLC (ethyl acetate/hexane = 1:4), Rf 0.28. MP: 191-193 °C, 189-190 °C (literature). ^{1}H NMR (300 MHz, $CDCl_3$): δ 7.74 (1H, d, *J* = 9.6 Hz), 7.63 (2H, m), 7.55 (3H, m), 7.47 (3H, m), 6.43

(1H, d, *J* = 9.6 Hz, C=CHCO). ^{13}C NMR (75 MHz, $CDCl_3$): δ 161.14, 154.74, 145.32, 143.35, 139.42, 129.35, 128.80, 128.38, 127.49, 123.60, 118.03, 116.59, 115.34.

2.4.17. 8-phenyl-2*H*-chromen-2-one (10g)

Synthesized from 3-phenyl salicylaldehyde. Yield (65 %). TLC (ethyl acetate/hexane = 1:4), Rf 0.22. MP: 138-140 °C. ^{1}H NMR (300 MHz, $CDCl_3$): δ 7.76 (1H, d, *J* = 9.9 Hz), 7.57 (3H, m), 7.48 (3H, m), 7.39 (2H, m), 6.45 (1H, d, *J* = 9.3 Hz, C=CHCO). ^{13}C NMR (75 MHz, $CDCl_3$): δ 160.76, 151.08, 144.08, 135.81, 133.36, 130.56, 129.76, 128.73, 128.25, 127.45, 124.64, 119.49, 116.88.

2.4.18. 6-(3',5'-dimethoxyphenyl)-2*H*-chromen-2-one (10h)

Yield (53%); ^{1}H NMR ($CDCl_3$): δ 7.77-7.65 (3H, m, Ar), 7.41 (1H, d, *J* = 9 Hz, 8-H), 6.69 (2H, m, Ar), 6.49 (2H, m), 3.85 (6H, s, 3',5'-OCH_3). ^{13}C NMR (75 MHz, $CDCl_3$): 161.26, 160.65, 155.49, 153.57, 143.42, 141.56, 137.77, 130.76, 126.11, 118.96, 117.21, 117.07, 105.47, 99.48, 55.47.

2.4.19. 6-(3', 4' ,5'-trimethoxyphenyl)-2*H*-chromen-2-one (10i)

Yield (50%); ^{1}H NMR ($CDCl_3$): δ 7.77 (2H, d, *J* = 9.6 Hz, 2',6'-H), 7.73 (1H, dd, *J* = 2.4, 8.4 Hz, 7-H), 7.63 (1H, d, *J* = 2.2Hz, 5-H), 7.41 (1H, d, *J* = 8.7 Hz, 8-H), 6.75 (1H, m), 6.49 (1H, d, *J* = 9.6 Hz, CHCO), 3.94 (6H, s, 3',5'-OCH_3), 3.90 (3H, s, 4'-OCH_3). ^{13}C NMR (75 MHz, $CDCl_3$): 160.05, 153.8, 153.61, 143.62, 138.22, 135.61, 130.95, 126.18, 119.22, 117.48, 117.39, 109.99, 61.24, 56.51.

2.4.20. 6-(naphthalene-1-yl)-2*H*-chromene-2-one (10j)

Yield: (55%); ^{1}H NMR ($CDCl_3$): δ 7.94-7.89 (2H, m, Ar),7.82 (1H, *J* = 8.4 Hz, Ar), 7.75 (1H, *J* = 9.6 Hz, 4-H), 7.66 (1H, *J* = 8.4 Hz, Ar), 7.59-7.41 (6H, m, Ar), 6.50

(1H, *J* = 9.6 Hz, CHCO). ^{13}C NMR (100 MHz, $CDCl_3$): 160.76, 153.38, 143.43, 138.19, 137.23, 133.81, 133.63, 131.45, 128.95, 128.48, 128.29, 127.17, 126.45, 126.16, 126.05, 125.39, 118.77, 117.07, 116.79.

2.4.21. 6-(naphthalene-2-yl)-2*H*-chromene-2-one (10k)

Yield: (63.8%); ^{1}H NMR ($CDCl_3$): δ 8.04 (1H, d, *J* = 1.6 Hz, 5-H), 7.97-7.94 (1H, d, J = 8.8 Hz, 4H), 7.93-7.88 (3H, m, Ar), 7.83-7.80 (2H, m, Ar), 7.72 (1H, dd, *J* = 1.6, 8.4 Hz, 7-H), 7.55-7.51 (2H, m ,Ar), 7.45 (1H, d, *J* = 8.4Hz, 8-H), 6.49 (1H, d, *J* = 9.6Hz, CHCO). ^{13}C NMR (100 MHz, $CDCl_3$): 206.89, 160.65, 153.48, 143.51, 136.67, 133.58, 132.72, 131.00, 128.82, 128.16, 127.71, 126.64, 126.35, 126.31, 125.92, 125.12. 119.13, 117.40, 117.11.

2.4.22. 6-(3,5-bis(trifluoromethyl)phenyl)-2H-chromen-2-one (10l)

Yield: 65 %. ^{1}H NMR ($CDCl_3$): δ 8.01 (2H, s), 7.89 (1H, s), 7.81-7.76 (2H, m), 7.73 (1H, d, *J*=2.4 Hz), 7.49 (1H, d, *J*=8.8 Hz), 6.53 (1H, d, *J*=9.6 Hz). ^{13}C NMR (75 MHz, $CDCl_3$): δ 160.08, 154.33, 142.86, 141.53, 134.71, 132.64, 132.30, 130.57, 127.14, 127.10, 126.45, 124.55, 121.47, 121.40, 119.42, 117.94, 117.82.

2.4.23. 6-(3-Nitrophenyl)-2H-chromen-2-one (10m)

Yield: 72 %. ^{1}H NMR ($CDCl_3$): δ 8.46 (1H,s), 8.27-8.24 (1H, m), 7.93-7.91 (1H, m), 7.81-7.78 (2H,m), 7.737 (1H, d, *J*=2 Hz), 7.66 (1H,t, *J*=8 Hz), 7.48 (1H, d, *J*=8.4 Hz), 6.53 (1H, d, *J*=9.2 Hz). ^{13}C NMR (75 MHz, $CDCl_3$): δ 160.23, 154.15, 142.99, 141.07, 135.21, 132.86, 130.55, 130.06, 126.33, 122.55, 121.88, 119.35, 117.82, 117.68.

2.4.24. General procedure for the synthesis of substituted Ethyl-4*H*-chromene-3-carboxylate compounds (CXL001-008, CXL017, CXL020, CXL021-CXL024)

Freshly cut sodium (0.096 mmol) was added to anhydrous ethanol (2 mL) followed by the addition of ethyl cyanoacetate (0.192 mmol). The reaction mixture was stirred at room temperature under an inert atmosphere for 30 min, followed by the addition of a solution of the corresponding coumarin (0.08 mmol) in anhydrous ethanol (1 mL). The resulting reaction mixture was stirred at room temperature. Upon consumption of the coumarin, the reaction mass was concentrated, diluted with water (30 mL) and extracted using methylene chloride (3 x 20 mL). The organics were combined, dried ($MgSO_4$) and the solvent removed under vacuum, to afford an oil. This crude oil was subjected to column chromatography to afford the pure product. Compounds CXL006-012 and CXL015 were prepared by Dr. Jignesh Doshi.

2.4.25. Ethyl 2-amino-4-(2-ethoxy-2-oxoethyl)-6-phenyl-4*H*-chromene-3-carboxylate (sHA 14-1, CXL001)

Yield: (53%); ^{1}H NMR ($CDCl_3$): δ 7.44 (7H, m, Ar), 7.03 (1H, d, *J* = 8.4 Hz, 8-H), 6.32 (2H, br s, NH_2), 4.36 (1H, dd, *J* = 4.5, 6.9 Hz, 4-H), 4.24 (2H, q, *J* = 7.2 Hz, $COOCH_2CH_3$), 4.02 (2H, q, *J* = 7.2 Hz, $COOCH_2CH_3$), 2.70 (1H, dd, *J* = 4.8, 15.0 Hz, HCHCO), 2.62 (1H, dd, *J* = 6.9, 15.0 Hz, HCHCO), 1.34 (3H, t, *J* = 6.9 Hz, $COOCH_2CH_3$), 1.12 (3H, t, *J* = 7.2 Hz, $COOCH_2CH_3$). ^{13}C NMR (75 MHz, $CDCl_3$): 171.88, 169.21, 161.61, 149.58, 140.43, 137.61, 128.92, 127.31, 127.19, 126.99, 126.52, 126.03, 116.276, 60.36, 59.69, 43.79, 31.48, 14.74, 14.21. HRMS-ESI (positive) calcd

for ($C_{22}H_{23}NO_5$ + Na)$^+$ 404.1468; found 404.08 (M+Na)$^+$. Anal. ($C_{22}H_{23}NO_5$) C, H, N. calcd C, 69.28; H, 6.08; N, 3.67. found C, 69.86; H, 6.24; N, 3.44.

2.4.26. Ethyl 2-amino-4-(2-ethoxy-2-oxoethyl)-4*H*-chromene-3-carboxylate (CXL002)

Yield (54%); ^{1}H NMR ($CDCl_3$): δ 7.21 (2H, m, Ar), 7.07 (1H, dt, *J* = 1.5, 7.5, 8.7 Hz, Ar H), 6.96 (1H, dd, *J* = 1.2, 8.1 Hz) 6.34 (2H, br s, NH_2), 4.29 (1H, dd, *J* = 4.8, 7.5 Hz, 4-H), 4.22 (2H, q, *J* = 6.9 Hz, $COOCH_2CH_3$), 4.03 (2H, q, *J* = 7.2 Hz, $COOCH_2CH_3$), 2.64 (1H, dd, *J* = 4.8, 15.0 Hz, HCHCO), 2.57 (1H, dd, *J* = 7.2, 14.7 Hz, HCHCO), 1.32 (3H, t, *J* = 7.2 Hz, $COOCH_2CH_3$), 1.15 (3H, t, *J* = 7.2 Hz, $COOCH_2CH_3$). ^{13}C NMR (75 MHz, $CDCl_3$): 171.69, 169.03, 161.38, 149.29, 131.38, 130.84, 128.03, 117.78, 116.87, 76.51, 60.59, 59.87, 43.56, 31.31, 14.79, 14.35. HRMS-ESI (positive) alcd for ($C_{16}H_{19}NO_5$ + Na)$^+$: 328.1155; found 328.1128 (M+Na)$^+$. Anal. ($C_{16}H_{19}NO_5$) C, H, N calcd C, 62.94; H, 6.27; N, 4.59 found C, 62.94; H 6.19; N, 4.52.

2.4.27. Ethyl 2-amino-6-bromo-4-(2-ethoxy-2-oxoethyl)-4*H*-chromene-3-carboxylate (CXL003)

Yield:(52 %); ^{1}H NMR ($CDCl_3$): δ 7.38 (1H, d, *J* = 2.4 Hz, 5-H), 7.29 (1H, dd, *J* = 2.4, 8.4 Hz, 7-H), 6.84 (1H, d, *J* = 9.0 Hz, 8-H), 6.30 (2H, br s, NH_2), 4.22 (3H, m, 4-H and $COOCH_2CH_3$), 4.05 (2H, q, *J* = 7.2 Hz, $COOCH_2CH_3$), 2.64 (1H, dd, *J* = 4.8, 15 Hz, HCHCO), 2.57 (1H, dd, *J* = 6.9, 15 Hz, HCHCO), 1.31 (3H, t, *J* = 7.2 Hz, $COOCH_2CH_3$), 1.18 (3H, t, *J* = 7.2 Hz, $COOCH_2CH_3$). ^{13}C NMR ($CDCl_3$): 171.69, 169.03, 161.38, 149.29, 131.38, 130.84, 128.03, 117.78, 116.87, 76.51, 60.59, 59.87, 43.56, 31.31, 14.79, 14.35. HRMS-ESI (positive) calcd for ($C_{16}H_{18}BrNO_5$ + Na^+):

406.0261; found, 406.0266 $(M+Na)^+$. Anal. ($C_{16}H_{18}BrNO_5$) C, H, N; calcd C, 50.02; H, 4.72; N, 3.65; found C, 50.54; H, 5.06; N, 3.64.

2.4.28. Ethyl 2-amino-4-(2-ethoxy-2-oxoethyl)-6-propyl-4*H*-chromene-3-carboxylate (CXL004)

Yield (53%); ^{1}H NMR ($CDCl_3$): δ 7.03 (1H, d, *J* = 1.8Hz, 5-H), 6.98 (1H, dd, *J* = 2.1Hz, 8.4Hz, 7-H), 6.86 (1H, d, *J* = 8.4Hz, 8-H), 6.28 (2H, br s, NH_2), 4.23 (3H, m, 4-H, $COOCH_2CH_3$), 4.02 (2H, q, *J* = 6.9 Hz, $COOCH_2CH_3$), 2.63 (1H, *J* = 14.7Hz, 7.5Hz, CH_2), 2.54 (1H, *J* = 14.7Hz, 7.5Hz, CH_2), 2.51 (2H, t, *J* = 7.5 Hz, $CH_2CH_2CH_3$), 1.586 (2H, m, $CH_2CH_2CH_3$), 1.32 (3H, t, *J* = 6.9 Hz, $COOCH_2CH_3$), 1.156 (3H, t, *J* = 6.9 Hz, $COOCH_2CH_3$), 0.904 (3H, t, *J* = 7.2 Hz, $CH_2CH_2CH_3$). ^{13}C NMR (75 MHz, $CDCl_3$): 171.96, 169.25, 161.83, 148.13, 138.84, 128.25, 127.75, 125.35, 115.58, 76.94. 60.26, 59.57, 43.90, 37.45, 31.44, 24.73, 14.72, 14.22, 13.81. HRMS-ESI (positive) calcd for $(C_{19}H_{25}NO_5 + Na)^+$ 370.1632; Found 370.1652 $(M+Na)^+$. Anal. ($C_{19}H_{25}NO_5$) C, H, N. calcd C, 65.69; H, 7.25; N, 4.03; found C, 65.23; H, 7.11; N, 3.90.

2.4.29. Ethyl 2-amino-6-(4-tert-butylphenyl)-4-(2-ethoxy-2-oxoethyl)-4*H*-chromene-3-carboxylate (CXL005)

Yield: (56%); ^{1}H NMR ($CDCl_3$): δ 7.45 (6H, m, Ar), 7.01 (1H, d, *J* = 8.7 Hz, 8-H), 6.34 (2H, br s, NH_2), 4.35 (1H, dd, *J* = 4.5, 6.6 Hz, 4-H), 4.24 (2H, q, *J* = 7.2 Hz, $COOCH_2CH_3$), 4.02 (2H, q, *J* = 7.2 Hz, $COOCH_2CH_3$), 2.69 (1H, dd, *J* = 5.1, 15.0 Hz, HCHCO), 2.62 (1H, dd, *J* = 6.6, 15.0 Hz, HCHCO), 1.33 (12H, m, $C(CH_3)_3$ and $COOCH_2CH_3$), 1.13 (3H, t, *J* = 7.2 Hz, $COOCH_2CH_3$). ^{13}C NMR (75 MHz, $CDCl_3$):171.88, 169.23, 161.63, 150.32, 149.38, 137.50, 137.43, 126.98, 126.60, 126.35,

125.94, 125.87, 116.19, 76.82, 60.33, 59.66, 43.77, 35.08, 34.66, 31.49, 14.74, 14.21. HRMS-ESI (positive) calcd for $(C_{26}H_{31}NO_5 + Na)^+$ 460.2120; found 460.2106 $(M+Na)^+$. Anal. ($C_{26}H_{31}NO_5$) C, H, N. calcd C, 71.37; H, 7.14; N, 3.2; found C, 69.72; H, 7.16; N, 3.12.

2.4.30. Ethyl 2-amino-4-(2-ethoxy-2-oxoethyl)-5-phenyl-4*H*-chromene-3-carboxylate (CXL006)

Yield: (51%); ^{1}H NMR ($CDCl_3$); δ 7.44 (7H, m, Ar), 7.03 (1H, d, *J* = 8.4 Hz, 8-H), 6.32 (2H, br s, NH_2), 4.36 (1H, dd, *J* = 4.5, 6.9 Hz, 4-H), 4.23 (2H, q, *J* = 7.2 Hz, $COOCH_2CH_3$), 4.02 (2H, q, *J* = 7.2 Hz, $COOCH_2CH_3$), 2.69 (1H, dd, *J* = 4.5, 14.7 Hz, HCHCO), 2.62 (1H, dd, *J* = 6.9, 14.7 Hz, HCHCO), 1.33 (3H, t, *J* = 6.9 Hz, $COOCH_2CH_3$), 1.12 (3H, t, *J* = 7.2 Hz, $COOCH_2CH_3$). ^{13}C NMR (75 MHz, $CDCl_3$):171.98, 169.29, 161.71, 149.68, 140.53, 137.71, 129.01, 127.40, 127.28, 127.08, 126.60, 126.14, 116.36, 76.95, 60.44, 59.77, 43.90, 31.59, 14.82, 14.29. HRMS-ESI (positive) calcd for $(C_{22}H_{23}NO_5 + Na)^+$ 404.1468; found 404.1464 $(M+Na)^+$. Anal. ($C_{22}H_{23}NO_5$) C, H, N; calcd C, 69.28; H, 6.08; N, 3.67; found C, 68.88; H, 6.05; N, 3.41.

2.4.31. Ethyl 2-amino-4-(2-ethoxy-2-oxoethyl)-7-phenyl-4*H*-chromene-3-carboxylate (CXL007)

Yield: (56%); ^{1}H NMR ($CDCl_3$): δ 7.41 (6H, m, Ar), 7.21 (1H, s, Ar), 7.15 (1H, s, Ar), 6.28 (2H, br s, NH_2), 4.28 (1H, dd, *J* = 4.5, 7.2 Hz, 4-H), 4.19 (2H, q, *J* = 6.9 Hz, $COOCH_2CH_3$), 4.00 (2H, q, *J* = 6.9 Hz, $COOCH_2CH_3$), 2.64 (1H, dd, *J* = 4.5, 15 Hz, HCHCO), 2.56 (1H, dd, *J* = 6.9, 15 Hz, HCHCO), 1.28 (3H, t, *J* = 7.2 Hz, $COOCH_2CH_3$), 1.12 (3H, t, *J* = 7.2 Hz, $COOCH_2CH_3$). ^{13}C NMR (75 MHz, $CDCl_3$):

172.03, 169.29, 161.74, 150.46, 141.93, 140.25, 129.05, 128.97, 127.82, 127.19, 124.77, 123.32, 114.52, 76.99, 60.45, 59.77, 43.84, 31.20, 14.83, 14.33. HRMS-ESI (positive) calcd for $(C_{22}H_{23}NO_5 + Na)^+$ 404.1468; found 404.1452 $(M+Na)^+$. Anal. ($C_{22}H_{23}NO_5$) C, H, N; calcd C, 69.28; H, 6.08; N, 3.67; found C, 70.00; H, 6.25; N, 3.62.

2.4.32. Ethyl 2-amino-4-(2-ethoxy-2-oxoethyl)-8-phenyl-4*H*-chromene-3-carboxylate (CXL008)

Yield: (54%); ^{1}H NMR ($CDCl_3$): δ 7.44 (5H, m, Ar), 7.22 (2H, m, Ar), 7.15 (1H, t, *J* = 7.2 Hz, Ar), 6.22 (2H, br s, NH_2), 4.36 (1H, dd, *J* = 4.8, 7.5 Hz, 4-H), 4.23 (2H, q, *J* = 7.5 Hz, $COOCH_2CH_3$), 4.06 (2H, q, *J* = 7.5 Hz, $COOCH_2CH_3$), 2.67 (1H, dd, *J* = 4.2, 14.7 Hz, HCHCO), 2.58 (1H, dd, *J* = 7.5, 14.7 Hz, HCHCO), 1.33 (3H, t, *J* = 7.2 Hz, $COOCH_2CH_3$), 1.17 (3H, t, *J* = 7.2 Hz, $COOCH_2CH_3$). ^{13}C NMR (75 MHz, $CDCl_3$): 171.98, 169.16, 161.72, 146.93, 137.42, 129.74, 129.41, 128.38, 128.01, 127.56, 126.53, 124.51, 77.21, 60.44, 59.74, 44.07, 31.87, 14.82, 14.35. HRMS-ESI (positive) calcd for $(C_{22}H_{23}NO_5 + Na)^+$ 404.1468; found 404.1471 $(M+Na)^+$. Anal. ($C_{22}H_{23}NO_5$) C, H, N; calcd C, 69.28; H, 6.08; N, 3.67; found C, 68.80; H, 6.64; N, 3.56.

2.4.33. Ethyl 2-acetamido-4-(2-ethoxy-2-oxoethyl)-6-phenyl-4*H*-chromene-3-carboxylate (CXL009)

sHA 14-1 (0.030 g, 0.078 mmol) was taken in acetic anhydride (2 mL). The resultant reaction mixture was heated under reflux for 8 h. Following this, the acetic anhydride was removed under reduced pressure. The crude residue was diluted with water and extracted with methylene chloride. The organics were combined, dried (anhydrous $MgSO_4$) and solvent removed under vacuum to afford an oily liquid. This was

subjected to column chromatography to afford **CXL009** as colorless oil. Yield (26 %). Also obtained was **CXL010** as colorless oil. Yield (48%); ^{1}H NMR ($CDCl_3$): δ 10.98 (1H, s, N-H), 7.45 (7H, m, Ar), 7.20 (1H, d, *J* = 8.1 Hz, 8-H), 4.44 (1H, dd, *J* = 5.1, 7.2 Hz, 4-H), 4.28 (2H, q, *J* = 7.2 Hz, $COOCH_2CH_3$), 4.03 (2H, q, *J* = 6.9 Hz, $COOCH_2CH_3$), 2.79 (1H, dd, *J* = 5.4, 15.3 Hz, HCHCO), 2.71 (1H, dd, *J* = 7.2, 15.3 Hz, HCHCO), 2.30 (3H, s, $NHCOCH_3$) 1.35 (3H, t, *J* = 7.2 Hz, $COOCH_2CH_3$), 1.12 (3H, t, *J* = 7.2 Hz, $COOCH_2CH_3$). ^{13}C NMR (75 MHz, $CDCl_3$): 171.45, 168.60, 168.24, 155.84, 149.33, 140.26, 138.71, 129.08, 127.62, 127.12, 127.09, 124.93, 117.14, 85.69, 61.10, 60.75, 43.71, 31.61, 25.89, 14.57, 14.29. HRMS-ESI (positive) calcd for $(C_{24}H_{25}NO_6 + Na)^+$ 446.1574; found 446.1597. Anal. ($C_{24}H_{25}NO_6.0.5C_6H_{14}$) C, H, N; calcd C, 69.62; H, 6.41; N, 2.73. found C, 69.62; H, 6.51; N, 2.87.

2.4.34. Ethyl 2-(N-acetylacetamido)-4-(2-ethoxy-2-oxoethyl)-6-phenyl-4*H*-chromene-3-carboxylate (CXL010)

Yield: (48%); ^{1}H NMR ($CDCl_3$); δ 7.45 (7H, m, Ar), 7.10 (1H, d, *J* = 2.7 Hz, 8-H), 4.58 (1H, dd, *J* = 5.4, 6.6 Hz, 4-H), 4.22 (2H, q, *J* = 7.2 Hz, $COOCH_2CH_3$), 4.05 (2H, q, *J* = 7.5 Hz, $COOCH_2CH_3$), 2.79 (1H, dd, *J* = 5.4, 15.3 Hz, HCHCO), 2.71 (1H, dd, *J* = 6.9, 15.0 Hz, HCHCO), 2.49 (3H, s, $N(COCH_3)$, 2.39 (3H, s, $N(COCH_3)$, 1.29 (3H, t, *J* = 7.2 Hz, $COOCH_2CH_3$), 1.14 (3H, t, *J* = 7.2 Hz, $COOCH_2CH_3$). ^{13}C NMR (75 MHz, $CDCl_3$):171.56, 171.42, 171.13, 164.48, 151.44, 150.31, 140.23, 139.09, 129.12, 127.70, 127.37, 127.15, 124.00, 116.87, 107.17, 77.28, 61.65, 60.93, 42.52, 33.92, 26.07, 25.75, 14.38, 14.29. HRMS-ESI (positive) calcd for $(C_{26}H_{27}NO_7 + Na)^+$ 488.168; found

488.1713. Anal. ($C_{26}H_{27}NO_7.0.5C_6H_{14}$) C, H, N; calcd C, 68.50; H, 6.74; N, 2.75; found C, 68.50; H, 6.17; N, 2.61.

2.4.35. Ethyl 2-(2-amino-3-cyano-6-phenyl-4*H*-chromen-4-yl)acetate (CXL011)

Freshly cut sodium (0.096 mmol) was taken in anhydrous ethanol (2 mL) followed by the addition of malononitrile (0.192 mmol) in anhydrous ethanol (0.5 mL). The reaction mixture was stirred at room temperature under an inert atmosphere for 30 min, followed by the addition of a solution of 6-phenylcoumarin (0.08 mmol) in ethanol (1 mL). The resulting reaction mixture was stirred at room temperature. Upon consumption of the 6-phenylcoumarin, the reaction mass was concentrated, diluted with water (30 mL) and extracted using methylene chloride (3 x 20 mL). The organics were combined, dried (anhydrous $MgSO_{4)}$ and the solvent removed under vacuum, to afford an oily liquid. This crude oil was subjected to column chromatography to afford the pure product as a cream solid. Yield (52 %); ^{1}H NMR ($CDCl_3$): δ 7.43 (7H, m, Ar), 7.04 (1H, d, J = 8.4 Hz, 8-H), 4.72 (2H, br s, NH_2), 4.12 (3H, m, 4-H and $COOCH_2CH_3$), 2.78 (1H, dd, J = 5.7, 15.3 Hz, HCHCO), 2.71 (1H, dd, J = 6, 15.6 Hz, HCHCO), 1.20 (3H, t, J = 7.2 Hz, $COOCH_2CH_3$). ^{13}C NMR (75 MHz, $CDCl_3$): 170.89, 160.95, 148.85, 140.01, 138.42, 129.08, 127.69, 127.28, 127.06, 126.83, 122.97, 119.92, 116.95, 61.11, 58.24, 43.75, 32.39, 14.48. HRMS-ESI (positive) calcd for $(C_{20}H_{18}N_2O_3 + Na)^+$ 357.1210; found 357.1204. Anal. ($C_{20}H_{18}N_2O_3$) C, H, N; calcd C, 71.84; H, 5.43; N, 8.38; found C, 71.14; H, 5.79; N, 7.95.

2.4.36. Isopropyl 2-amino-4-(2-isopropoxy-2-oxoethyl)-6-phenyl-4*H*-chromene-3-carboxylate: (CXL012)

Synthesized from 6-phenyl coumarin with anhydrous isopropanol as solvent using similar procedure as outlined in the general procedure. Yield: (48%); ^{1}H NMR ($CDCl_3$): δ 7.42 (7H, m, Ar), 7.02 (1H, d, *J* = 8.4 Hz, 8-H), 6.30 (2H, br s, NH_2), 5.11 (1H, m, $COOCH(CH_3)_2$), 4.92 (1H, m, $COOCH(CH_3)_2$), 4.34 (1H, dd, *J* = 4.5, 7.2 Hz, 4-H), 2.67 (1H, dd, *J* = 4.2, 15.0 Hz, HCHCO), 2.61 (1H, dd, *J* = 7.2, 14.7 Hz, HCHCO), 1.33 (3H, d, *J* = 6.6 Hz, $COOCH(CH_3)_2$), 1.31 (3H, d, *J* = 6.6 Hz, $COOCH(CH_3)_2$), 1.12 (3H, d, *J* = 6.6 Hz, $COOCH(CH_3)_2$), 1.04 (3H, d, *J* = 6.6 Hz, $COOCH(CH_3)_2$). ^{13}C NMR (75 MHz, $CDCl_3$): 171.26, 161.65, 161.52, 149.65, 140.55, 137.63, 128.99, 127.38, 127.08, 126.57, 126.09, 116.35, 67.75, 67.71, 66.82, 59.76, 44.15, 31.61, 22.56, 22.34, 21.92, 14.83. ESI-MS (positive): m/z 432.08 $(M+Na)^+$. Anal. ($C_{24}H_{27}NO_5$) C, H, N; calcd C, 70.40; H, 6.65; N, 3.42; found C, 70.27; H, 5.85; N, 3.85.

2.4.37. Ethyl 2-amino-4-(2-oxo-2-(piperidin-1-yl)ethyl)-6-phenyl-4*H*-chromene-3-carboxylate (CXL013)

Piperidine (0.096 mmol) was taken in anhydrous ethanol (2 mL) followed by the addition of ethyl cyanoacetate (0.192 mmol). The resultant solution was stirred at room temperature under an inert atmosphere for 30 min, followed by the addition of a solution of 6-phenylcoumarin (0.08 mmol) in ethanol (1 mL). The resulting reaction mixture was stirred at room temperature and upon consumption of the 6-phenylcoumarin, it was concentrated to half its volume. The reaction mass was then diluted with water (30 mL) and extracted using methylene chloride (3 x 20 mL). The organics were combined, dried

(anhydrous $MgSO_4$) and the solvent removed under reduced pressure, to afford a solid residue. This residue was subjected to column chromatography to afford the pure product as a cream solid. Yield (28 %); ^{1}H NMR ($CDCl_3$): δ 7.51 (3H, m, Ar), 7.38 (4H, m, Ar), 7.03 (1H, d, *J* = 8.4 Hz, 8-H), 6.32 (2H, br s, NH_2), 4.40 (1H, dd, *J* = 4.2, 9 Hz, 4-H), 4.24 (2H, q, *J* = 6.9 Hz, $COOCH_2CH_3$), 3.59-3.11 (4H, m, $N(CH_2)_2$), 2.70 (1H, dd, *J* = 4.5, 13.8 Hz, HCHCO), 2.56 (1H, dd, *J* = 9.3, 13.8 Hz, HCHCO), 1.6-1.3 (6H, m, $(CH_2)_3$), 1.34 (3H, t, *J* = 6.9 Hz, $COOCH_2CH_3$). ^{13}C NMR (75 MHz, $CDCl_3$): 169.47, 169.41, 161.81, 149.66, 140.56, 137.55, 128.98, 127.87, 127.35, 127.11, 126.45, 116.29, 78.04, 59.82, 47.13, 42.79, 42.56, 32.26, 26.47, 25.63, 24.67, 14.84. HRMS-ESI (positive) calcd for $(C_{25}H_{28}N_2O_4 + Na)^+$ 443.1937; found 443.1954. Anal ($C_{25}H_{28}N_2O_4$) C, H, N; calcd C, 71.41; H, 6.71; N, 6.66;found C, 71.25; H 6.92; N, 7.02.

2.4.38. Ethyl 2-amino-4-(2-morpholino-2-oxoethyl)-6-phenyl-4*H*-chromene-3-carboxylate (CXL014)

Synthesized from 6-phenylcoumarin, morpholine, and ethyl cyanoacetate following similar procedure as for **CXL013** to afford a solid. Yield (30 %); ^{1}H NMR ($CDCl_3$); δ 7.43 (7H, m, Ar), 7.04 (1H, d, *J* = 8.4 Hz, 8-H), 6.34 (2H, br s, NH_2), 4.42 (1H, dd, *J* = 5.1, 9.3 Hz, 4-H), 4.24 (2H, q, *J* = 7.2 Hz, $COOCH_2CH_3$), 3.49 (4H, m, $(OCH_2)_2$), 3.25 (4H, m, $(CON(CH_2)_2$), 2.68 (1H, dd, *J* = 4.8, 13.8 Hz, HCHCO), 2.58 (1H, dd, *J* = 9, 13.8 Hz, HCHCO), 1.33 (3H, t, *J* = 6.9 Hz, $COOCH_2CH_3$). ^{13}C NMR (75 MHz, $CDCl_3$): 169.87, 169.25, 161.83, 149.74, 140.32, 137.69, 129.07, 127.67, 127.50, 127.05, 126.61, 126.26, 116.39, 77.85, 66.91, 66.56, 59.88, 46.54, 42.01, 41.89, 32.30, 14.87. HRMS-ESI (positive) calcd for $(C_{24}H_{26}N_2O_5 + Na)^+$ 445.1734; found 445.1754.

Anal. ($C_{24}H_{26}N_2O_5$.0.22 CH_2Cl_2) C, H, N; calcd C, 65.89; H, 6.03; N, 6.34; found C, 65.89; H, 6.45; N, 6.34.

2.4.39. Ethyl 2-amino-4-(2-oxo-2-(piperazin-1-yl)ethyl)-6-phenyl-4*H*-chromene-3-carboxylate: (CXL015)

Synthesized from 6-phenylcoumarin, piperazine, and ethyl cyanoacetate following similar procedure as for **CXL013** and using benzene as a solvent to afford an oil. Yield (58%); ^{1}H NMR ($CDCl_3$): δ 7.43 (7H, m, Ar), 7.04 (1H, d, *J* = 8.1 Hz, 8-H), 6.32 (2H, br s, NH_2), 4.41 (1H, dd, *J* = 4.2, 8.7 Hz, 4-H), 4.24 (2H, q, *J* = 6.9 Hz, $COOCH_2CH_3$), 3.52-3.18 (4H, m, 2 x $N(CH_2)$), 2.69 (6H, m, CH_2CO and 2 x CH_2), 1.33 (3H, t, *J* = 6.9 Hz, $COOCH_2CH_3$). ^{13}C NMR (75 MHz, $CDCl_3$): 169.60, 169.18, 161.73, 149.58, 140.27, 137.451, 128.91, 127.61, 127.30, 126.93, 126.39, 116.21, 59.73, 47.11, 46.12, 45.759, 42.58, 42.20, 32.14, 14.74. HRMS-ESI (positive) calcd for ($C_{24}H_{27}N_3O_4$+ Na)$^+$ 444.2066 found 444.2056. Anal. ($C_{24}H_{27}N_3O_4$) C, H, N; calcd C, 68.55; H, 6.23; N, 9.99; found C, 61.89; H, 5.94; N, 8.74.

2.4.40. Ethyl 2-amino-4-(2-(diethylamino)-2-oxoethyl)-6-phenyl-4*H*-chromene-3-carboxylate (CXL016)

Synthesized from 6-phenylcoumarin, diethylamine, and ethyl cyanoacetate following the general procedure for **5m** to afford a solid. Yield (53%); ^{1}H NMR ($CDCl_3$): δ 7.53 (3H, m, Ar), 7.40 (3H, m, Ar), 7.31 (1H, m, Ar), 7.02 (1H, d, *J* = 8.1 Hz, 8-H), 6.31 (2H, br s, NH_2), 4.49 (1H, dd, *J* = 4.2, 9 Hz, 4-H), 4.25 (2H, q, *J* = 6.9 Hz, $COOCH_2CH_3$), 3.27 (2H, m, $CONCH_2CH_3$), 2.99 (2H, m, $CONCH_2CH_3$), 2.61 (1H, dd, *J* = 4.5, 14.1 Hz, HCHCO), 2.53 (1H, dd, *J* = 9, 14.1 Hz, HCHCO) 1.34 (3H, t, *J* = 7.2 Hz,

$COOCH_2CH_3$), 0.89 (6H, m, 2 x $CONCH_2CH_3$). ^{13}C NMR (75 MHz, $CDCl_3$): 170.30, 169.37, 161.63, 149.48, 140.37, 137.41, 128.84, 127.76, 127.22, 126.96, 126.24, 116.11, 78.19, 59.71, 42.35, 42.06, 40.36, 32.02, 14.78, 14.30, 13.13. HRMS-ESI (positive) calcd for $(C_{24}H_{28}N_2O_4 + Na)^+$ 437.1940 found 437.1925. Anal. ($C_{24}H_{28}N_2O_4$) C, H, N; calcd C, 70.57; H, 6.91; N, 6.86; found C, 70.31; H, 6.71; N, 6.54.

2.4.41. Ethyl 2-amino-6-(3', 5'-dimethoxyphenyl)-4-(2-ethoxy-2-oxoethyl)-4*H*-chromene-3-carboxylate (CXL017)

Yield (52%); ^1H NMR ($CDCl_3$): δ 7.45 (1H, d, *J* = 2.1 Hz, 5-H), 7.39 (1H, dd, *J* = 2.4, 8.4 Hz, 7-H), 7.01 (1H, d, *J* = 8.4 Hz, 8-H), 6.60 (2H, d, *J* = 2.4 Hz, 2',6'-H), 6.45 (1H, t, *J* = 2.1 Hz, 4'-H), 4.35 (1H, dd, *J* = 5.1, 6.9 Hz, 4-H), 4.23 (2H, q, *J* = 6.9 Hz, $COOCH_2CH_3$), 4.02 (2H, q, *J* = 6.9 Hz, $COOCH_2CH_3$), 3.84 (6H, s, 3', 5'-OCH_3), 2.69 (1H, dd, *J* = 4.8, 14.7 Hz, HCHCO), 2.62 (1H, dd, *J* = 7.2, 15.0 Hz, HCHCO), 1.33 (3H, t, *J* = 7.2 Hz, $COOCH_2CH_3$), 1.13 (3H, t, *J* = 7.2 Hz, $COOCH_2CH_3$). ^{13}C NMR (75 MHz, $CDCl_3$); 171.94, 169.28, 161.69, 161. 29, 149.84, 142.76, 137.65, 127.31, 126.69, 126.08, 116.30, 105.34, 99.44, 60.44, 59.79, 55.66, 43.86, 31.59, 14.83, 14.33. ESI-MS (positive): m/z 464.47 $(M+Na)^+$. Anal. ($C_{24}H_{27}NO_7$) C, H, N; calcd C, 65.29; H, 6.16; N, 3.17; found C, 63.78; H, 6.92; N, 3.26.

2.4.42. Ethyl 2-amino-4-(2-ethoxy-2-oxoethyl)-6-(3'-hydroxy-5'-methoxyphenyl)-4*H*-chromene-3-carboxylate (CXL018)

CXL017 (0.050 g, 0.12 mmol) was dissolved using anhydrous methylene chloride followed by addition of molecular sieves (3 Å). The resultant solution was stirred for an hour at -78 °C to remove any residual moisture. Boron tribromide (BBr_3) (0.61 mmol)

was slowly added to this solution. The resultant mixture was stirred at -78 °C for 1 h. The reaction mixture was then gradually warmed to 0 °C, stirring was continued at this temp for 1 h. Finally, after 3 h the reaction was quenched using saturated aq. sodium bicarbonate solution, followed by extraction using ethyl acetate. The organic layer was dried using $MgSO_4$ and the solvent was removed under pressure to get the crude product. The crude mixture was subjected to column chromatography using (2:1) (Hexane : ethyl acetate) to get **CXL018**.Yield (25%). Also obtained was **CXL019** in (30%) yield. ^{1}H NMR ($CDCl_3$); δ 7.43 (1H, d, *J* = 2.1 Hz, 5-H), 7.37 (1H, dd, *J* = 2.1,8.4 Hz, 7-H), 6.99 (1H, d, *J* = 8.4 Hz, 8-H), 6.65 (1H, dd, *J* = 1.5, 2.1 Hz, 2'-H), 6.60 (1H, dd, *J* = 1.5, 2.1 Hz, 6'-H), 6.39 (1H, t, *J* = 2.1 Hz, 4'-H), 5.15 (1H, br s, OH), 4.34 (1H, dd, *J* = 4.8, 6.6 Hz, 4-H), 4.23 (2H, q, *J* = 6.9 Hz, $COOCH_2CH_3$), 4.02 (2H, q, *J* = 6.9 Hz, $COOCH_2CH_3$), 3.83 (3H, s, OCH_3), 2.65 (1H, dd, *J* = 4.5, 15 Hz, HCHCO), 2.62 (1H, dd, *J* = 6.9, 14.7 Hz, HCHCO), 1.33 (3H, t, *J* = 6.9 Hz, $COOCH_2CH_3$), 1.13 (3H, t, *J* = 6.9 Hz, $COOCH_2CH_3$). ^{13}C NMR (75 MHz, $CDCl_3$); 171.94, 169.28, 161.69, 161. 29, 149.84, 142.76, 137.65, 127.31, 126.69, 126.08, 116.30, 105.34, 86.2, 60.44, 55.66, 43.86, 31.59, 14.83, 14.33.ESI-MS (positive): m/z 450.16. $(M+Na)^+$

2.4.43. Ethyl 2-amino-6-(3', 5'-dihydroxyphenyl)-4-(2-ethoxy-2-oxoethyl)-4*H*-chromene-3-carboxylate (CXL019).

Yield (30%); ^{1}H NMR ($CDCl_3$): δ 7.36 (1H, d, *J* = 2.1 Hz, 5-H), 7.31 (1H, dd, *J* = 2.1, 8.1 Hz, 7-H), 6.95 (1H, d, *J* = 8.1 Hz, 8-H), 6.58 (2H, d, *J* = 2.1 Hz, 2', 6'-H), 6.37 (1H, t, *J* = 2.1 Hz, 4'-H), 5.78 (2H, bs, 2 x OH), 4.32 (1H, dd, *J* = 4.8, 6.6 Hz, 4-H), 4.23 (2H, q, *J* = 7.2 Hz, $COOCH_2CH_3$), 4.02 (2H, q, *J* = 7.2 Hz, $COOCH_2CH_3$), 2.67 (1H, dd,

J = 4.8, 14.4 Hz, HCHCO), 2.62 (1H, dd, *J* = 6.6, 14.4 Hz, HCHCO), 1.33 (3H, t, *J* = 7.2 Hz, $COOCH_2CH_3$), 1.12 (3H, t, *J* = 7.2 Hz, $COOCH_2CH_3$). ^{13}C NMR (75 MHz, $CDCl_3$); 170.81, 166.75, 163.95, 157.32, 157.25, 150.22, 142.5, 137.65, 127.85, 126.82, 122.85, 117.39, 106.63, 106.57, 102.16, 62.67, 61.48, 51.47, 38.45, 35.80, 14.49, 14.02. ESI-MS (positive): m/z 436.15. $(M+Na)^+$

2.4.44. Ethyl 2-amino-4-(2-ethoxy-2-oxoethyl)-6-(3', 4', 5'-trimethoxyphenyl)-4*H*-chromene-3-carboxylate (CXL020)

Yield (60%); ^1H NMR ($CDCl_3$): δ 7.43 (1H, d, *J* = 2.1 Hz, 5-H), 7.39 (1H, dd, *J* = 2.1, 8.4 Hz, 7-H), 7.03 (1H, d, *J* = 8.4 Hz, 8-H), 6.7 (2H, s, 2', 6'-H), 6.34 (1H, br s, NH_2), 4.37 (1H, dd, *J* = 4.8, 7.2 Hz, 4-H), 4.26 (2H, q, *J* = 6.9 Hz, $COOCH_2CH_3$), 4.06 (2H, q, *J* = 6.9 Hz, $COOCH_2CH_3$), 3.92 (6H, s, 3',5'- OCH_3), 3.88 (3H, s, 4'-OCH_3), 2.72 (1H, dd, *J* = 4.8, 14.4 Hz, HCHCO), 2.65 (1H, dd, *J* = 7.2, 14.4 Hz, HCHCO), 1.35 (3H, t, *J* = 7.5 Hz, $COOCH_2CH_3$), 1.16 (3H, t, *J* = 7.2 Hz, $COOCH_2CH_3$). ^{13}C NMR (75 MHz, $CDCl_3$); 171.71, 169, 161.45, 153.45, 149.41, 137.58, 136.31, 126.95, 126.31, 116.07, 104.18, 60.95, 60.17, 59.54, 56.18, 43.69, 31.34, 14.57, 14.10. ESI-MS (positive): m/z 494.5. $(M+Na)^+$

2.4.45. Ethyl 2-amino-4-(2-ethoxy-2-oxoethyl)-6-(naphthalen-1-yl)-4*H*-chromene-3-carboxylate (CXL021)

Yield(55%);^1H NMR ($CDCl_3$): δ 7.91 (1H, m, Ar), 7.86 (2H, m, Ar), 7.52-7.36(5H, m, Ar), 7.33-7.30 (1H, m, Ar), 7.09 (1H, d, *J* = 6.3 Hz, 8-H), 6.19 (2H, br s, NH_2), 4.37 (1H, dd, *J* = 5.1, 6.9 Hz, 4-H), 4.26 (2H, q, *J* = 6.9 Hz, $COOCH_2CH_3$), 4.03 (2H, q, *J* = 6.9 Hz, $COOCH_2CH_3$), 2.68 (1H, dd, *J* = 4.8, 14.4 Hz, HCHCO), 2.62 (1H,

dd, *J* = 6.6, 14.4 Hz, HCHCO), 1.33 (3H, t, *J* = 7.2 Hz, $COOCH_2CH_3$), 1.12 (3H, t, *J* = 7.2 Hz, $COOCH_2CH_3$). ^{13}C NMR (75 MHz, $CDCl_3$); 170.37, 167.76, 160.39, 148.35, 138.52, 136.19, 133.08, 130.94, 129.28, 128.72, 127.66, 127.08, 126.29, 125.49, 125.277, 125.2, 124.75, 115.27, 63.45, 60.65, 60.02, 44.45, 32.35, 25.78, 15.79, 15.28. ESI-MS (positive): m/z 454.48. $(M+Na)^+$

2.4.46. Ethyl 2-amino-4-(2-ethoxy-2-oxoethyl)-6-(naphthalen-2-yl)-4*H*-chromene-3-carboxylate (CXL022)

Yield (54%) ^1H NMR ($CDCl_3$): δ 7.98 (1H, s), 7.91-7.85 (3H, m), 7.70-7.67 (1H, m), 7.61-7.60 (1H, d, *J* = 2.1 Hz), 7.55-7.46 (3H, m), 7.09(1H, d, J= 8.4Hz, 8-H), 6.34 (2H, br s, NH_2), 4.40 (1H, dd, *J* = 4.8, 7.2 Hz, 4-H), 4.25 (2H, q, *J* = 7.2 Hz, $COOCH_2CH_3$), 4.02 (2H, q, *J* = 7.2 Hz, $COOCH_2CH_3$), 2.67 (1H, dd, *J* = 4.4, 14.8 Hz, HCHCO), 2.62 (1H, dd, *J* = 7.6, 14.8 Hz, HCHCO), 1.34 (3H, t, *J* = 8 Hz, $COOCH_2CH_3$), 1.13 (3H, t, *J* = 7.2 Hz, $COOCH_2CH_3$). ^{13}C NMR (75 MHz, $CDCl_3$); 171.74, 167.76, 161.46, 149.54, 137.36, 133.08, 132.52, 130.94, 128.45, 128.12, 127.63, 127.29, 126.63, 126.34, 126.05, 125.92, 125.42, 125.28, 116.24, 60.23, 59.546, 43.70, 31.39, 25.78, 14.57, 14.07. ESI-MS (positive): m/z 454.48. $(M+Na)^+$

2.4.47. Ethyl 2-amino-6-(3,5-bis(trifluoromethyl)phenyl)-4-(2-ethoxy-2-oxoethyl)-4H-chromene-3-carboxylate (CXL023)

Yield: 55 %. ^1H NMR ($CDCl_3$): δ 7.95 (2H, s), 7.83 (1H, s), 7.51 (1H, d, *J*=2.0 Hz), 7.45 (1H, dd, *J*=2.4 Hz, 8.4 Hz), 7.11 (1H, d, *J*=8.4 Hz), 6.4 (2H, bs), 4.40-4.37 (1H, m), 4.27 (2H, q, *J*=7.2 Hz), 4.07 (2H, q, *J*=7.2 Hz), 2.74-2.6 (2H, m), 1.35 (3H, t, *J*=7.2 Hz), 1.17 (3H, t, *J*=7.2 Hz). ^{13}C NMR (75 MHz, $CDCl_3$): δ 171.56, 168.87, 161.16,

150.58, 142.39, 134.36, 132.31, 131.98, 127.34, 126.72, 121.95, 120.79, 116.76, 60.34, 59.66, 43.56, 31.22, 14.54, 14.06. MS (ESI, positive) m/z 517.27. Calcd for $C_{24}H_{21}F_6NO_5$: 517.13.

2.4.48. Ethyl 2-amino-4-(2-ethoxy-2-oxoethyl)-6-(3-nitrophenyl)-4H-chromene-3-carboxylate (CXL024)

Yield: 45 %. ^{1}H NMR ($CDCl_3$): δ 8.39-8.38 (1H, m), 8.19-8.16 (1H, m), 7.87-7.85 (1H, m), 7.6 (1H, t, *J*=8.0 Hz), 7.53 (1H, d, *J*=2.4 Hz), 7.47 (1H, dd, *J*=2.0 Hz, 8.4 Hz), 7.1 (1H, d, *J*=8.4 Hz), 6.4 (2H, bs), 4.39-4.36 (1H, m), 4.27 (2H, q, *J*=6.8 Hz), 4.07 (2H, q, *J*=7.2 Hz), 2.73-2.61 (2H, m), 1.35 (3H, t, *J*=7.2 Hz), 1.17 (3H, t, *J*=6.8 Hz). ^{13}C NMR (75 MHz, $CDCl_3$): δ 171.65, 168.89, 161.24, 150.34, 148.72, 141.96, 134.84, 132.69, 129.75, 127.27, 126.54, 121.92, 121.61, 116.62, 60.31, 59.63, 43.56, 31.24, 14.56, 14.08. MS (ESI, positive) m/z 426.4. Calcd for $C_{25}H_{29}NO_8Na$: 426.14.

2.4.49. Cell cultures

CCl-240™ (HL60), CRL-2257™ (HL60/MX2), CCL-119™ (CCRF-CEM), CRL-2264™ (CCRF-CEM/CT) cells were purchased from ATCC, the NALM-6 cell line was originally characterized at the University of Minnesota and kindly provided by Dr Tucker Lebien.[143] HL60 cell line was grown in IMDM glutamax media supplemented with 20% FBS. HL60/MX2, CCRF-CEM and CCRF-CEM/CT cells were grown in RPMI 1640 purchased from ATCC supplemented with 10% FBS. The NALM-6 cell line was cultured in RPMI 1640 (Invitrogen) medium supplemented with 10 mM HEPES, 1 mM sodium pyruvate, 4.5 g/L glucose, 1.5 g/L sodium bicarbonate, 10% FBS, and 1%

penicillin-streptomycin (antibiotic). All cell lines were incubated at 37 ºC with 5% CO_2 in air atmosphere.

2.4.50. Cell viability measurement

The *in vitro* cytotoxicity of these small molecules was assayed by determining their ability to inhibit growth of tumor cells. In brief, tumor cells were plated in a 96 - well plate (at a density of 1 x 10^4 cells/well), and were treated with a series of dilutions of test compounds of varied concentrations with 1 % DMSO in the final cell medium (cells treated with medium containing 1 % DMSO served as a control). After a 48 h treatment, the relative cell viability in each well was determined by using a Cell Titer-Blue Cell Viability Assay kit, according to manufacturer's protocol. The IC_{50} of each candidate was determined by fitting the relative viability of the cells to the drug concentration by using a dose-response model in Prism program from GraphPad Software, Inc. (San Diego, CA).

2.4.51. Preparation of recombinant Bcl-2, Bcl-X_L, and Mcl-1 proteins

A pET-25b(+) vector inserted with the DNA sequence encoding Bcl-2ΔC21 fused with a His_6 tag was a generous gift from Jialing Lin at the University of Okalahoma; pET-29b(+) vectors inserted with the DNA sequence encoding Bcl-wΔC22 fused with a His_6 tag and the DNA sequence encoding Bcl-X_LΔloopΔC40 fused with a His_6 tag respectively were generous gifts from Kalle Gehring at McGill University. pMCSG9(+) vector inserted with the DNA sequence encoding MCl-1(171-326aa) with a MBP and a His_6 tag was a generous gift from Dr, Barry Finzel.The plasmids were transformed into the *Escherichia coli* strains ER2566 (New England Biolab., MA)and BL21 (DE3) cells. The expression of the fusion proteins was induced by 1 mM IPTG and the fusion proteins

were purified by Ni-NTA resin by following a native protein purification protocol provided by the manufacture (Qiagen, CA). The purity of the recombinant proteins was characterized by SDS-PAGE and Coommassie blue staining. Recombinant proteins were concentrated using centrifugal filter devices (Millipore, MA) and dialyzed against PBS buffer containing 15% glycerol, 1 mM DTT. The concentration of the recombinant protein was determined by the Bradford method using BSA as a standard, and stored at -20 °C.

2.4.52. Fluorescence Polarization (FP) Assays

The Bak BH3 (GQVGRQLAIIGDDINR) peptide was synthesized at the Oligonucleotide & Peptide Synthesis Facility at the University of Minnesota, purified by HPLC. The purified peptide was labeled with Oregon Green 488® fluorescein at the N terminus following the manufacture's protocol (Promega, CA), purified by HPLC, characterized by MS, and named as Flu-Bak. Flu-Bak was dissolved in ddH_2O and stored at -20 °C as aliquots. FP assay was conducted using a GENios Pro plate reader (Tecan US, NC) with all assays performed in triplicate, each assay performed twice.

To determine the binding affinity of the Flu-Bak peptide with an anti-apoptotic Bcl-2 protein, a series of 2-fold dilutions of the anti-apoptotic Bcl-2 protein was prepared in a PBS solution, pH 7.0 with 45 nM Flu-Bak peptide and 1 mM DTT. The solutions were incubated at 23 °C for one hour (the time-course study of binding process of Flu-Bak peptide to all the anti-apoptotic Bcl-2 proteins demonstrated that the binding interaction reached equilibrium within 5 min). To each well in a 96-well half-area black plate (Corning, NY) the solution (50 μl) was added and fluorescence polarization (in mP

unit) was measured. The binding affinity of Flu-Bak to the anti-apoptotic Bcl-2 protein was determined by fitting the FP changes to the concentrations of the protein using a single-site saturation binging model in GraphPad (San Diego, CA).

To determine the binding interactions of small molecules to an anti-apoptotic Bcl-2 protein, a series of 3-fold dilutions of small molecules were prepared in DMSO. To each well in a 96-well half-area black plate, 5 µl of the small molecule stock solution was added. A PBS solution (pH 7.0, 1 mM DTT) containing 50 nM Flu-Bak peptide and the amount of the anti-apoptotic Bcl-2 protein that resulted in 60% of Flu-Bak peptide binding to the anti-apoptotic Bcl-2 protein was prepared and incubated at 23 °C for one hour. To each well the solutions of Flu-Bak peptide and the anti-apoptotic Bcl-2 protein (45 µl) were added by auto-injection at a rate of 200 µl/second. The sample was incubated at 23 °C for one hour and the fluorescence polarization (in mP unit) was measured (The 10% DMSO in the final solution was found to have no interference to the binding interaction of Flu-Bak to the anti-apoptotic Bcl-2 proteins). Small-molecule controls included dose-response measurements in the absence of proteins to assess for any interactions between the compounds and the Flu-Bak peptide. Inhibitory constant (Ki) was determined by fitting the FP values to the concentrations of the small molecule using a single-site competition model for fluorescence polarization based competition assay established in this laboratory in GraphPad (San Diego, CA).

2.4.53. Caspase-3/7 activation assay

Apo-ONE® Homogeneous Caspase-3/7 Assay kit was used to measure the caspase-3/7 activity according to the manufacturer's instructions. Briefly, Apo-ONE®

Caspase-3/7 reagent (50 μL) was added to each well containing 50 μL of treated cell suspension (4×10^4 cells) in a 96-well plate. The suspension in the wells were mixed gently and incubated at 37 °C for 30 – 60 min. The fluorescence intensity of the sample in each well was measured with excitation at 485 nm and emission at 530 nm. Caspase-3/7 activity in each well was normalized to the vehicle-treated control.

2.4.54. Synergism assay (performed by Dr. Jignesh Doshi)

Synergistic interactions between sHA 14-1 and test agents (Fas ligand or Dexamethasone) were examined by using median dose-effect analysis as described by Chou and Talalay.[144] Briefly, tumor cells were treated with serial dilutions of each agent individually and in combination at a fixed dose ratio for 48 h. The cytotoxic effects of the treatment were measured by evaluating the cell viability using the cell viability assay and the long-term survival assay. Fractional effect was calculated as fraction of cells killed by the individual agent or the combination, in treated versus untreated cells. Median dose-effect analysis was performed using CompuSyn program from ComboSyn, Inc. (Paramus,NJ). The software computes combination index (CI) values based on the following equation: CI = (D)1/(Dx)1 + (D)2/(Dx)2 + (D)1(D)2/(Dx)1(Dx)2, where(D)1 and (D)2 are the doses of drug 1 and drug 2 that have x effect when used in combination and (Dx)1 and(Dx)2 are the doses of drugs 1 and 2 that have the same x effect when used alone. The CI values indicate synergism (<1), additivity (1), or antagonism (>1). The CIs of 0.1–0.3, 0.3–0.7, and 0.7–0.85 are considered strong synergism, synergism, and moderate synergism, respectively.

2.4.55. Statistical analysis

All biological experiments, including *in vitro* cytotoxicity assay, caspase-3/7 activation assay and synergism assay were performed at least twice with triplicates in each experiment. Representative results are depicted in this report. Data are presented as means ± S.D., and comparisons were made using Student's *t* test. A probability of 0.05 or less was considered statistically significant.

CHAPTER 3*

3. Mechanism of action of CXL017

3.1. Introduction

In the previous chapter, we discussed the design, synthesis and mechanism of action of the stable analog sHA 14-1. Although sHA 14-1 was a stable analog, it was 2-fold less potent than HA 14-1. A thorough SAR study of sHA 14-1, led to the development of CXL017, which is 27-fold more potent than sHA 14-1 and 12-fold more potent than HA 14-1 in Jurkat cells. While the SAR studies on sHA 14-1 were ongoing, a more in-depth investigation on the mechanism of sHA 14-1 was also underway. Since anti-apoptotic Bcl-2 family proteins can localize to the ER and regulate apoptosis through calcium homeostasis, it was hypothesized that anti-apoptotic Bcl-2 inhibitors can potentially affect cellular calcium homeostasis. We found that sHA 14-1 rapidly induced an increase in cytosolic calcium through release of ER calcium storage in a dose-dependent manner.[145] We also discovered that sHA 14-1 partially blocked thapsigargin (a known SERCA inhibitor)-induced ER calcium release in a dose-dependent manner, suggesting that sHA 14-1 may induce ER calcium release through the SERCA pathway.[145] In addition to the effects on ER calcium and SERCA activity, like

---

*Parts of this chapter have been reproduced with permission from {Das, S. G. et al. Structure-activity relationship and molecular mechanisms of ethyl 2-amino-4-(2-ethoxy-2-oxoethyl)-6-phenyl-4h-chromene-3-carboxylate (sHA 14-1) and its analogues. *J Med Chem* **2009,** 52, 5937-49}. Copyright {2009} American Chemical Society and from {Das, S. G. et al. Structure–Activity Relationship and Molecular Mechanisms of Ethyl 2-Amino-6-(3,5- dimethoxyphenyl)-4-(2-ethoxy- 2-oxoethyl)-4H-chromene- 3-carboxylate (CXL017) and Its Analogues *J Med Chem* **2011,** 54, 5937-48}. Copyright {2011} American Chemical Society

thapsigargin, sHA 14-1 treatment also led to induction of ATF4, an indication of ER stress, in leukemic cells.[145] These results suggest that sHA 14-1 has a functional effect on the ER similar to thapsigargin. As a Bcl-2 antagonist, sHA 14-1 induced a loss of mitochondrial membrane potential ($\Delta\psi m$) and caspase-9 activation in various leukemic cells. Overall these results suggest that the action of sHA 14-1 involves both organelles – ER and mitochondria, through antagonizing SERCA and anti-apoptotic Bcl-2 family proteins. The capacity of a small molecule such as sHA 14-1 to bind multiple intracellular targets may be an attractive strategy to overcome drug resistance that emerges as a consequence of multi-gene mutation. Given the unique mechanism of action of sHA 14-1, the goal of the present study was to elucidate if CXL017, a more potent analog of sHA 14-1, also has these unique properties.

3.2. Results and Discussion

3.2.1. Fluorescent polarization binding assay

FP assay was used to determine if CXL017 could inhibit the interaction between the anti-apoptotic Bcl-2 proteins and the Bak BH3 peptide. Although CXL017 was a more potent analog of sHA 14-1, CXL017 showed decreased potency in the FP assay with an IC_{50} of >1mM. As mentioned before, the FP assay has its flaws and therefore based on this assay we cannot conclude that CXL017 does not interact with or modulate Bcl-2 proteins. Furthermore, it is possible that CXL017 like its predecessor sHA 14-1 is a dual inhibitor of Bcl-2 and SERCA. If this is true CXL017 might be preventing the interaction between anti-apoptotic Bcl-2 protein and SERCA. Since the current FP assay only studies the ability of anti-apoptotic Bcl-2 proteins to displace Bak BH3 peptide, it

might not be able to fully encompass the complexity of the interactions of Bcl-2 protein with other proteins of interest. With all this in consideration, we continued to study if CXL017 eliminated cancer cells via activating the apoptotic pathway.

3.2.2. Ability of CXL017 to induce Caspase-3/7 activation in NALM-6 cells

To determine if CXL017 induced apoptosis via Caspase-3/7 activation as seen for its predecessor sHA 14-1, we treated NALM-6 cells with varying concentrations of CXL017 and sHA 14-1 for a period of 24 h. The caspase-3/7 activation in the treated cells was measured using the Apo-ONE® Homogeneous Caspase-3/7 Assay kit. Our results show that treatment of NALM-6 cells with varying concentrations of CXL017 and sHA 14-1 induces caspase-3/7 activation in a dose-dependent manner. Moreover, consistent with its increased cytotoxicity, CXL017 induced higher caspase-3/7 activation at a much lower concentration than sHA 14-1. (Figure 3.1)

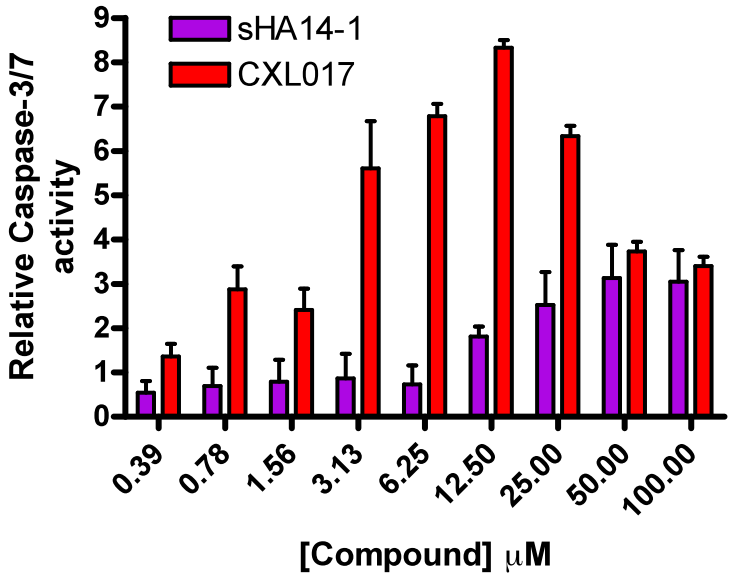

Figure 3.1. Dose-response caspase-3/7 activation in NALM-6 cells induced after treatment with CXL017 and sHA 14-1 for 24 h

3.2.3. Induction of PARP cleavage in NALM-6 cells by CXL017

Poly(ADP-ribose) polymerase (PARP) is a protein involved in a number of cellular processes including DNA repair and programmed cell death. PARP cleavage is carried out by caspases during apoptosis and is a biomarker for apoptosis. NALM-6 cells treated with varying concentrations of CXL017 for 24 h show a dose-dependent increase in PARP cleavage with the distinct cleavage band observable from 3.1 μM of CXL017. Complete cleavage was observed at 25 μM. In comparison, a slight cleavage was observed with sHA 14-1 at a concentration of 50 μM (Figure 3.2). Thus, these results further emphasize that CXL017 is a more potent analog of sHA 14-1, and induces Caspase-3/7 activation and PARP cleavage in a dose-dependent manner.

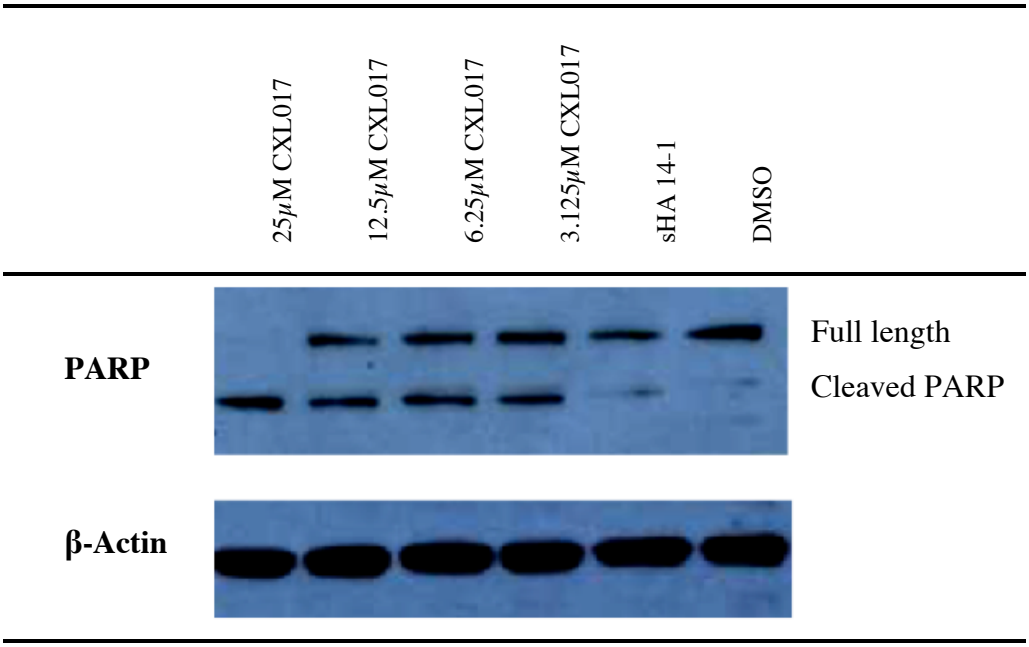

Figure 3.2. Dose-dependent PARP cleavage in NALM-6 cells treated with CXL017 and sHA 14-1 (50 μM) for 24 h

3.2.4. Activity in drug resistant cancer cell lines

Overcoming drug resistance is an important feature of sHA 14-1, and hence further studies were carried out on CXL017 to determine its ability to overcome drug resistance. We evaluated the ability of CXL017 to target drug-resistant cells like HL60/MX2 and CCRF-CEM/CT. Interestingly, both HL60/MX2 and CCRF-CEM/CT cells demonstrated collateral sensitivity (more sensitive to CXL017 than their corresponding parent cells) to CXL017 (Figure 3.3). We also tested a known Bcl-2 inhibitor ABT-737 in the HL60/MX2 and CCRF-CEM/CT cells for comparison. Contrary to the results observed for CXL017, HL60/MX2 cells were resistant to ABT-737 while CCRF-CEM/CT cells were collaterally sensitive to ABT-737 (Figure 3.4). We

evaluated thapsigargin (a known SERCA inhibitor) in these cell lines as well and our results show that HL60/MX2 cells were collaterally sensitive to thapsigargin while CCRF-CEM/CT cells showed slight resistance to thapsigargin (Figure 3.5). These results taken together show that like sHA 14-1, CXL017 also has a unique profile different from traditional Bcl-2 and SERCA inhibitors.

A

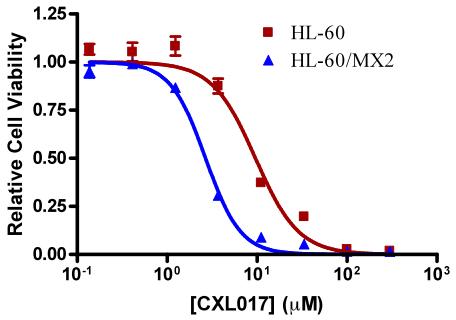

	HL60	HL60/MX2
IC_{50} (μM)	10.7 ± 0.5	2.4 ± 0.2

B

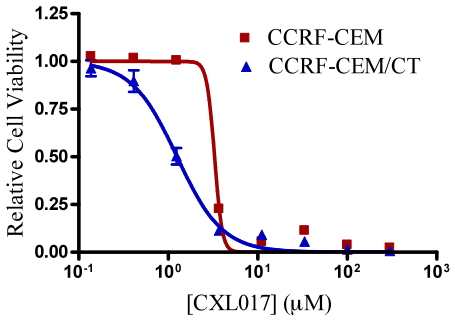

	CCRF-CEM	CCRF-CEM/CT
IC_{50} (μM)	3.34 ± 0.03	1.73 ± 0.24

Figure 3.3. Sensitivity of A) mitoxantrone resistant HL60 cells and B) camptothecin resistant CCRF-CEM cells to CXL017

A

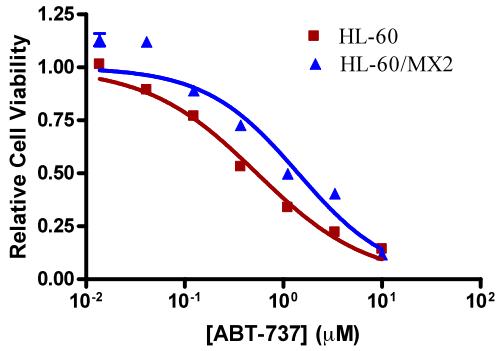

	HL60	HL60/MX2
IC_{50} (μM)	0.57 ± 0.11	1.5 ± 0.7

B

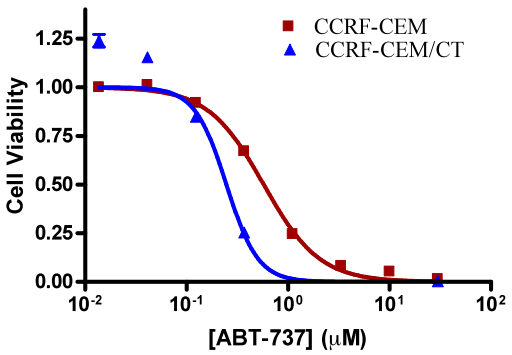

	CCRF-CEM	CCRF-CEM/CT
IC_{50} (μM)	0.45 ± 0.11	0.14 ± 0.09

Figure 3.4. Sensitivity of A) mitoxantrone resistant HL60 cells and B) camptothecin resistant CCRF-CEM cells to ABT-737

A

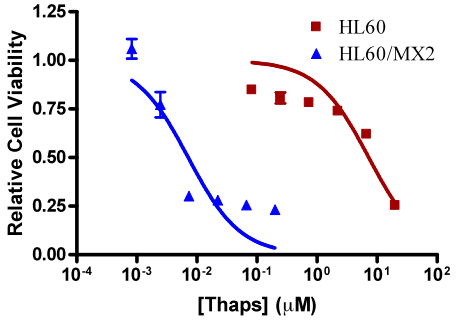

	HL60	HL60/MX2
IC_{50} (μM)	3 ± 0.11	0.0065 ± 0.0003

B

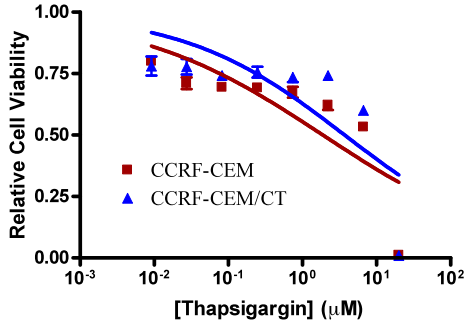

	CCRF-CEM	CCRF-CEM/CT
IC_{50} (μM)	1.9 ± 0.1	4.0 ± 0.4

Figure 3.5. Sensitivity of A) mitoxantrone resistant HL60 cells and B) camptothecin resistant CCRF-CEM cells to thapsigargin

To further evaluate the scope of CXL017 in targeting drug resistant cancers, we acquired several additional drug resistant cancer cell lines, such as HL60/DNR, K562/HHT300, CCRF-CEM/VLB100, selected for resistance towards daunorubicin (DNR), homoharringtonine (HHT), and vinblastine (VLB) respectively. We first evaluated these cell lines for their potential cross-resistance to standard therapies (Table 3.1). Our results show that these drug-resistant cell lines reveal cross-resistance to all standard therapies tested. Evaluation of CXL017 in these cell lines again revealed that none of these resistant cell lines show cross-resistance to CXL017 (Table 3.1), and one cell line (HL60/DNR) may be collaterally sensitive to CXL017. These results further support the unique ability of CXL017 to target drug resistant malignancies.

Table 3.1. Cross-resistance (ratio of IC_{50} in resistant cell lines relative to that in parent cell lines) of MDR cancer cell lines for standard therapies and CXL017

Resistant Cell line	Cross-resistance					
	Doxorubicin	Vincristine	Ara-C	Taxol	MX	CXL017
HL60/DNR	80 ± 21	> 1000	1.3 ± 0.5	>1000	7.5 ± 0.6	0.77 ± 0.15
K562/HHT300	32 ± 11	> 1000	2.2 ± 0.1	91 ± 15	11 ± 0.5	0.93 ± 0.15
CCRF-CEM/VLB100	6.1 ± 2.1	> 1000	0.88 ± 0.16	266 ± 16	2.0 ± 0.5	1.32 ± 0.02

Results are the mean of two independent experiments with triplicate in each experiment.

3.2.5. Synergism

Subsequently combination studies were carried out to evaluate the potential of CXL017 to function as a chemosensitizer to help overcome drug resistance. Specifically, studies of CXL017 in combination with mitoxantrone (MX) and camptothecin (CT) in

HL60/MX2 and CCRF-CEM/CT cells, respectively, were carried out to determine if CXL017 could sensitize the resistant cells. The combination index (CI) of these drugs was analyzed using the Chou and Talalay method (Table 3.2).[144] Moderate synergistic effect was observed when CXL017 was administered in combination with MX in HL60/MX2 cells while combination of CXL017 with CT in CCRF-CEM/CT cells showed antagonism. We also tested if CXL017 could synergize with ABT-737 in HL60/MX2 cells, our results showed that CXL017 demonstrated good synergism with ABT-737. To further expand the scope of CXL017, synergism studies in combination with vincristine or taxol in the three new MDR cell lines were carried out. Our results show that CXL017 synergizes with these clinically used drugs with a CI of ~ 0.5-0.8 in all of the three MDR cell lines (Table 3.2). These results overall suggest that CXL017 can be used in combination with standard therapies to treat drug resistant cancer cells.

Table 3.2. Synergism studies of sHA 14-1 with Mitoxantrone, Camptothecin, Vincristine, Taxol and ABT-737

Treatment	Combination Index (CI)				
	HL60/MX2	CCRF-CEM/CT	HL60/DNR	K562/HHT300	CCRF-CEM/VLB100
Mitoxantrone + CXL017	0.74 ± 0.12				
Camptothecin + CXL017		1.59 ± 0.74			
Vincristine + CXL017			0.61	0.56	0.55
Taxol + CXL017			0.77	0.53	0.53
ABT-737 + CXL017	0.33 ± 0.10				

The MDR cell lines were treated with single drugs mitoxantrone, camptothecin vincristine, taxol, ABT-737 and CXL017 or in combination in a fixed ratio for 48 hrs. The fixed ratios used for CXL017 with mitoxantrone is 2:1,with camptothecin is 1:4 and with ABT-737 is 2:1. The fixed ratios used for CXL017 with vincristine are 2.5:1, 5:1 and 1:1; and with taxol are 8:1, 8:1 and 1:1 for HL60/DNR, K562/HHT300 and CCRF-CEM/VLB100 respectively. The CI (combination index) was calculated by the combination index equation of Chou and Talalay. CI < 1, CI = 1, and CI > 1 indicate synergism, additive effect, and antagonism, respectively.

3.2.6. Activity of CXL017 in NCI-60 cell lines

The NCI-60 human tumor cell line anticancer drug screen was developed in the late 1980's and has been used for a variety of purposes such as identifying potential anticancer drug candidates, determining the molecular target of a compound, gene and chemosensitization profiling.[146] We used the NCI-60 cell line screen to evaluate the activity profile of CXL017. Notably, CXL017 was active across the entire NCI cell panel

with a mean GI_{50} value of 1.04 μM (Table 3.3). Very interestingly, the natural MDR cell line, HCT-15, and *in vitro* drug selected MDR cell line, NCI/ADR-RES, are both sensitive to treatment by CXL017 with GI_{50} values of 0.55 μM and 0.49 μM, respectively (Table 3.3). Further analysis of the NCI data suggests that CXL017 was generally more effective against leukemia, colon cancer, melanoma and breast cancer cells, but shows decreased activity in renal, ovarian and non-small cell lung cancer cells. These results suggest that CXL017 may be useful for the treatment of a variety of different cancers including naturally occurring MDR cancers.

Table 3.3. Cytotoxicity of CXL017 in μM across a panel of 60 cancer cell lines from NCI.

Panel/cell lines	GI_{50} (μM)	Panel/cell lines	GI_{50} (μM)
Leukemia		**Melanoma**	
HL-60(TB)	0.35	UACC-62	0.55
K-562	0.39	M14	0.55
SR	0.45	LOX IMVI	0.72
CCRF-CEM	0.81	SK-MEL-5	0.89
MOLT-4	0.80	SK-MEL-2	1.4
RPMI-8226	1.9	SK-MEL-28	2.6
Non-Small Cell Lung Cancer		UACC-257	12
NCI-H460	0.54	**Ovarian Cancer**	
NCI-H522	0.62	OVCAR-3	0.32
HOP-62	0.89	NCI/ADR-RES	0.49
A549/ATCC	1.2	IGROV1	0.93
EKVX	1.3	SK-OV-3	1.4
HOP-92	1.4	OVCAR-8	3.8
NCI-H23	2.0	OVCAR-5	4.1
NCI-H322M	4.0	OVCAR-4	5.2
NCI-H226	4.4	**Renal Cancer**	
Colon Cancer		A498	0.36
HT29	0.39	CAKI-1	0.71
HCT-116	0.42	UO-31	1.4
SW-620	0.49	ACHN	1.5
KM12	0.50	786-0	2.3
HCT-15	0.55	RXF 393	2.5
COLO 205	1.2	SN12C	2.8
HCC-2998	2.5	TK-10	3.4
CNS Cancer		**Prostate Cancer**	
SF-295	0.48	PC-3	0.83
SF-539	0.49	DU-145	1.5
U251	0.63	**Breast Cancer**	
SF-268	1.1	HS 578T	0.32
SNB-75	1.3	MCF7	0.45
SNB-19	1.9	MDA-MB-468	0.67
Melanoma		BT-549	0.77
MDA-MB-435	0.27	MDA-MB-231/ATCC	1.5
MALME-3M	0.39	T-47D	3.7

3.2.7. COMPARE study

We have already demonstrated that CXL017 has a unique profile like its predecessor sHA 14-1 when compared to ABT-737 and thapsigargin. To explore the potential similarity of CXL017 to other compounds tested in the NCI-60 cell line screen, we used the COMPARE algorithm provided by NCI to measure the similarity of CXL017 (the seed compound) in responses to the 60 cell lines of an entire database of compounds. It then ranks all the compounds in the entire database in their order of similarity towards the seed compound, in which a compound with a rank 1 signifies highest similarity in the possible mechanism of action to the seed compound. Using this approach, we compared the mean GI_{50} profile ("fingerprint") of CXL017 to the standard agents. The standard agent database includes 171 compounds ranging from cancer treatment new drug applications, investigational new drug applications, to compounds of particularly high interest at the NCI. The similarity pattern to that of the seed is expressed using a Pearson's correlation coefficient (PCC). A PCC value of > 0.5 is generally considered significant based on previous reports.[147, 148]

Our COMPARE analysis results show that compound CXL017 is unique in its mechanism of action with little correlation to "standard" agents; specifically, none of the 171 compounds tested, which include some clinically used agents, show a PCC value of > 0.5 to CXL017 in the COMPARE analysis (Table 3.4). These data suggest that CXL017 is a scaffold with a unique mechanism of action, potentially accounting for its novel ability to selectively eliminate drug resistant cancers. It is interesting to note that the first 5 compounds with the best correlation to CXL017's mechanism of action are

either antimetabolites or antimitotic agents. Thus, further investigations to determine if CXL017 has any antimitotic or antimetabolite function may shed some light towards discovering the cellular target of CXL017.

Table 3.4. List of the top compounds with growth inhibitory patterns similar to CXL017 (NSC no. S753690)

Seed NSC: S753690 (5) Seed level :GI_{50}
EXP ID. AVGDATA High Conc.: -4.0
Data base: Standard Agents

Rank	PCC	NSC No.	Name	Mechanism	Hi Conc.
1	0.50	S35212	Trimetrexate	Antimetabolite/antifolate	-6.0
2	0.49	S163501	Acivicin	Antimetabolite	-4.0
3	0.48	S126771	Dichloroallyl lawsone	Antimetabolite	-3.6
4	0.48	S153858	Maytansine	Antimitotic agent	-3.6
5	0.48	S332598	Rhizoxin	Antimitotic agent	-4.3
14	0.40	S49842	Vinblastine	Antimitotic agent	-5.6
16	0.39	S619003	Vincristine	Antimitotic agent	-5.0
21	0.38	S19893	5-Fluorouracil	Antimetabolite	-4.0
22	0.38	S740	Methotrexate	Antimetabolite/antifolate	-3.6
32	0.36	S125973	Taxol	Antimitotic agent	-6.0

3.2.8. Pharmacokinetic studies

Given that CXL017 can selectively target drug resistant cells *in vitro*, we next examined the ability of CXL017 to target drug-resistant cells *in vivo.* We performed this experiment in a series of steps. To begin, we performed an *in vitro* stability assay to determine the half-life of CXL017 in blood obtained from mice. Our results show that CXL017 has good stability in blood with a half-life of > 8 h (Figure 3.6).

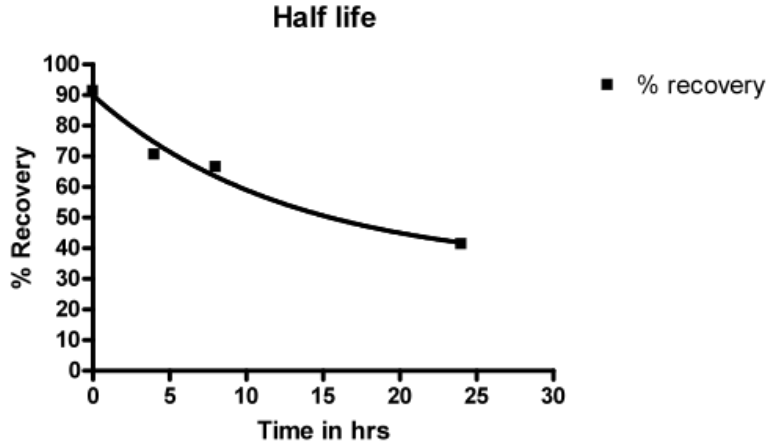

Figure 3.6. Stability of CXL017 in blood

We then moved on to perform a maximum tolerated dose (MTD) and pharmacokinetic study *in vivo*. In this study 32 mice were divided into 4 groups, with each group containing 8 Female B6C3F1 mice. Group 1 was treated with vehicle (DMSO), Group 2 was treated with 25 mg/kg of CXL017, Group 3 was treated with 50 mg/kg of CXL017 and Group 4 was treated with 100 mg/kg of CXL017 as shown in Table 3.5. The mice were given an i.p injection of CXL017 in DMSO at the required dose once a day for 5 consecutive days. On day 5 all mice were sacrificed, 2 mice per group, at 1 h, 2 h, 4 h, and 8 h time points after injection of CXL017. They were bled and the blood collected was spun at 14,000 rpm for 5 min and the serum was collected and stored at – 80 °C for pharmacokinetic studies. Our results showed that CXL017 was well tolerated by mice with no significant change in bodyweight observed in any of the treatment groups (Figure 3.7A). Moreover, pharmacokinetic studies showed that the

highest serum concentration of CXL017 reached in blood was about 4 µM in group 4 (100 mg/kg/day) (Figure 3.7 B).

Table 3.5. Description of the different groups used for the MTD study

No. of Mice	Group No.	Treatment
8	1	DMSO alone
8	2	25 mg/kg/day CXL017 in DMSO
8	3	50 mg/kg/day CXL017 in DMSO
8	4	100 mg/kg/day CXL017 in DMSO

A

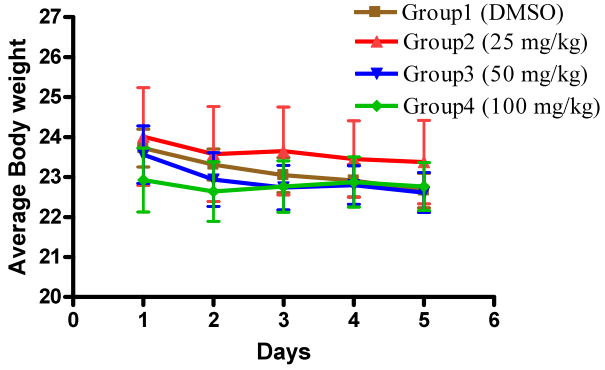

B

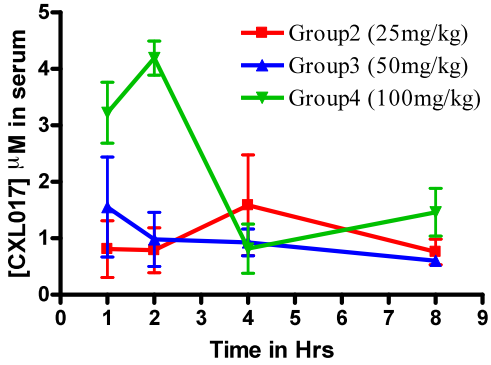

Figure 3.7. A) Average body weight of mice for 5 days B) Plasma concentration curve of CXL017

3.2.9. *In vivo* therapeutic efficacy evaluation

Based on the MTD and pharmacokinetic study results, we decided to perform an *in vivo* study with 100 mg/kg/day of CXL017. We have previously demonstrated that HL60/MX2 cells display collateral sensitivity to CXL017 *in vitro*. In order to determine if HL60/MX2 cells demonstrate collateral sensitivity to CXL017 *in vivo*, we developed a

xenograft mouse model by subcutaneously injecting HL60/MX2 (right flank) and HL60 cells (left flank) into the same mouse. The tumors were then allowed to grow to a size of $40mm^3$, followed by treatment with CXL017 for a period of 3 weeks at dose of 100 mg/kg/day for 6 days a week. The body weights of the mice were monitored during the entire course of the treatment and no significant change was observed due to CXL017 treatment (Fig. 3.8A). Our results show that CXL017 demonstrates significant reduction of tumor size in the resistant tumors when compared to the vehicle treated control mice (Fig. 3.8C). No significant reduction of tumor size was observed in the parent HL60 induced tumors (Fig. 3.8B). Thus, CXL017 demonstrates selectivity towards MDR cancer cell lines both *in vitro* and *in vivo*, making it a potential candidate for further development. The lack of efficacy of CXL017 in HL60 derived tumors is probably due to its poor bioavailability as its peak plasma concentration in the mice, although higher than the IC_{50} for HL60/MX2, was lower than the IC_{50} in the HL60 cell line (Figure 3.7 B)

A

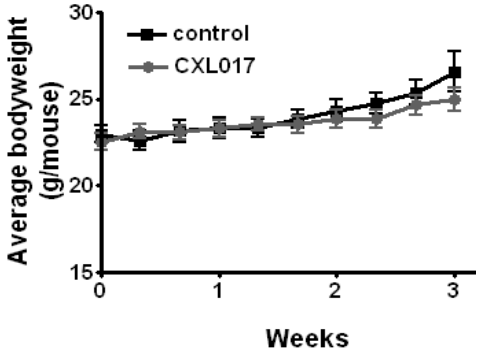

B

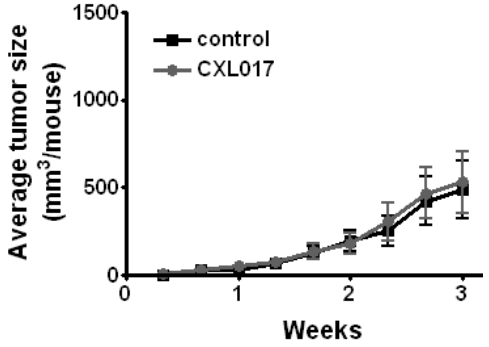

C

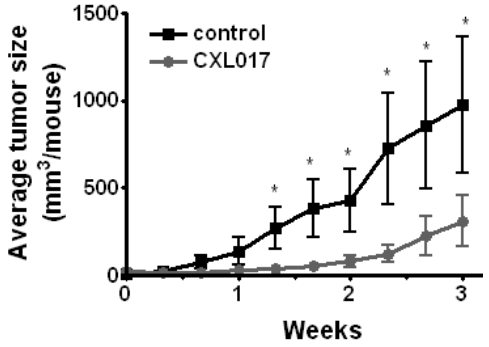

Figure 3.8. Effect of CXL017 100mg/kg i.p. on A) Body weight B) the growth of parent HL60 tumors in SCID mice C) the growth of resistant HL60/MX2 tumors in SCID mice. *-indicates significant difference from vehicle control, P< 0.05.

3.2.10. Chiral purification

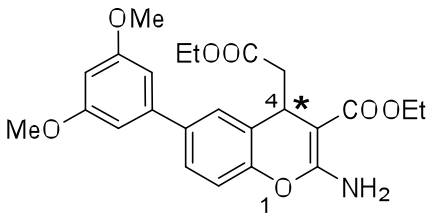

Figure 3.9. Structure of CXL017

As shown in Figure 3.9, compound CXL017 has one chiral center at position 4 on the chromene core. Our study so far has only evaluated the racemate of CXL017. Therefore, we were intrigued to determine whether the optically pure isomers of compound CXL017 would present a different *in vitro* activity profile. For this purpose, we used a chiral HPLC column to separate the two enantiomers. The optical rotation of the enantiomers was determined using polarimetry. The optical rotation for one enantiomer was (+) 0.107 (c 1.0, MeOH) and that for the other enantiomer was (−) 0.102 (c 1.0, MeOH). The two enantiomers were evaluated for their cytotoxicity and selectivity in HL60 and HL60/MX2 cancer cells. The results show that (−)-CXL017 is about 13-fold more cytotoxic than the (+)-CXL017 while there is no significant change with respect to selectivity (Table 3.6). An important thing to notice was that although the (−)-CXL017 enantiomer was more active than (+)-enantiomer, there was not much difference between the activity of the racemate CXL017 and the (−) enantiomer in HL60 and HL60/MX2 cells. Therefore for future studies we continued to use the racemic form of CXL017.

A (Racemate)

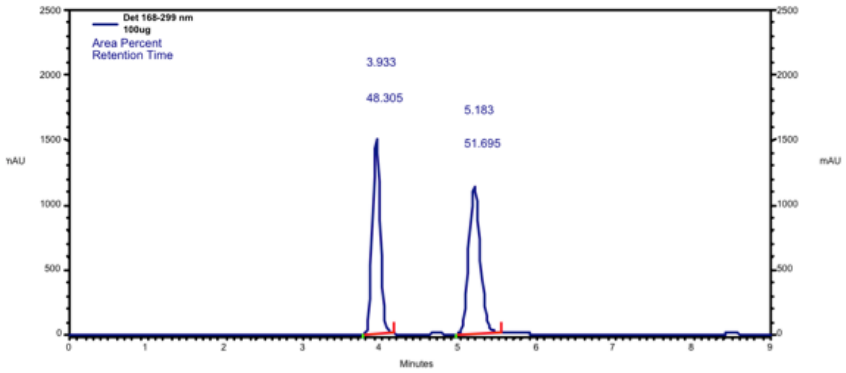

B (+) enantiomer

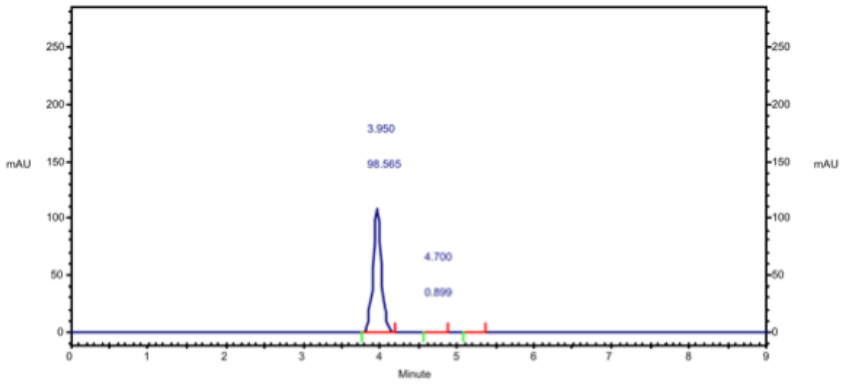

C (–) enantiomer

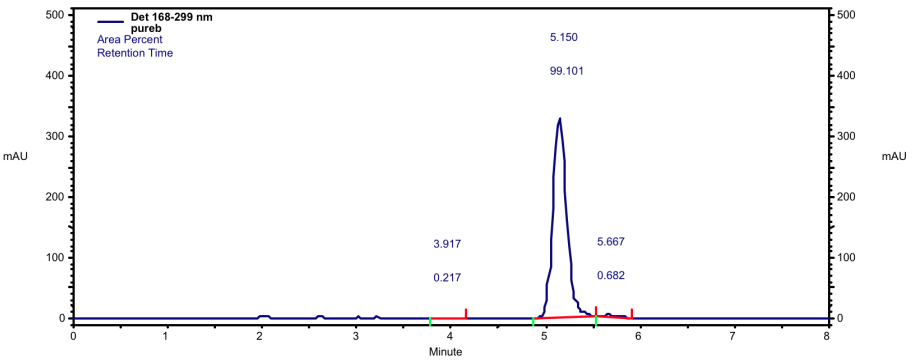

Figure 4.0. HPLC trace for the chiral purification of CXL017. A, Racemate B, (+) enantiomer and C, (–) enantiomer

Table 3.6. IC_{50} values (μM) of enantiomers of CXL017 in MDR cell lines

Cell lines	**CXL017**	**(+) enantiomer**	**(−) enantiomer**
HL60	10.7 ± 0.5	82.6 ± 1.4	6.1 ± 0.1
HL60/MX2	2.4 ± 0.2	21.8 ± 1.8	1.9 ± 0.1
Selectivity	4.4	3.8	3.2

3.3. Conclusion

The ability to selectively target MDR cancer cells is one crucial factor for future cancer therapy development. With respect to this, we have identified compound CXL017 as a potential lead. In this study, we show that CXL017 induces cell death via apoptosis as characterized by activation of caspase-3/7 and induction of PARP cleavage in a dose-dependent manner. We also demonstrate that a variety of MDR cells show no cross-resistance to CXL017. CXL017 synergizes with several standard anticancer agents in MDR cells, including vincristine, taxol, and mitoxantrone. Additionally, we have shown that CXL017 is effective across the panel of NCI-60 cell lines and seems to have a unique mechanism of action based on its low correlation with standard agents tested. Most importantly, we have established that CXL017 significantly and selectively suppresses the growth of tumors derived from the MDR cancer cell line, HL60/MX2, *in vivo*. Finally we have shown that (−) enantiomer for compound CXL017 is about 13 times more active than the (+) enantiomer. However there is no difference in their selectivity towards MDR cancer cells. The significant difference in cytotoxicity and lack of difference in selectivity

of the enantiomers suggests that CXL017 and its analogs have distinct cellular targets responsible for cytotoxicity and selectivity, which are currently under investigation. In conclusion, we have demonstrated that compound CXL017 reveals unique mechanism of action to selectively kill MDR cancer cell lines, which merits further investigation for its potential as a drug candidate for the treatment of MDR cancers.

3.4. Experimental procedures

3.4.1. Chiral separation of CXL017 racemate

The chiral separation was done using a RegisPack chiral column (5μm, 250mm x 4.6mm) (Product # 783104, Regis technologies). The enantiomers of CXL017 were separated using 70:30 (Hexane: IPA) with a flow rate of 1.5 ml/min. The retention time for the (+) enantiomer was 3.8 min and for the (−) enantiomer was 5.0 min. The optical rotation for one enantiomer was (+) 0.107 (c 1.0, MeOH) and that for the other enantiomer was (−) 0.102 (c 1.0, MeOH).

3.4.2. Cell cultures

CCL-240 (HL60) and CRL-2258 (HL60/MX2) cells were purchased from ATCC. K562/HHT300 and HL60/DNR cell lines were developed by Dr. Tang. CCRF-CEM and CCRF-CEM/VLB100 were developed by Dr. Beck. HL60 cell line was grown in IMDM Glutamax media supplemented with 20% FBS. All other cell lines were grown in RPMI 1640 media purchased from ATCC supplemented with 10% FBS. All cell lines were incubated at 37 ºC with 5% CO_2 in air atmosphere.

3.4.3. Cell viability measurement

The *in vitro* cytotoxicity of these small molecules were assayed by determining their ability to inhibit the growth of the tumor cells. In brief, the tumor cells were plated in a 96 - well plate (the density of 1 x 10^4 cells/well). The cells were treated with a series of dilutions of the test compounds of varied concentrations with 1 % DMSO in the final cell medium (cells treated with medium containing 1 % DMSO served as a control). After a 48 h treatment, the relative cell viability in each well was determined by using a CellTiter-Blue Cell Viability Assay kit. The IC_{50} of each candidate was determined by fitting the relative viability of the cells to the drug concentration by using a dose-response model in Prism program from GraphPad Software, Inc. (San Diego, CA).

3.4.4. Caspase-3/7 activation assay

Apo-ONE® Homogeneous Caspase-3/7 Assay kit was used to measure the caspase-3/7 activity according to the manufacturer's instructions. Briefly, Apo-ONE® Caspase-3/7 reagent (50 μL) was added to each well containing 50 μL treated cell suspension (4 × 10^4 cells) in a 96-well plate. The suspension in the wells were mixed gently and incubated at 37 °C for 30 – 60 min. The fluorescence intensity of the sample in each well was measured with excitation at 485 nm and emission at 530 nm. Caspase-3/7 activity in each well was normalized to the vehicle-treated control.

3.4.5. Western blot analysis

Cultured cells were plated at a density of 4x10^6 cells/well in six well plates. Cells were treated with the test compounds with various concentrations and incubated at 37 °C for 24 h. After 24 h cells were harvested and washed with ice-cold phosphate-buffered

saline (PBS). Cell pellets were suspended in RIPA (25 mM Tris•HCl pH 7.6, 150 mM NaCl, 1% NP-40, 1% sodium deoxycholate, 0.1% SDS) buffer supplemented with 1% protease inhibitor from Sigma. The cell suspension was incubated on ice for 30 min and centrifuged at 12000 × *g* for 10 min. The supernatant was collected and the protein concentration in the supernatant was quantified by Bradford method with BSA as the standard. Samples were separated at 150 V through electrophoresis for 1 h on 12% SDS-PAGE. The proteins were blotted to polyvinylidine fluoride (PVDF) membrane from Millipore (Boston, MA) and probed with the following antibodies described; the anti-PARP (9532) antibody (Cell Signaling Technology) was used at a final dilution of (1:300) and the anti-β-actin antibody (Sigma–Aldrich) was used at a final dilution of (1:40000). Bound antibodies were detected using appropriate peroxidase-coupled secondary antibodies followed by detection using the supersignal chemiluminescence system from Pierce (Rockford, IL).

3.4.6. Synergism assay

Synergistic interactions of CXL017 with vincristine were examined by using median dose–effect analysis as described by Chou and Talalay.[144] Briefly, tumor cells were treated with serial dilutions of each agent individually and in combination simultaneously at a fixed dose ratio for 48 h. The fixed ratios used for (vincristine with CXL017) are 1:2.5, 1:5, and 1:1 and for (taxol with CXL017) are 1:8 and 1:1 for HL60/DNR, K562/HHT300 and CCRF-CEM/VLB100 respectively. The fixed dose ratios used for CXL017 with mitoxantrone is 2:1, with camptothecin is 1:4 and with ABT-737 is 2:1. The cytotoxic effects of the treatment were measured by evaluating the

cell viability using the cell viability assay and the long-term survival assay. Fractional effect was calculated as fraction of cells killed by the individual agent or the combination, in treated versus untreated cells. Median dose effect analysis was performed using CompuSyn program from ComboSyn, Inc. (Paramus,NJ). The software computes combination index (CI)values based on the following equation: CI = (D)1/(Dx)1 + (D)2/(Dx)2 + (D)1(D)2/(Dx)1(Dx)2, where(D)1 and (D)2 are the doses of drug 1 and drug 2 that have x effect when used in combination and (Dx)1 and(Dx)2 are the doses of drugs 1 and 2 that have the same x effect when used alone. The CI values indicate synergism (<1), additivity (1), or antagonism (>1). The CIs of 0.1–0.3, 0.3–0.7, and 0.7–0.85 are considered to indicate strong synergism, good synergism, and moderate synergism, respectively.

3.4.7. Pharmacokinetic and MTD studies

In this study 32 mice were divided into 4 groups, with each group containing 8 Female B6C3F1 mice each. To determine the optimal dose for efficacy evaluation, CXL017 was administered to mice at a daily dose of 100, 50, and 25 mg/kg of bodyweight in carrier (*DMSO), 0.05 mL*) via *i.p.* injection for 5 days. Group 1 was treated with vehicle (DMSO), Group 2 was treated with 25 mg/kg of CXL017, Group 3 was treated with 50 mg/kg of CXL017 and Group 4 was treated with 100 mg/kg of CXL017. Mice were monitored daily for toxicity and euthanized with CO_2 respiration at different time points (1, 2, 4, and 8 h) after the final CXL017 injection. Serum concentrations of CXL017 were determined by HPLC.

3.4.8. *In vivo* Therapeutic Efficacy Evaluation (Performed by Dr. Xing)

For *in vivo* anticancer potential evaluation, female athymic nude mice obtained from Harland were maintained in a laminar airflow cabinet under pathogen-free conditions and used at 6 to 12 weeks of age. The protocol for animal experiments was approved by the Institutional Animal Care and Use Committee (IACUC) of the research animal resources facility at the University of Minnesota. Upon arrival, all mice were maintained on standard diet and housed in the pathogen-free animal quarters at the University of Minnesota Cancer Center. After one week of acclimation, HL60 cells (5 x 10^6 in 0.1 mL PBS : Metrigel (v/v 1:1)) were implanted subcutaneously into the left flank of each mouse. At the same time, HL60/MX2 cells (5 x 10^6 in 0.1 ml PBS : Metrigel (v/v 1:1)) were implanted subcutaneously into the right flank of the same mouse. Formation of a bulla indicated a satisfactory injection. Tumors were measured three times a week with a caliper. Tumor volumes were calculated using the following formula: $1/2 \times w_1 \times w_2 \times w_2$ (w_1 the largest tumor diameter and w_2 the smallest tumor diameter). When tumors induced by HL60/MX2 reached ~40 mm^3, mice were randomized into two groups with similar distribution in HL60/MX2 induced tumor size and bodyweight, ten mice each group. Mice in Group 1 were given carrier (*PEG400 : EtOH (v/v 2:1), 0.1 mL*) alone via i.p. injection. Mice in Group 2 were given CXL017 (100 mg/kg of body weight). Treatment was once a day for three weeks. Mice were CO_2 euthanized with tumors removed and weighed.

Chapter 4

4. Development of drug-resistant cell lines

4.1. Introduction

Multidrug resistance (MDR) in cancer is a phenomenon in which administration of a single chemotherapeutic agent causes cross-resistance of cancer cells to a variety of therapies even with different mechanism of action. Development of MDR against standard therapies is a major challenge in the treatment of cancer. Therefore, anti-cancer agents that can re-sensitize MDR cancer cells to chemotherapy not only bring forth the opportunity to greatly improve patient response but also provide valuable tools complementary to standard biological approaches to help understand MDR mechanisms. Over-expression of anti-apoptotic Bcl-2 proteins plays a key role in MDR development in cancer. Thus antagonizing anti-apoptotic Bcl-2 proteins provides a viable strategy to overcome MDR. In the previous sections, we have discussed the design and synthesis of 4H-chromene analogs based on a putative Bcl-2 inhibitor HA 14-1, culminating in the development of CXL017 with an average IC_{50} value of 1μM in over 60 different NCI cancer cell lines.[140, 149] In addition, we showed that a variety of MDR cancer cell lines demonstrated collateral sensitivity towards CXL017 *in vitro*.[140, 149] Specifically, HL60/MX2 MDR cancer cells were 4-fold more sensitive to treatment of CXL017 than the parent HL60 cells. More importantly, CXL017 significantly and selectively suppressed the growth of tumors derived from the MDR cancer cell line, HL60/MX2, *in vivo*. These results show that CXL017 demonstrates selectivity towards MDR cancer cell lines both *in vitro* and *in vivo*, making it a potential candidate for further development.

Although CXL017 demonstrated selectivity towards a variety of MDR cancer cells that were not exposed to CXL017, we were intrigued to know the effect of prolonged exposure to CXL017 on MDR cancer cells, which is the focus of the present study. Specifically, we examined if HL60/MX2 cells could acquire drug resistance towards CXL017 upon prolonged exposure.

4.2. Results and discussion

4.2.1. Multidrug resistant HL60/MX2 cell line over-expresses Mcl-1, Bax, Bak, SERCA2 and SERCA3 but does not over-express P-gp nor breast cancer resistance protein (BCRP)

Before we exposed the HL60/MX2 cells to CXL017 for a prolonged period, we fully characterized these cells to determine the possible reason for the increased selectivity of CXL017 towards these cell lines. As we have described before, HL60/MX2 is a MDR variant of HL60 cells, which demonstrates cross-resistance to mitoxantrone, doxorubicin, and cisplatin.[140] This cell line has previously been characterized to demonstrate an atypical MDR phenotype, i.e. it does not over-express MDR receptors like P-gp by western blotting. However, the conclusion was questionable given that no positive control for P-gp was used in that study and no other ABC members had been analyzed.[150] Since ABC transporter proteins commonly play an important role in drug-induced development of MDR in cancers, we first investigated the expression levels of various ABC transporter proteins in these cell lines. A FACS analysis of P-gp and BCRP expression on HL60 and HL60/MX2 cell lines showed that there is no difference in the expression of these transporters between these cell lines (Figure 4.1A and B). This is in

accordance with a previous report,[150] suggesting that the mechanism for MDR in HL60/MX2 is not likely through ABC efflux pumps.

Given the importance of anti-apoptotic Bcl-2 family proteins in MDR and the fact that HL60/MX2 cells greatly over-express Mcl-1 protein, we further characterized these cell lines to study the protein expression levels of various pro-apoptotic Bcl-2 (Bax and Bak) proteins. Interestingly, contrary to our expectation, pro-apoptotic proteins like Bax and Bak were found to be upregulated in the resistant cell lines similar to the trend observed for anti-apoptotic proteins Mcl-1 (Figure 4.1C). The MDR nature of HL60/MX2 suggests that the upregulation of the anti-apoptotic Bcl-2 family proteins (i.e. Mcl-1) likely outweighs the over-expression of the pro-apoptotic Bax and Bak proteins in programmed cell death regulation.

Based on the potential dual function of CXL candidates on Bcl-2 family proteins and SERCA proteins[145] and their reported physical interactions,[27-29] we also characterized the expression levels of SERCA2 and SERCA3 in these cell systems. It was found that HL60/MX2 has significantly elevated levels of SERCA2 and SERCA3 proteins (Figure 4.1C). Given that Bcl-2 family proteins and SERCA both regulate ER calcium content, we also characterized the ER calcium content in these cell lines. Our results show that HL60/MX2 cells have significantly increased ER calcium levels in comparison to HL60 cells (Figure 4.1D). Taken together these characteristics of HL60 and HL60/MX2 suggest that these cell lines provide a valuable system to study MDR using CXL017 as a chemical tool.

4.2.2. HL60/MX2 cell line fails to develop stable resistance to CXL017 upon prolonged exposure

To determine whether HL60/MX2 cells could develop resistance towards CXL017 upon prolonged exposure, HL60 and HL60/MX2 cells were cultured in the presence of increasing concentrations of CXL017 and Ara-C respectively for a period of 6 months. The newly derived cells named as HL60/CXL017, HL60/MX2/CXL017, HL60/Ara-C, and HL60/MX2/Ara-C were then evaluated for their sensitivity to CXL017 and Ara-C. Ara-C was used for comparison in this experiment, as it is the major first line therapy for treatment of AML. To determine if the cell lines exposed to drug for 6 months demonstrate stable resistance, they were cultured in the absence of drug for a period of 2 months and then re-evaluated for their drug sensitivity. The cell lines thus obtained were named as HL60/MX2/CXL017/NT and HL60/MX2/Ara-C/NT respectively. HL60/MX2 cells exposed to CXL017 for different time periods (2 and 4 months) were used for mechanistic investigation, named as HL60/MX2/CXL017-2 and HL60/MX2/CXL017-4 respectively. For additional comparison, HL60/MX2 cells were exposed to ABT-737 (a Bcl-2 inhibitor) and Thapsigargin (TG) (a SERCA inhibitor) for a period of 3 months, denoted as HL60/MX2/ABT-737 and HL60/MX2/TG, respectively.

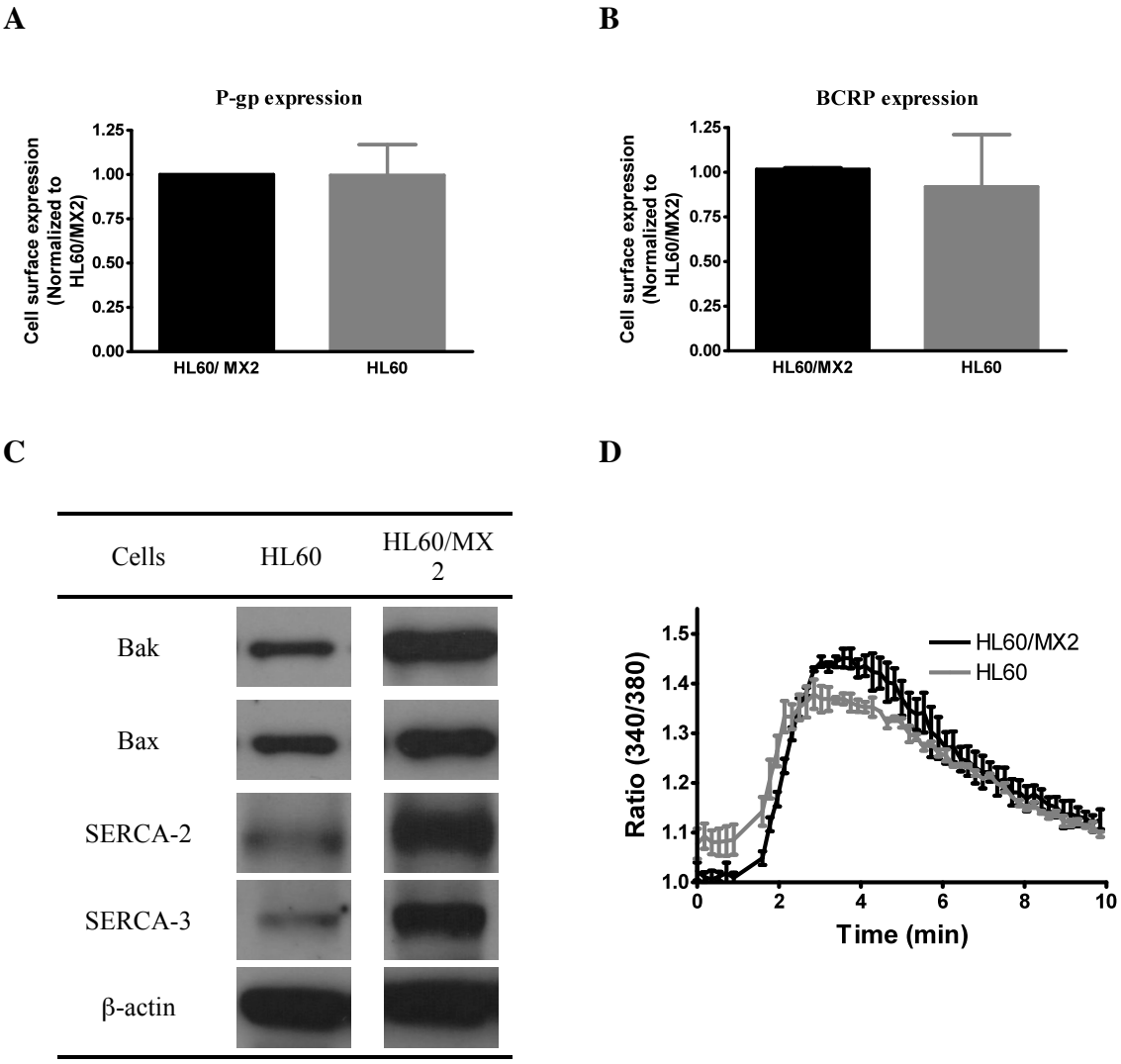

Figure 4.1. Characterization of HL60 and HL60/MX2 cell line

A, Flow cytometric analysis, three independent experiments were averaged and depict the fold difference of P-gp expression between HL60 and HL60/MX2. B, The data represented is an average of three independent experiments and depict the fold difference of BCRP expression between HL60 and HL60/MX2. C, Western blot analysis of HL60 and HL60/MX2 for Bax, Bak, SERCA2 and SERCA3, β-Actin was used as a protein loading control. Three independent experiments were conducted with similar results. D, ER calcium content in HL60/MX2 cells is higher than HL60. Three independent experiments were averaged and the ratio of 340/380 nm was plotted with the shown error bars. (Western blot analysis and ER calcium content study was performed by David Hermanson)

Interestingly, after 6 months exposure, HL60/MX2 cells developed a 2.5-fold resistance to CXL017 (Figure 4.2A), which was transient as the resistance was lost when such cells were cultured in the absence of CXL017 (HL60/MX2/CXL017/NT) (Figure 4.3A). HL60 on the other hand developed only 1.3-fold resistance towards CXL017 after exposure for 6 months (Figure 4.2B). However, both HL60 and HL60/MX2 develop over a 2000-fold resistance towards Ara-C (Figure 4.2C and 4.2D, Table 4.1); that remains unchanged even after removing Ara-C treatment for 2 months (Figure 4.3B for HL60/MX/Ara-C/NT). Since, no change was observed between HL60/MX2/Ara-C and HL60/MX2/Ara-C/NT cells, the HL60/MX2/Ara-C cells were used for later studies. These results show that both HL60 and HL60/MX2 cells fail to develop stable resistance towards CXL017 upon prolonged exposure. To determine if this behavior was unique to CXL017 and whether it depends on the dual mechanism of action of CXL017 on Bcl-2 family proteins and SERCA, we also exposed HL60/MX2 cells to ABT-737 and TG for 3 months. HL60/MX2 cells developed over 10-fold stable resistance to ABT-737 and about 3-fold resistance to TG (Figure 4.4A and B). These results show that the lack of resistance towards CXL017 observed in HL60 and HL60/MX2 cells upon prolonged exposure is unique and inhibiting Bcl-2 family proteins or SERCA alone is not sufficient to achieve such an outcome.

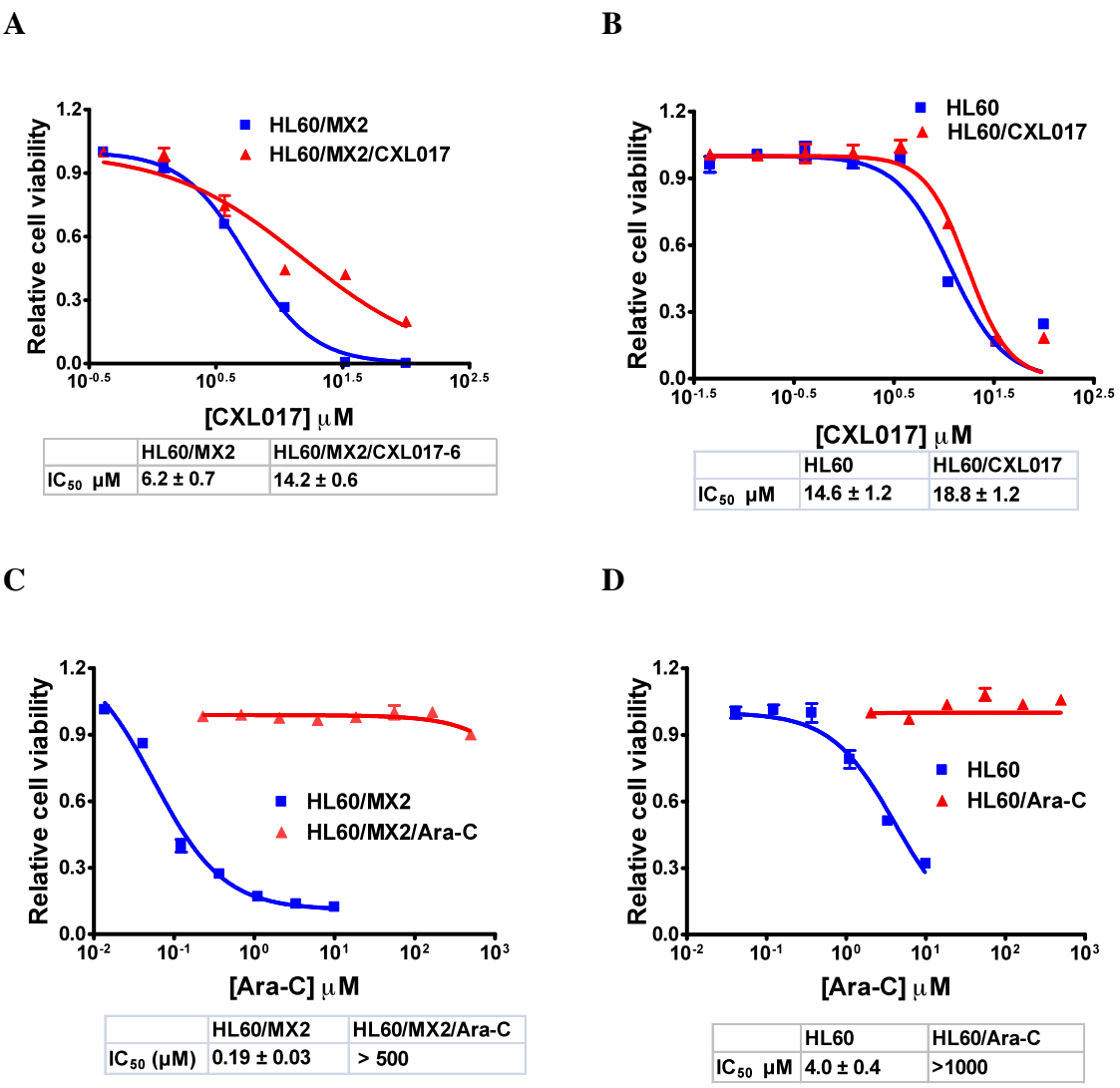

	HL60/MX2	HL60/MX2/CXL017-6
IC_{50} μM	6.2 ± 0.7	14.2 ± 0.6

	HL60	HL60/CXL017
IC_{50} μM	14.6 ± 1.2	18.8 ± 1.2

	HL60/MX2	HL60/MX2/Ara-C
IC_{50} (μM)	0.19 ± 0.03	> 500

	HL60	HL60/Ara-C
IC_{50} μM	4.0 ± 0.4	>1000

Figure 4.2. In vitro cytotoxicity of CXL017 and Ara-C in HL60 and HL60/MX2 cells exposed to the drugs for 6 months

A, dose-dependent effect of CXL017 on the cell viability of HL60/MX2 and HL60/MX2/CXL017 cells. B, dose-dependent effect of CXL017 on the cell viability of HL60 and HL60/CXL017 cells. C, dose-dependent effect of Ara-C on the cell viability of HL60/MX2 and HL60/MX2/Ara-C cells. D, dose-dependent effect of Ara-C on the cell viability of HL60 and HL60/Ara-C cells

A B

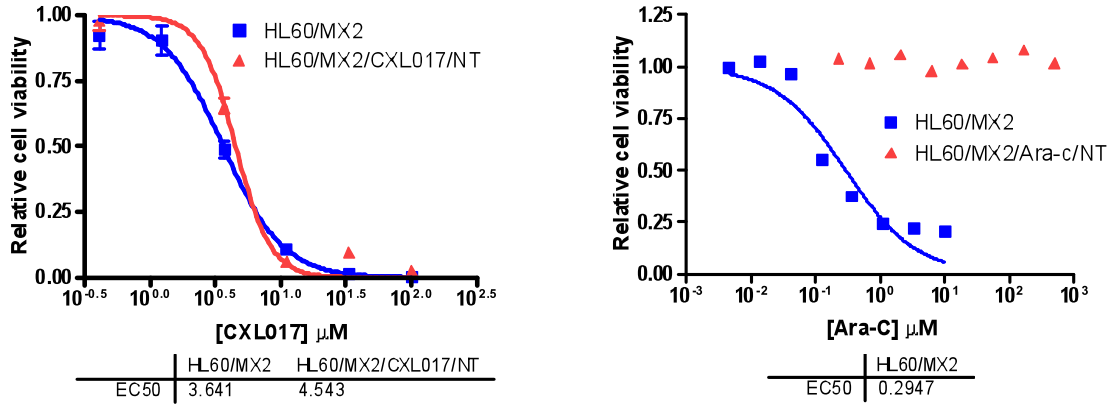

Figure 4.3. *In vitro* cytotoxicity of CXL017 and Ara-C in HL60/MX2/CXL017/NT and HL60/MX2/Ara-C /NT cells.

A, HL60/MX2/CXL017/NT cells lose the transient resistance towards CXL017 upon culturing in the absence of CXL017 for 2 months. B, HL60/MX2/Ara-C/NT cells demonstrate stable resistance when cultured in the absence of Ara-C.

A B

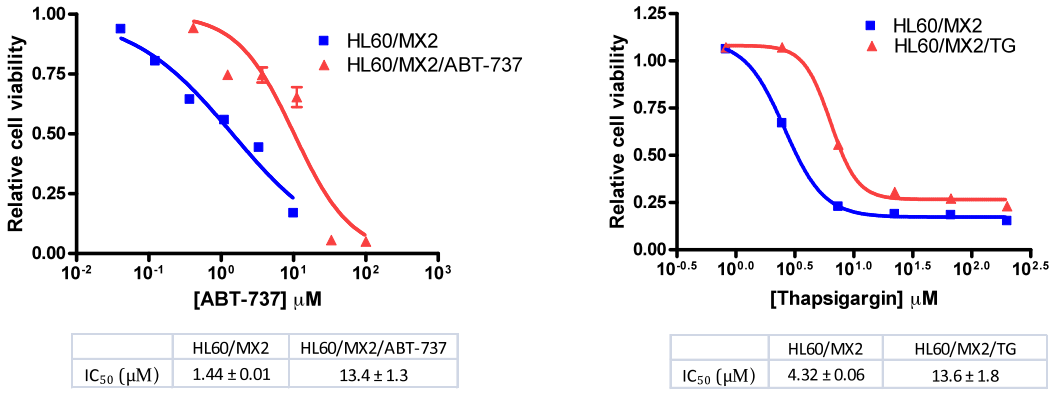

Figure 4.4. *In vitro* cytotoxicity of ABT-737 and Thapsigargin in HL60/MX2/ABT-737 and HL60/MX2/TG cells

A, HL60/MX2/ABT-737 develops 10-fold resistance to ABT-737 in 3months. B, HL60/MX2/TG develops 3-fold resistance to thapsigargin in 3months.

4.2.3. HL60/MX2 cells exposed to CXL017 demonstrate collateral sensitivity towards standard chemotherapeutic agents

Although HL60/MX2 cells failed to develop stable resistance to CXL017, it remains to be determined if these cells acquire MDR after prolonged exposure to CXL017. Therefore, we evaluated the cytotoxicity of standard anticancer agents against HL60/MX2/CXL017 cells and HL60/MX2/Ara-C cells. As expected, our results show that HL60/MX2/Ara-C cells demonstrate cross-resistance against all the agents tested except etoposide and CXL017 (Table 4.1). Very surprisingly, HL60/MX2/CXL017 cells demonstrate (10 to 100-fold) collateral sensitivity towards all the agents tested, particularly the main-line therapies (Table 4.1), except thapsigargin, which gains ~ 30-fold resistance. In comparison, HL60/MX2/ABT-737 and HL60/MX2/TG cells do not demonstrate any extent of collateral sensitivity to mitoxantrone (Figure 4.5). In addition, HL60/CXL017 cells that do not demonstrate resistance to CXL017 also reveal moderate levels of collateral sensitivity towards standard therapy like mitoxantrone and Ara-C (Table 4.1).

Table 4.1. IC_{50} values of various anticancer agents in the cell exposed to CXL017 and Ara-C for 6 months

Compounds	HL60	HL60/MX2	HL60/MX2/CXL017	HL60/MX2/Ara-C	HL60/CXL017
	((IC_{50} (nM) ± SEM)[a]				
MX	16 ± 2	724 ± 81	6.5 ± 0.8	1870 ± 400	9.02 ± 0.5
Dox	140 ± 16	1223 ± 336	60.7 ± 9.4	1800 ± 400	137 ± 4.8
Ara-C	4000 ± 390	362 ± 86	33.5 ± 4	> 500000	2057 ± 281
Etoposide	1620 ± 63	14600 ± 1400	360 ± 20	18900 ± 3100	1300 ± 360
CXL017	14600 ± 1200	4200 ± 690	14200 ± 600	3400 ± 400	18800 ± 1200
ABT-737	1391 ± 380	2740 ± 170	232 ± 15	8800 ± 500	1250 ± 215
Thaps	3000 ± 105	6.5 ± 0.2	192 ± 9.0	24 ± 3	38 ± 2.9

[a]Data represented are an average of three independent experiments with their SEM

These results prompted us to determine how quickly cancer cells could develop collateral sensitivity to the standard agents upon CXL017 exposure. Therefore, we tested the sensitivity of HL60/MX2 cells exposed to CXL017 for 2 months (HL60/MX2/CXL017-2) and for 4 months (HL60/MX2/CXL017-4) against all the standard agents (Table 4.2). Our results show that HL60/MX2/CXL017-4 cells demonstrate similar sensitivity towards the standard agents as observed with HL60/MX2/CXL017 cells while HL60/MX2/CXL017-2 overall shows no difference relative to HL60/MX2. Very interestingly, HL60/MX2/CXL017/NT cells that have lost their resistance towards CXL017 still retain collateral sensitivity towards standard agents

(Table 4.2) but lose their resistance to TG. These findings suggest that cells exposed to CXL017 are re-sensitized to standard agents as early as 4 months after exposure and such collateral sensitivity is stable in the absence of further CXL017 challenge.

Table 4.2. IC_{50} values of various anticancer agents in cells exposed to CXL017 2-6 months

Compounds	HL60/MX2	HL60/MX2/CXL017-2	HL60/MX2/CXL017-4	HL60/MX2/CXL017	HL60/MX2/CXL017/NT
	(IC_{50} (nM) ± SEM)[a]				
MX	724 ± 81	1205 ± 70	3.7 ± 1.1	6.5 ± 0.8	4.1 ± 0.1
Dox	1223 ± 336	2251 ± 737	52 ± 18	61 ± 9.0	54.7 ± 7.0
Ara-C	362 ± 86	1988 ± 703	39 ± 12	34 ± 4.0	13.2 ± 7.4
Etoposide	14600 ± 1400	12700 ± 1500	220 ± 40	360 ± 20	230 ± 22
CXL017	4200 ± 690	6200 ± 600	6600 ± 900	14200 ± 600	4600 ± 500
ABT-737	2740 ± 170	2559 ± 488	486 ± 109	232 ± 15	307 ± 63
TG	6.5 ± 0.2	8.9 ± 1.4	94 ± 29	192 ± 9.0	14.5 ± 4.5

[a] Data represented are an average of three independent experiments with their SEM

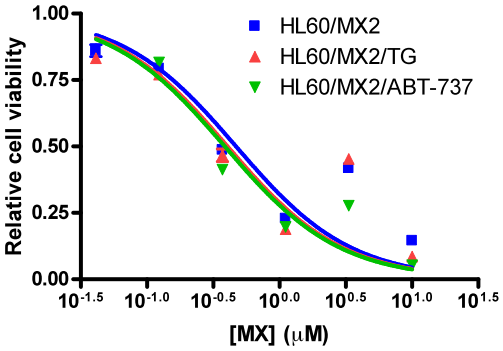

	HL60/MX2	HL60/MX2/TG	HL60/MX2/ABT-737
IC_{50} (μM)	0.41 ± 0.04	0.32 ± 0.06	0.46 ± 0.05

Figure 4.5. *In vitro* cytotoxicity of Mitoxantrone in HL60/MX2/TG and HL60/MX2/ABT-737 cells

4.2.4. CXL017 exposure causes significant changes in Bcl-2 family proteins, SERCA proteins, and ER calcium content but no changes in P-gp and BCRP

In order to explore the potential mechanism for the collateral sensitivity observed in CXL017 exposed cells, HL60/MX2 cells exposed to CXL017 were evaluated for changes among Bcl-2 family proteins and SERCA proteins via western blot analysis with HL60/MX2/Ara-C cells included for comparison. The levels of Bak proteins remain unchanged amongst the HL60/MX2 cell lines irrespective of treatment history. Bcl-X_L protein was significantly over-expressed in HL60/MX2/CXL017-4, HL60/MX2/CXL017, and HL60/MX2/CXL017/NT cells but not in cells with other treatment regimens (Figure 4.6, Lanes 4-6). In clear contrast to Bcl-X_L, the level of Mcl-1

and Bax was heavily down regulated in cell lines exposed to CXL017 for 4 months or longer, which are sensitized to standard therapies. No significant changes were observed in cells with the other treatment regimens (Figure 4.6, Lanes 4-6). There was a slight decrease in the level of Bcl-2 protein among cells exposed to CXL017 for ≥ 2 months, while its level bounced back in HL60/MX2/CXL017/NT cells (Figure 4.6, Lane 3 and 6). The fact that Bcl-2 levels started decreasing in HL60/MX2/CXL107-2 cells, which were not yet sensitized to standard therapy, and the levels bounced back in HL60/MX2/CXL017/NT cells, which continue to be sensitive towards standard therapies, suggests that the protein level changes in Bcl-2 among these cells is not responsible for the CXL017 induced re-sensitization. However, there is a possibility that the decrease in Bcl-2 levels in the CXL017 exposed cells is responsible for the transient resistance observed towards CXL017. Contrary to the effects of CXL017 exposure, Ara-C exposure to HL60/MX2 cells had no effect on any of the Bcl-2 family proteins evaluated, supporting that these changes are CXL017 specific and the Bcl-2 family proteins are involved in the mechanism of action of CXL017 (Figure 4.6, Lane 1).

In summary, based on the reported functions of Mcl-1, and the correlation observed with its expression levels and the drug sensitivity profiles of HL60/MX2 exposed to CXL017 (Table 2), the down-regulation of Mcl-1 is likely responsible for the increased sensitivity of these cell lines to standard therapies. There is literature precedent showing that over-expression of Mcl-1 can lead to MDR.[46, 115, 151] Furthermore, independent research groups have shown that down regulation of Mcl-1 using siRNA resensitizes resistant cancer cells to chemotherapy.[152-154] Altogether, these results indicate

that lowered Mcl-1 expression in CXL017 exposed HL60/MX2 cells is one of the factors responsible for the re-sensitization of these cells to therapy. The role of up-regulation of Bcl-X_L and down-regulation of Bax in the CXL017 exposed cells is not clear, as these protein changes based on their function should have induced resistance in these cell lines. However, it is possible that the extent of changes in Bcl-X_L and Bax was not sufficient to counterbalance the loss of Mcl-1. It is also possible that BH3 only members of the Bcl-2 family proteins are regulating the activity of Bcl-X_L and Bax proteins in these cell lines.[155] Investigation on the levels of BH3 only proteins in these cell lines is currently underway.

In addition to changes in the Bcl-2 family proteins, the drug-resensitized cell lines reveal a further over-expression of the SERCA2 and SERCA3 with > 2 months CXL017 treatment (Figure 4.6, Lanes 4-6). Starting at 4 months treatment, both SERCA2 and SERCA3 proteins were heavily upregulated and stayed elevated through the 6 months treatment with a slight dip in HL60/MX/CXL017/NT. The HL60/MX2/Ara-C cell line had much weaker changes in SERCA proteins with a slight increase in the level of SERCA2 and a slight reduction in that of SERCA3 (Figure 4.6, Lane 1). Nonetheless, the up-regulation of SERCA2 and SERCA3 and the reduction of ER calcium content may account for the resistance of the cells to thapsigargin treatment (Table 4.2), again distinguishing CXL017 from a typical SERCA inhibitor.

Finally, ER calcium content was also measured for HL60/MX2, HL60/MX2/CXL017-2, HL60/MX2/CXL017-4, HL60/MX2/CXL017/NT, and HL60/MX2/Ara-C (Figure 4.7). HL60/MX2/CXL017-4 and HL60/MX2/CXL017/NT

cells both had significantly lower levels of ER calcium compared to HL60/MX2 cells despite having increased levels of SERCA2 and SERCA3. This is in contrast to what was observed between HL60 to HL60/MX2 cell lines where HL60/MX2 cells have increased levels of both SERCA and calcium. It has been shown in literature that cells lacking Bax and Bak demonstrate decreased ER calcium content when compared to wild type.[156, 157] Therefore, it is also possible that the decrease in ER calcium content in drug-resensitized cells is due to the down regulation of Bax in these cells. There was no difference in ER calcium content in the HL60/MX2/CXL017-2 or HL60/MX2/Ara-C cell lines in comparison to HL60/MX2.

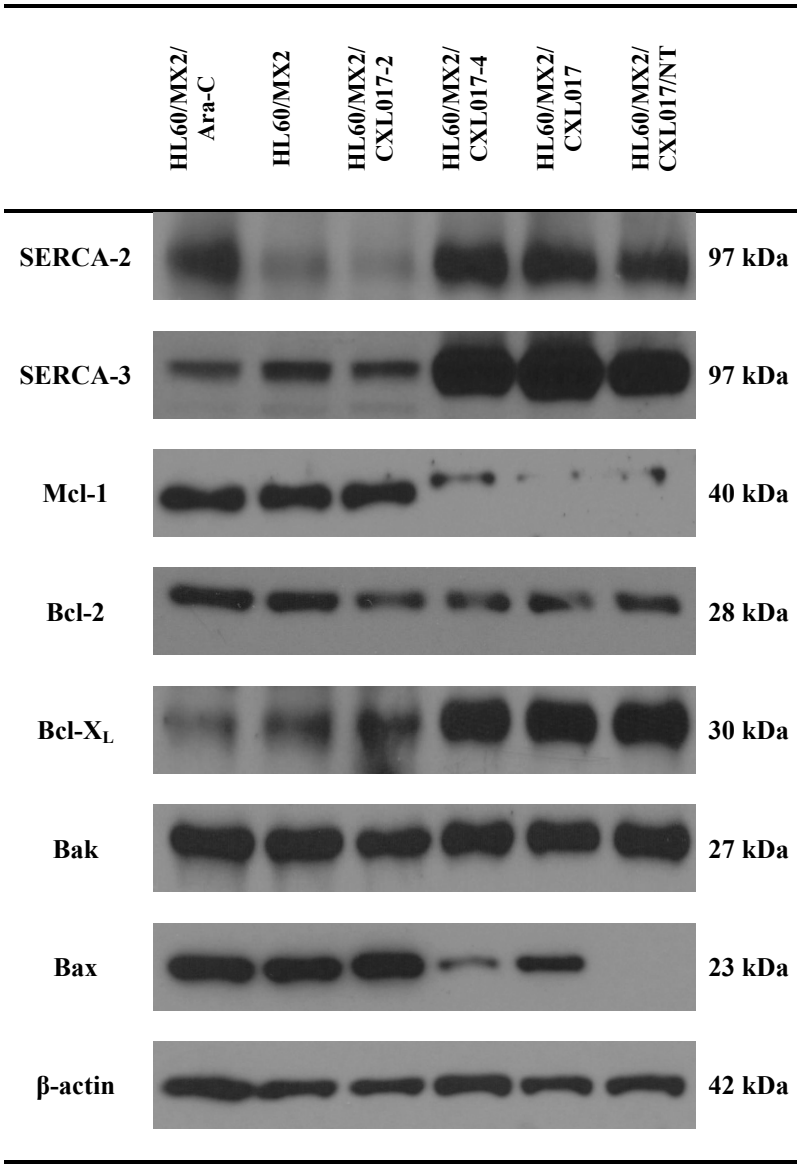

Figure 4.6. Western Blotting analysis of CXL017 treated HL60/MX2 Cells

Total cell lysates from HL60/MX2/Ara-C, HL60/MX2, HL60/MX2/CXL017-2, HL60/MX2/CXL017-4, HL60/MX2/CXL017, or HL60/MX2/CXL017/NT were separated by SDS-PAGE and immunoblotted with mouse monoclonal anti-SERCA2, SERCA3, Bcl-2, Bax, or rabbit polyclonal anti-Mcl-1, Bcl-X_L, or Bak. Mouse monoclonal anti-Actin was used as a protein loading control. Three independent experiments were conducted with similar results. (Performed by David Hermanson)

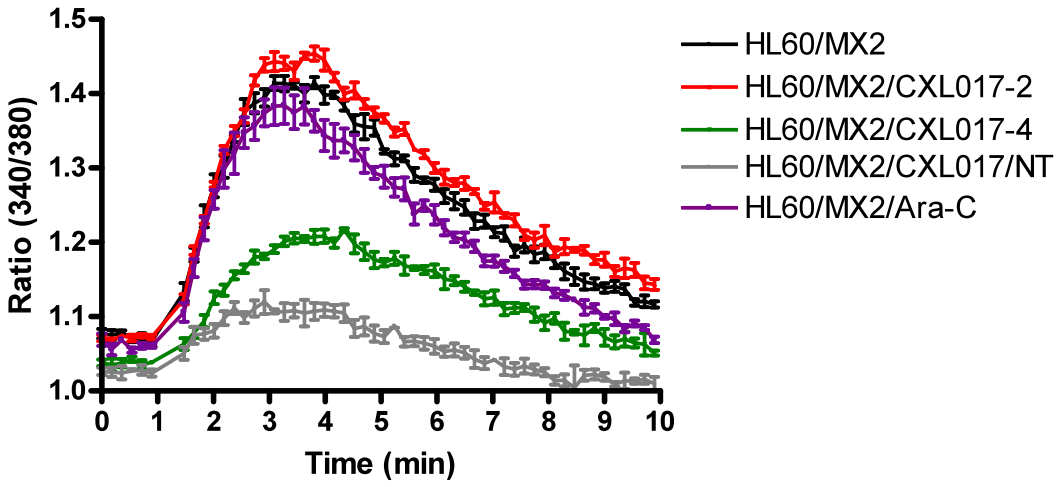

Figure 4.7. Endoplasmic reticulum calcium content in HL60/MX2 cells exposed to CXL017 and Ara-C

ER calcium levels were measured in HL60/MX2, HL60/MX2/CXL017-2, HL60/MX2/CXL017-4, HL60/MX2/CXL017/NT, or HL60/MX2/Ara-C. Three independent experiments were averaged and the ratio of 340/380 nm was plotted with the shown error bars. HL60/MX2/CXL017-4 and HL60/MX2/CXL017/NT show significantly lower levels of ER calcium release by TG. (Performed by David Hermanson)

In order to determine if ABC transporter proteins had any role in the increased sensitivity of the CXL017 exposed cells towards chemotherapy, we measured the levels of P-gp and BCRP in these cell lines. As we have observed in HL60 and HL60/MX2 cells, exposure of CXL017 or Ara-C did not introduce clear and significant changes in P-gp and BCRP (Figure 4.8A and B), eliminating the potential involvement of ABC transporter proteins in CXL017 induced collateral sensitivity in HL60/MX2 cells.

Overall, we have observed strong correlation between CXL017 induced sensitivity towards standard therapies and the levels of Mcl-1 and ER calcium content among these cell lines. The calcium content changes among these cells indicate that raised levels of ER calcium content may play a role in acquired drug resistance in HL60/MX2 cells and altering the ER calcium content may be an effective way to overcome drug resistance. The specific role of these changes is currently under investigation.

A B

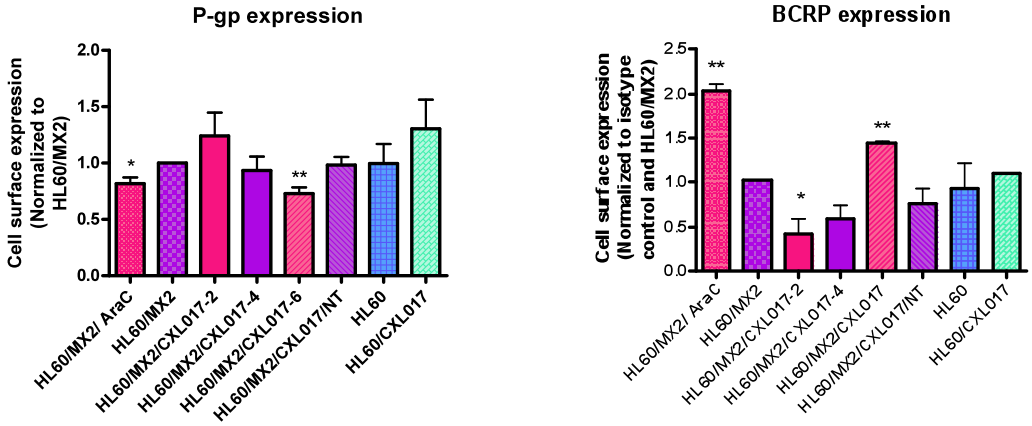

Figure 4.8. Flow cytometric analysis of P-gp and BCRP expression in HL60/MX2 cells exposed to CXL017 and Ara-C.

A, The data represented is an average of three independent experiment and depicts the fold difference of P-gp expression in comparison to HL60/MX2, * signifies $P< 0.05$. B, The data represented is an average of three independent experiment and depicts the fold difference of BCRP expression in comparison to HL60/MX2, * signifies $P \leq 0.05$, ** signifies $P \leq 0.01$.

4.3. Conclusion

In summary, in this study we demonstrate that HL60/MX2 failed to develop stable resistance to CXL017 upon prolonged exposure. On the contrary, HL60/MX2 acquired greater than 2000-fold resistance to cytarabine (Ara-C) – the major first-line chemotherapy for the treatment of acute myeloid leukemia (AML). The failure of HL60/MX2 cells to develop resistance towards CXL017 is of particular importance as rapid development of resistance to chemotherapy is a major concern in cancer therapy. In addition, remarkably, instead of acquiring further cross-resistance, HL60/MX2 cells exposed to CXL017 were re-sensitized to standard therapies (10 to 100-fold) after exposure to CXL017 for 4 months. Western blotting analyses revealed that exposure to CXL017 for 4 months significantly down-regulates Mcl-1 and Bax but causes up-regulation of Bcl-X_L, SERCA2, and SERCA3 proteins. CXL017 exposure also causes a reduction in ER calcium content. Given the well-established functions of Bcl-2 family proteins and ER calcium in drug resistance, our results suggest that the reduction in Mcl-1 and the decrease in ER calcium content are responsible for CXL017 induced chemosensitization of MDR cancer cells. These results taken together demonstrate the unique biological activity of CXL017 and strongly support the clinical potential of CXL017-based cancer therapies with minimum risk of acquired drug resistance, particularly against MDR malignancies.

4.4. Experimental procedures

4.4.1. Chemicals and Reagents

CXL017 [Ethyl-2-amino-6-(3,5-dimethoxyphenyl)-4-(2-ethoxy-2-oxoethyl)-4*H*-chromene-3-carboxylate] was synthesized and characterized by NMR and mass spectrometry, as previously described. ABT-737 was synthesized following published procedures. [158] Fura-2AM was from Invitrogen (Carlsbad, CA). TG was obtained from Acros Organics (Geel, Belgium). All the drugs including mitoxantrone, Ara-C, etoposide, and doxorubicin were obtained from commercial sources. Probenecid was obtained from Sigma-Aldrich (St Louis, MO). CellTiter-Blue Assay Kit was from Promega (Madison, WI). The SERCA2 (1:300), SERCA3 (1:200), Mcl-1 (1:400), Bcl-X_L (1:750), Bax (1:200) antibodies were from Santa Cruz Biotechnology, Inc. (Santa Cruz, CA) and used at the specified dilution respectively. The anti-Bak antibody was from Millipore (address) and was used at a final dilution of 1:300. The anti-Bcl-2 antibody (1:1000), the anti-β-actin (1:40000) antibody, the anti-mouse (1:3000) secondary antibodies were from Sigma–Aldrich (St. Louis, MO) and used at the specified dilution respectively.

4.4.2. Cell Culture

HL60 and HL60/MX2 were purchased from ATCC. HL60 cell line and its derivative cell lines were grown in IMDM glutamax media supplemented with 20% FBS. HL60/MX2 cell line and its derivative cell lines were grown in RPMI 1640 supplemented with 10% FBS. All cell lines were incubated at 37 °C with 5% CO_2 in air atmosphere.

4.4.3. Evaluation of Cell Viability

Leukemic cells were plated at a density of 1 x 10^4 cells/well in a 96-well round-bottom plate. Test compounds were added at varying concentrations in 0.5-1% DMSO and cells treated with medium containing the same amount of DMSO served as a control. After a 48 h treatment, relative cell viability in each well was determined using the CellTiter-Blue Cell Viability Assay. The IC_{50} of each compound was determined by fitting the relative viability of the cells to the drug concentration, using a dose-response model in Prism program from GraphPad Software, Inc. (San Diego, CA).

4.4.4. Determination of ER Calcium Content

Cells at a density of 1 x 10^6 cells/mL were incubated in medium containing 5 μM Fura-2AM and 2.5 mM probenecid at room temperature in the dark for 1 h. The cells were then washed once with cold PBS and re-suspended to a concentration of 2 x 10^6 cells/mL in medium containing 2.5 mM probenecid. 750 μL of the cell suspension was added to a cuvette with 735 μL media containing 100 mM EGTA and 2.5 mM probenecid. The cell suspension was mixed by pipetting slowly. Under this condition, the cell media contained negligible amount of free calcium. Therefore, the cells had no extracellular calcium source. Fluorescence emission was measured for 1 min followed by adding 15 μL DMSO solution of thapsigargin, and readings were continued for another 9 min. Readings were obtained on a dual wavelength fluorometer (Cary Eclipse, Varian, Palo Alto, CA) with excitation wavelengths alternating between 340 and 380 nm and an emission wavelength of 510 nm.

4.4.5. Western Blotting Analysis

Western blotting was conducted using standard chemiluminescent techniques, as previously described.[141] Following overnight incubation in primary antibody at 4°C, the blot was washed and secondary staining was accomplished using corresponding IgG conjugated to HRP. Protein loading was assessed using anti-beta actin.

4.4.6. Flow Cytometry Analysis

To detect and quantify P-gp and breast cancer resistance protein (BCRP), cells (1×10^6) were blocked with normal mouse serum for 10 min, followed by incubation for 1 h with phycoerythrin (PE)-conjugated UIC2 (Anti-Human P-gp PE) (ebiosciences, CA), PE-conjugated 5D3(Anti-Human BCRP PE) (ebiosciences, CA) with PE conjugated isotype IgG1 as control. After 1 h of incubation, the cells were washed and fixed in 50 µL of 10% formalin overnight at 4°C. The fluorescence intensity was measured using a flow cytometer (BD FACS calibur, BD Biosciences). Protein level was determined by subtracting the mean fluorescence intensity of the control antibody from each specific antibody (P-gp-IgG1, BCRP-IgG1). For each sample, 25,000 events were collected.

4.4.7. Development of Drug Resistant Cell Lines

HL60 and HL60/MX2 cell lines were exposed to increasing concentration of CXL017 and Ara-C respectively *in vitro*, starting at the IC_{20} value for a period of 6 months with gradual increase of drug concentration while maintaining the survival of most cells. Cell medium was changed twice a week. The sensitivity of these cells to the corresponding drugs was monitored once a month, in which the cells were grown in the absence of drug for a period of 7 days and then evaluated for the sensitivity using cell

viability assay. To determine if the cell lines exposed to drug for 6 months demonstrate stable resistance, they were cultured in the absence of drug for a period of 2 months and then re-evaluated for their drug sensitivity. For additional comparison, HL60/MX2 cells were exposed to ABT-737 (a known Bcl-2 inhibitor) and TG (a known SERCA inhibitor) for a period of 3 months, using the same protocol mentioned earlier.

4.4.8. Statistical Analysis

All biological experiments, including *in vitro* cytotoxicity assays, calcium assays, flow cytometry and western blot, were performed at least three times. Representative results are depicted in this report. Data are presented as means ± Standard error of the mean (SEM), and comparisons were made using Student's *t* test. A probability of 0.05 or less was considered statistically significant.

CHAPTER 5*

5. SAR studies of CXL017 and its analogs to develop a more potent and selective compound to target drug resistant malignancies

5.1. Introduction

Thus far we have demonstrated a unique ability of CXL017 to selectively target MDR cancer cells *in vitro* and *in vivo*. We have also shown that CXL017 can synergize with a variety of anticancer agents in MDR cancer cells. In addition, CXL017 has potent cytotoxicity in the NCI-60 panel of cell lines with an average IC_{50} value of 1.04 μM. Most importantly, MDR cancer cells did not develop resistance to CXL017 upon prolonged exposure and instead of gaining cross-resistance were more sensitive to standard therapies. Given these unique features of CXL017, there is a need to understand the importance of various functional groups on CXL017 towards its cytotoxicity and selectivity in MDR cells.

Previous SAR studies of CXL017 mainly focused on its cytotoxicity in Jurkat cells. Therefore in this study, we expand the SAR of CXL017 to study the effect of functional groups on both its cytotoxicity and selectivity in HL60/MX2 MDR cells. Since CXL017 has two methoxy groups on the 3' and 5' position on the phenyl ring relative to sHA 14-1, resulting in ~10-fold improvement in cytotoxicity in both HL60 and

---

*Parts of this chapter have been reproduced with permission from {Das, S. G. et al. Structure–Activity Relationship and Molecular Mechanisms of Ethyl 2-Amino-6-(3,5- dimethoxyphenyl)-4-(2-ethoxy- 2-oxoethyl)-4H-chromene- 3-carboxylate (CXL017) and Its Analogues *J Med Chem* **2011,** 54, 5937-48}.

HL60/MX2 cells, we designed molecules (CXL025-028) (Table 5.1) to investigate the importance of the number of methoxy groups and their position on the phenyl ring. Previous SAR studies have also shown that the phenyl ring plays an important role in the activity of sHA 14-1; therefore, we evaluated compounds (CXL002-008) (Table 5.2) to determine the effect of the phenyl substitution on selectivity towards MDR cells. Compounds (CXL005, 018, 019, 029, 030) (Table 5.3) were chosen to study the effect of electron donating groups (EDG) on the phenyl ring while compounds CXL023 and CXL024 were evaluated to determine the effect of electron withdrawing groups (EWG). Previous SAR study results also show that substitution at the 4' position on the phenyl ring decreases activity. Here we have expanded our SAR to include fused and extended ring system analogs (CXL021, 022 and 031) (Table 5.3) to further understand the impact of sterics on the activity and selectivity of CXL017. We also designed molecules (CXL032-037) (Table 5.4) with various alkyl and alkynyl groups on the ester at the 3rd and 4th position to evaluate the effect of modulating chain length and flexibility on the ester functionality. To explore the importance of ester functionality at the 3rd and 4th position on the chromene ring, analogs (CXL011-016) (Table 5.5) were evaluated. Finally, the role of the amino functionality at the 2nd position of the chromene ring was explored with the help of compounds CXL038, CXL009 & CXL010 (Table 5.4, 5.5). These compounds were evaluated in HL60 and HL60/MX2 (the drug resistant cell line) to evaluate their cytotoxicity and selectivity.

5.2. Results and Discussion

5.2.1. Chemistry

Compounds (CXL002-CXL024) were synthesized previously with their synthesis and characterization reported in chapter 2. The structures of the new series of 4H-chromene derivatives, designed based on our lead compound CXL017, are depicted in Figure 5.1. Compounds (CXL025-028) were synthesized from their corresponding boronic acids with overall yields of ~ 70%. Compounds (CXL032-037) with various alkyl or alkynyl groups on the ester functionality were synthesized by treating 3′, 5′-dimethoxy phenyl coumarin **(10h)** with ethyl cyanoacetate in the presence of various sodium alkoxides generated in situ as outlined in Scheme 5.1 with overall yields ranging from 45-60%.

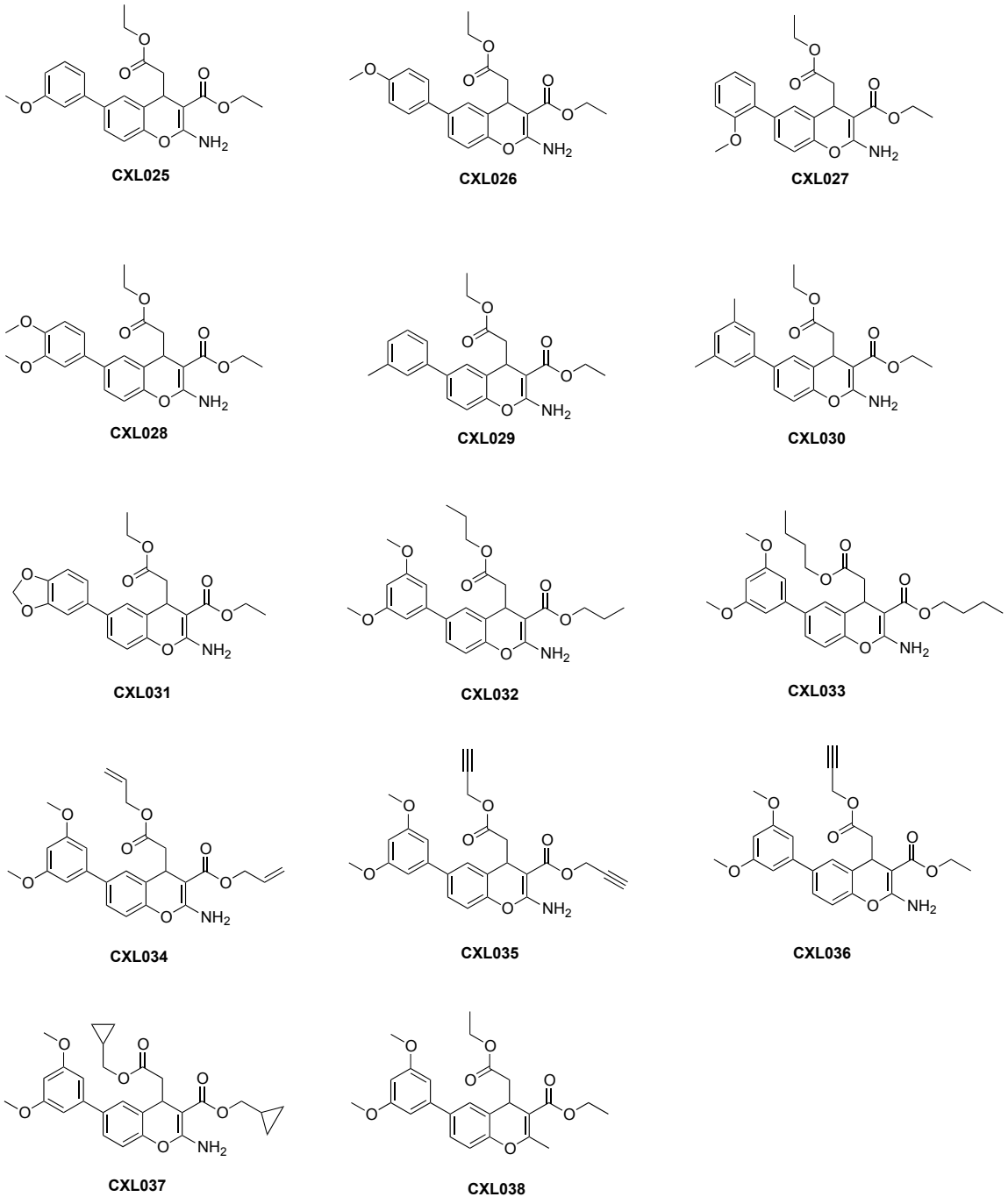

Figure 5.1. Structure of the new series of CXL017 analogs

Compound CXL038 was synthesized from 3′, 5′-dimethoxy phenyl salicylaldehyde **(9h)** using the method described in Scheme 5.2.[159] Briefly, **9h** was

converted to the ester intermediate **11** using a Wittig reaction with 72% yield. Intermediate **11** then underwent an oxa-Michael/Michael addition sequence with ethyl buta-2, 3-dieonate to give compound CXL038 in 82 % yield.

Scheme 5.1. Synthesis of CXL032-037 and CXL034

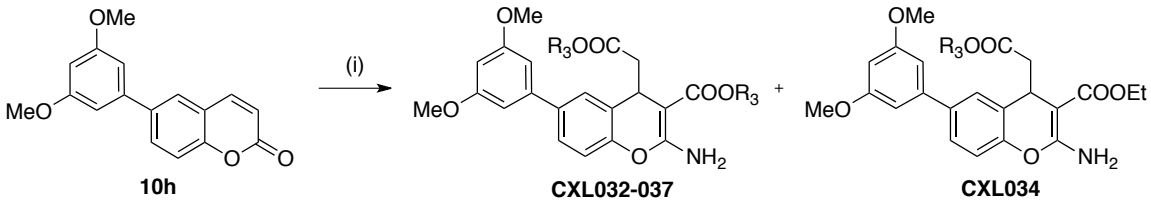

Reagents and condition: (i) Ethyl cyanoacetate, R^3OH, $NaOR^{3,}$ room temp.

Scheme 5.2. Synthesis of CXL038

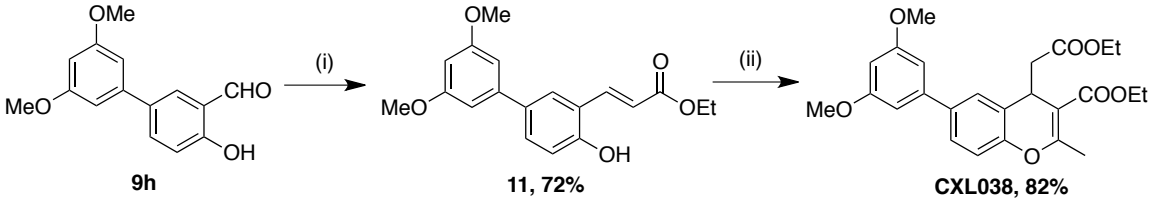

Reagents and condition: (i) $Ph_3P{=}CHCO_2Et$, Toluene, 80 °C (ii) $H_2C{=}C{=}CHCO_2Et$, K_2CO_3 (10 mol%), DMSO, 120°C.

5.2.2. *In vitro* cytotoxicity in HL60 and HL60/MX2 cells

The *in vitro* cytotoxicity results of sHA 14-1, CXL017, 020 and CXL025-28 (Table 5.1) revealed that the number of methoxy groups on the phenyl ring played an important role in the activity. For example, compound sHA14-1 with no methoxy groups shows a significant loss in activity in comparison with analog CXL025 (one methoxy at 3' position) and CXL017 (two methoxy groups at 3' and 5' position). Interestingly, further increasing the number of methoxy groups (CXL020) led to decreased activity in the

HL60/MX2 cells. A possible reason for this observation could be the change in sterics of the ring on addition of a third methoxy group at the 4' position. This observation was further supported by the data from compound CXL026-CXL028 (Table 5.1). Compounds CXL026 and CXL027 that have methoxy groups at 4' and 2' positions of the phenyl ring, respectively, showed decreased activity in comparison to CXL025 that has a methoxy group at the 3' position. In addition, CXL028 with methoxy groups at 3' and 4' position was less active than CXL017. Taken together, these data suggest that the number and relative position of the methoxy groups play an important role in the activity of CXL017.

We showed previously that removal of the phenyl group from the 6^{th} position of the chromene ring leads to a decrease in activity in Jurkat cells.[140] A similar trend was observed when these analogs (CXL002-CXL004) (Table 5.2) were tested in HL60 and HL60/MX2 cells. In addition, moving the phenyl ring to positions 5, 7 and 8 (CXL006-CXL008) on the chromene core also led to a decrease in activity (Table 5.2), suggesting that the 6-phenyl is probably optimal for activity

Table 5.1. IC_{50} values (μM) of analogs 2, CXL025-028 in HL60 and HL60/MX2

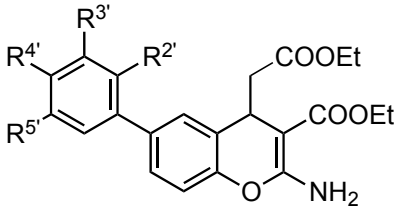

Cmpd.	$R^{2'}$	$R^{3'}$	$R^{4'}$	$R^{5'}$	HL60 IC_{50} ± SEM[a]	HL60/MX2 IC_{50} ± SEM[a]	Selectivity HL60/(HL60/MX2)
CXL017	H	OMe	H	OMe	10.7 ± 0.5	2.43 ± 0.18	4.41
sHA 14-1	H	H	H	H	91.0 ± 0.3	23.2 ± 1.5	3.93
CXL025	H	OMe	H	H	38.7 ± 1.2	9.7 ± 0.5	4.02
CXL020	H	OMe	OMe	OMe	33.3 ± 0.8	28.1 ± 1.0	1.19
CXL026	H	H	OMe	H	66.6 ± 0.3	15.1 ± 0.6	4.41
CXL027	OMe	H	H	H	68.4 ± 1.3	16.0 ± 0.3	4.28
CXL028	H	OMe	OMe	H	54.6 ± 7.2	14.5 ± 0.4	3.77

[a] Results are given as the mean of three independent experiments with triplicate in each experiment

When analogs with EDG (CXL029, 030, 018, 019 and 005) (Table 5.3) were tested, we found that small lipophilic groups like methyl (CXL029, CXL030) led to an improvement in activity, while bulky lipophilic groups, such as *t*-butyl in CXL005, led to a decrease in activity possibly due to unfavorable steric interactions as observed for CXL020. Interestingly, replacing the lipophilic groups with hydrophilic groups like hydroxyl (CXL018, CXL019) also led to a decrease in activity, suggesting that small lipophilic functional groups were optimal for activity. We also tested the effect of EWG

on the phenyl ring (CXL023 & CXL024) and found that substituting electron withdrawing groups led to a decrease in activity.

Table 5.2. IC_{50} values (μM) of analogs CXL002-008 in HL60 and HL60/MX2

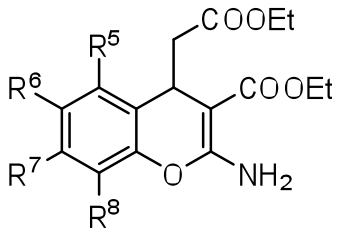

Cmpd.	R^5	R^6	R^7	R^8	HL60 IC_{50} ± SEM[a]	HL60/MX2 IC_{50} ± SEM[a]	Selectivity HL60/(HL60/MX2)
CXL002	H	H	H	H	202 ± 10	99.1± 2.3	2.04
CXL003	H	Br	H	H	74.4 ± 5.6	35.4 ± 0.7	2.10
CXL004	H	*n*-Pr	H	H	79.2 ± 4.2	46.7 ± 1.9	1.70
CXL006	Ph	H	H	H	56.8 ± 2.0	38.7 ± 1.2	1.47
CXL007	H	H	Ph	H	84.5 ± 4.2	34.3 ± 5	2.47
CXL008	H	H	H	Ph	87.3 ± 6.5	44.4 ±3.4	1.97

[a] Results are given as the mean of three independent experiments with triplicate in each experiment.

As observed in an earlier SAR study,[140] steric bulkiness at the 4' position on the phenyl ring led to a decrease in activity. To further explore the importance of the 4' position, we introduced rigidity and flexibility in the scaffold with fused and extended ring system analogs (CXL021-CXL031) (Table 5.3). All of these analogs show a

decrease in activity in comparison to CXL017, further supporting that increased sterics leads to decreased activity.

Table 5.3. IC_{50} values (μM) of analogs CXL029-031 in HL60 and HL60/MX2

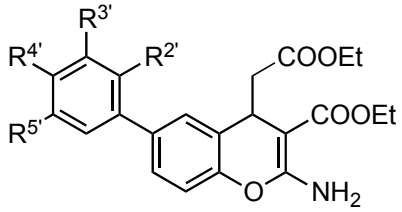

Cmpd.	$R^{2'}$	$R^{3'}$	$R^{4'}$	$R^{5'}$	HL60 IC_{50} ± SEM[a]	HL60/MX2 IC_{50} ± SEM[a]	Selectivity HL60/(HL60 /MX2)
CXL029	H	Me	H	H	12.2 ± 0.6	4.3 ± 0.05	2.82
CXL030	H	Me	H	Me	7.29 ± 0.4	2.46 ± 0.2	2.97
CXL018	H	OH	H	OMe	84.5 ± 8.9	11.9 ± 1.6	7.10
CXL019	H	OH	H	OH	> 400	67.5 ± 5.7	5.93
CXL005	H	H	*t*-BuPh	H	48.3 ± 0.5	24.4 ± 0.4	1.98
CXL023	H	CF_3	H	CF_3	264.5 ± 5.7	81.3 ± 0.5	3.26
CXL024	H	NO_2	H	H	39.2 ± 4.7	13.4 ± 0.76	2.92
CXL021	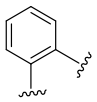		H	H	39.5 ± 2.8	15.1 ± 1.9	2.61
CXL022	H			H	57.7 ± 1.9	18.2 ± 1.7	3.17
CXL031	H			H	73.1 ± 1.5	19.2 ± 0.5	3.82

[a] Results are given as the mean of three independent experiments with triplicate in each experiment.

Previously, we showed that changes on the ester did not significantly affect the activity in Jurkat cells.[140] In this study, we evaluated the ester functionality by designing analogs with various alkyl and alkynyl substitutions at the ester position (CXL032-CXL037) (Table 5.4). Interestingly, replacing the ethyl ester with an *n*-propyl (CXL032) slightly improves activity. However, a further increase in chain length to the *n*-butyl ester (CXL033) led to a significant decrease in activity. Interestingly, introducing unsaturation in the propyl group led to a further improvement in activity (CXL034 & CXL035). Analog CXL035 with a propargyl group on the ester is the most active compound with an IC_{50} of (1.53μM) in HL60 cells and an IC_{50} of (0.64μM) in HL60/MX2 cells, about 4 to 7-fold more active than CXL017.

Table 5.4. IC_{50} values (μM) of analogs CXL032-038 in HL60 and HL60/MX2

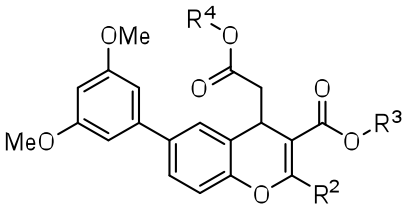

Cmpd.	R^2	R^3	R^4	HL60 IC_{50} ± SEM[a]	HL60/MX2 IC_{50} ± SEM[a]	Selectivity HL60/(HL60/MX2)
CXL032	NH_2	*n*-Pr	*n*-Pr	7.6 ± 0.3	3.9 ± 0.3	1.97
CXL033	NH_2	*n*-Bu	*n*-Bu	32 ± 1.7	14.1 ± 0.5	2
CXL034	NH_2	Allyl	Allyl	4.7 ± 0.3	2.5 ± 0.1	1.62
CXL035	NH_2	C_3H_3	C_3H_3	1.5 ± 0.1	0.64 ± 0.01	2.38
CXL036	NH_2	Et	C_3H_3	4.7 ± 0.2	1.87 ± 0.06	2.54
CXL037	NH_2	Cyclopropyl methyl	Cyclopropylmethyl	6.7 ± 0.5	3.55 ± 0.45	1.87
CXL038	Me	Et	Et	63.6 ± 7.4	9.55 ± 0.90	6.66

[a] Results are given as the mean of three independent experiments with triplicate in each experiment.

Other positions on the chromene core, including the 2nd, 3rd and 4th positions, were also explored. The amino group at the 2nd position was evaluated by acetylation (CXL009 & CXL010) (Table 5.5) or replacement by a methyl (CXL038) (Table 5.4), which resulted in a loss in activity suggesting that the amino group was optimal for

activity. Replacing the ester with CN or amide led to a slight decrease in activity (Table 5.5), suggesting that the ester functionality may be optimal for activity.

Table 5.5. IC_{50} values (μM) of analogs CXL011-010 in HL60 and HL60/MX2

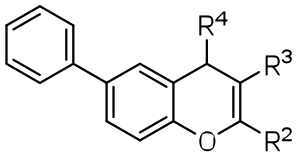

Cmpd.	R^2	R^3	R^4	HL60 IC_{50} ± SEM[a]	HL60/MX2 IC_{50} ± SEM[a]	Selectivity HL60/(HL60 /MX2)
CXL011	NH_2	CN	OEt	76.1 ± 1.1	26.5 ± 5.7	2.87
CXL012	NH_2	CO_2i-Pr	CO_2i-Pr	74.3 ± 6.5	22.1 ± 1.5	3.37
CXL013	NH_2	CO_2Et	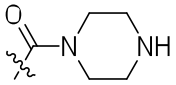	24.9 ± 2.5	38.8 ± 1.04	0.64
CXL014	NH_2	CO_2Et	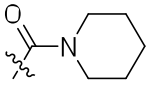	57 ± 6	23.4 ± 3.2	2.44
CXL015	NH_2	CO_2Et	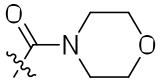	> 400	> 400	1.00
CXL016	NH_2	CO_2Et	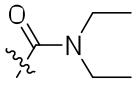	60.0 ±2.7	31.1 ± 1.9	1.93
CXL009	NH(COMe)	CH_2CO_2Et	CO_2Et	79.6 ± 5	44.9 ± 3.8	1.77
CXL010	$N(COMe)_2$	CH_2CO_2Et	CO_2Et	58.9 ± 4.4	45.8 ± 2.2	1.29

[a] Results are given as the mean of three independent experiments with triplicate in each experiment.

5.2.3. Selectivity towards MDR resistant HL60/MX2 cells

The selectivity of these analogs towards MDR resistant cell lines was determined based on the ratio of their IC_{50} in HL60 cells to that in HL60/MX2 cells. We used the Bonferroni multiple comparison test of statistical analysis to classify the compounds into three categories based on their selectivity ratio and statistical analysis. Compounds with selectivity ratios between 0.5-2.0 had a $p > 0.05$, indicating that they are likely to be non-selective. Analogs with a selectivity ratio of 2-4 had a $p < 0.01$ and were considered to have medium selectivity. Analogs with a selectivity ratio of > 4 had a $p < 0.001$ and were considered to have significant selectivity (Figure 5.2).

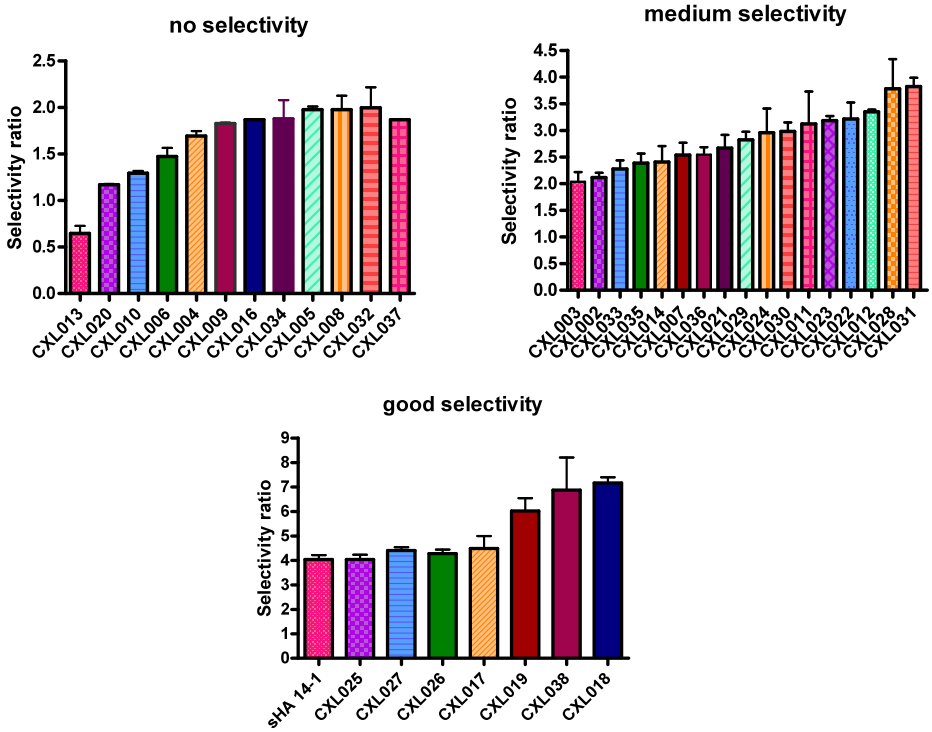

Figure 5.2. Classification of CXL series of analogs based on their selectivity ratio and statistical analysis using Bonferroni test

Based on such criteria, 13 analogs demonstrate no selectivity, 17 analogs demonstrate medium selectivity while 8 analogs (sHA 14-1, CXL017, CXL025, CXL026, CXL027, CXL018, CXL019, and CXL038) demonstrate significant selectivity with CXL018, CXL019, and CXL038 being most selective. Our results show that removing a phenyl group (CXL002-CXL004) from CXL017 led to a decrease in selectivity (Table 5.2). However, removing the methoxy groups (CXL025) or replacing them with other electron donating groups such as a methyl (CXL030) does not change the selectivity (Tables 5.1 and 5.3). In addition, replacing an EDG with an EWG such as NO_2 or CF_3 does not cause significant change in selectivity. These data overall suggest that electronic effect are unlikely to play an essential role in the selectivity of CXL017 towards drug resistant cells. Interestingly, converting the methoxy to a hydroxyl group, compounds CXL018 & CXL019 (Table 5.3), led to an improvement in selectivity, suggesting the hydrophilic nature of a hydroxyl group might play a role in the improved selectivity. Sterically hindered molecules like (CXL021-CXL031) do not show much change in selectivity in comparison to CXL017, indicating that sterics do not play a major role in selectivity of CXL017. Converting the amino group at the second position to a methyl group (CXL038) (Table 5.4) improves the selectivity, suggesting that introducing lipophilic groups at the 2^{nd} position might lead to more selective candidate.

5.3. Conclusion

In conclusion, the results of our current SAR studies suggest that there is no correlation between the selectivity and cytotoxicity of CXL017 analogs in cancer cells.

For example, adding a methoxy group to CXL025 at 5' position (CXL017) improves activity no change in selectivity. On the other hand, replacing a methoxy with a hydroxy (CXL017 vs. CXL018) leads to decreases in activity but improvement in selectivity. Similarly, replacement of the amino group from CXL017 with a methyl (compound CXL038) led to a slight decrease in cytotoxicity but improvement in selectivity. Nonetheless, both selectivity and cytotoxicity of CXL017 are very sensitive to functional modifications.

With our current SAR study we have also developed a more potent and selective analog of CXL017, compound CXL035, which is 4-fold more potent than CXL017. We were also able to improve the selectivity of CXL017 with compounds, CXL030 and CXL038, with a selectivity of 7.1 and 6.7 respectively towards HL60/MX2 MDR cells relative to the parent HL60 cells. Taken together our study has led to the discovery of a series of analogs that selectively target drug resistant cancer cells with the potential for the treatment of drug resistant cancers.

5.4. Experimental procedures

5.4.1. General Procedure for the Synthesis of Salicylaldehydes

5-Bromosalicylaldehyde (1 g, 4.97 mmol), K_2CO_3 (2.061 g, 14.91 mmol), boronic acid (0.9954g, 5.47 mmol), triphenylphosphine (TPP) (1 mol %), and $Pd(OAc)_2$ (1 mol %) were taken in DME:water (1:1) (12 mL). The mixture was stirred at room temperature under an atmosphere of nitrogen for 24 h. The reaction mixture was acidified using HCl (1N) on an ice bath, followed by extraction with ethyl acetate. The extracts were

combined, dried ($MgSO_4$), and the solvent was removed under vacuum. The crude solid was purified by flash chromatography to isolate the desired salicylaldehyde.

5.4.2. 4-Hydroxy-3'-methoxy-[1,1'-biphenyl]-3-carbaldehyde

Yield: 71 %. ^{1}H NMR ($CDCl_3$): δ 11.01 (1H, s), 9.98 (1H, s), 7.76-7.78 (2H, m), 7.37 (1H, t, *J*=4.0 Hz), 7.13 (1H, d, *J*=7.6 Hz), 7.06-7.08 (2H, m), 6.90 (1H, dd, *J*=2.0 Hz, 8.4 Hz), 3.87 (3H, s). ^{13}C NMR (75 MHz, $CDCl_3$): δ 196.66, 161.08, 160.12, 140.83, 135.77, 133.17, 131.92, 130.03, 120.68, 119.08, 118.11, 112.60, 112.55, 55.35.

5.4.3. 4-Hydroxy-4'-methoxy-[1,1'-biphenyl]-3-carbaldehyde

Yield: 76 %. ^{1}H NMR ($CDCl_3$): δ 10.96 (1H, s), 9.97 (1H, s), 7.70-7.74 (2H, m), 7.47-7.49 (2H, m), 7.05 (1H, d, *J*=8.4 Hz), 6.98-7.07 (2H, m), 3.86 (3H, s). ^{13}C NMR (75 MHz, $CDCl_3$): δ 196.70, 160.54, 159.20, 135.45, 133.07, 131.93, 131.34, 127.66, 120.70, 118.05, 114.41, 55.39.

5.4.4. 4-Hydroxy-2'-methoxy-[1,1'-biphenyl]-3-carbaldehyde

Yield: 65 %. ^{1}H NMR ($CDCl_3$): δ 11.02 (1H, s), 9.93 (1H, s), 7.70-7.73 (2H, m), 7.29-7.36 (2H, m), 7.01-7.06 (3H, m), 3.83 (3H, s). ^{13}C NMR (75 MHz, $CDCl_3$): δ 196.78, 160.63, 156.36, 138.43, 134.47, 130.38, 128.94, 128.67, 121.01, 120.34, 117.24, 111.24, 111.07, 55.55.

5.4.5. 4-Hydroxy-3',4'-dimethoxy-[1,1'-biphenyl]-3-carbaldehyde

Yield: 78 %. ^{1}H NMR ($CDCl_3$): δ 10.97 (1H, s), 9.97 (1H, s), 7.70-7.73 (2H, m), 7.04-7.10 (3H, m), 6.95 (1H, d, *J*=8.4 Hz), 3.96 (3H, s), 3.93 (3H, s). ^{13}C NMR (75 MHz, $CDCl_3$): δ 196.67, 160.64, 149.35, 148.72, 135.56, 133.26, 132.40, 131.46, 120.67, 118.96, 118.06, 111.62, 109.96, 56.02.

5.4.6. 4-Hydroxy-3'-methyl-[1,1'-biphenyl]-3-carbaldehyde

Yield: 67 %. ^{1}H NMR ($CDCl_3$): δ 10.99 (1H, s), 9.98 (1H, s), 7.76 (2H, m), 7.35 (3H, m), 7.18 (1H, m), 7.07 (1H, d, *J*=8.4 Hz), 2.43 (3H, s). ^{13}C NMR (75 MHz, $CDCl_3$): δ 196.69, 160.92, 139.32, 138.66, 135.79, 133.46, 131.86, 128.90, 128.15, 127.39, 123.70, 120.71, 118.06, 21.54.

5.4.7. 4-Hydroxy-3',5'-dimethyl-[1,1'-biphenyl]-3-carbaldehyde

Yield: 53 %. ^{1}H NMR ($CDCl_3$): δ 10.99 (1H, s), 9.99 (1H, s), 7.77 (2H, m), 7.18 (2H, s), 7.07 (1H, d, *J*=8.4 Hz), 7.02 (1H, s), 2.40 (6H, s). ^{13}C NMR (75 MHz, $CDCl_3$): δ 196.72, 160.86, 139.31, 138.56, 135.83, 133.57, 131.85, 129.03, 124.52, 120.68, 117.98, 21.39.

5.4.8. 5-(Benzo[d][1,3]dioxol-5-yl)-2-hydroxybenzaldehyde

Yield: 58 %. ^{1}H NMR ($CDCl_3$): δ 10.96 (1H, s), 9.95 (1H, s), 6.67 (2H, m), 7.01 (3H, m), 6.88 (1H, d, *J*=8.0 Hz), 6.01 (2H, s). ^{13}C NMR (75 MHz, $CDCl_3$): δ 196.64, 160.70, 148.33, 147.17, 135.54, 133.73, 133.14, 131.53, 120.65, 120.12, 118.08, 108.73, 107.19, 101.28.

5.4.9. General Procedure for the Synthesis of Coumarin

To *N,N*-dimethylacetamide (1.98 mmol) stirred at 0 ºC, phosphorus oxychloride (1.98 mmol) was added slowly. The reaction mixture was allowed to stir at 0 ºC for 30 min followed by addition of the corresponding salicylaldehyde (0.99 mmol). The reaction mass was then heated at 68-70 ºC for 3 h. Following this, the reaction mass was cooled to room temperature and saturated $NaHCO_3$ solution (10 mL) was added to it. The reaction mass was heated at 68-70 ºC for another 30 min, cooled, and acidified (1 N HCl),

followed by extraction with methylene chloride. The extracts were combined, dried (anhydrous $MgSO_4$), and concentrated under reduced pressure to afford a residue, which upon column chromatography afforded the desired coumarin.

5.4.10. 6-(3-Methoxyphenyl)-2H-chromen-2-one

Yield: 79 %. ^{1}H NMR ($CDCl_3$): δ 7.75 (2H, m), 7.66 (1H, d, *J*=2.4 Hz), 7.36-7.41 (2H, m), 7.14-7.17 (1H, m), 7.09 (1H, t, *J*=2.0 Hz), 6.92-6.95 (1H, m), 6.46 (1H, d, *J*=9.2 Hz), 3.88 (3H, s). ^{13}C NMR (75 MHz, $CDCl_3$): δ 160.68, 160.11, 153.51, 143.45, 140.89, 137.69, 130.78, 130.07, 126.11, 119.51, 119.01, 117.25, 117.08, 113.01, 112.98, 55.57.

5.4.11. 6-(2-Methoxyphenyl)-2H-chromen-2-one

Yield: 82 %. ^{1}H NMR ($CDCl_3$): δ 7.74 (1H, d, *J*=9.6 Hz), 7.70 (1H, dd, *J*=2.4 Hz, 8.4 Hz), 7.63 (1H, d, *J*=2.0 Hz), 7.34-7.38 (2H, m), 7.31 (1H, dd, *J*=2.0 Hz, 7.6 Hz), 6.99-7.07 (2H, m), 6.44 (1H, d, *J*=9.6 Hz), 3.83 (3H, s). ^{13}C NMR (75 MHz, $CDCl_3$): δ 160.97, 156.34, 153.07, 143.73, 135.02, 133.36, 130.69, 129.28, 128.73, 128.54, 121.02, 118.52, 116.61, 116.46, 111.27, 55.56.

5.4.12. 6-(3,4-Dimethoxyphenyl)-2H-chromen-2-one

Yield: 75 %. ^{1}H NMR ($CDCl_3$): δ 7.76 (1H, d, *J*=9.6 Hz), 7.71 (1H, dd, *J*=2.0 Hz, 8.4 Hz), 7.61 (1H, d, *J*=2.4 Hz), 7.38 (1H, d, *J*=8.4 Hz), 7.13 (1H, dd, *J*=2.0 Hz, 8.4 Hz), 7.07 (1H, d, *J*=2.0 Hz), 6.96 (1H, d, *J*=8.4 Hz), 6.46 (1H, d, *J*=9.6 Hz), 3.97 (3H, s), 3.93 (3H, s). ^{13}C NMR (75 MHz, $CDCl_3$): δ 160.73, 153.13, 149.38, 149.04, 143.45, 137.72, 132.36, 132.36, 130.52, 125.62, 119.45, 119.01, 117.21, 117.04, 111.61, 110.30, 56.04.

5.4.13. 6-(m-Tolyl)-2H-chromen-2-one

Yield: 84 %. ^{1}H NMR ($CDCl_3$): δ 7.75 (2H, m), 7.66 (1H, d, *J*=2.0 Hz), 7.34-7.40 (4H, m), 7.21 (1H, d, *J*=6.4 Hz), 6.46 (1H, d, *J*=9.4 Hz), 2.44 (3H, s). ^{13}C NMR (75 MHz, $CDCl_3$): δ 160.74, 153.38, 143.50, 139.38, 138.70, 137.97, 130.79, 128.93, 128.54, 127.84, 126.04, 124.15, 119.00, 117.21, 117.01, 21.53.

5.4.14. 6-(3,5-Dimethylphenyl)-2H-chromen-2-one

Yield: 79 %. ^{1}H NMR ($CDCl_3$): δ 7.76 (1H, d, *J*=9.4 Hz), 7.72 (1H, d, *J*=2.0 Hz), 7.65 (1H, d, *J*=2.4 Hz), 7.19 (2H, s), 6.46 (1H, d, *J*=9.2 Hz), 2.40 (6H, s). ^{13}C NMR (75 MHz, $CDCl_3$): δ 160.79, 153.33, 143.53, 139.38, 138.61, 138.09, 130.82, 129.42, 126.02, 124.97, 118.96, 117.13, 116.96, 21.39.

5.4.15. 6-(Benzo[d][1,3]dioxol-5-yl)-2H-chromen-2-one

Yield: 72 %. ^{1}H NMR ($CDCl_3$): δ 7.72 (1H, d, *J*=8.8 Hz), 7.66 (1H, dd, *J*=2.4 Hz, 8.8 Hz), 7.58 (1H, d, *J*=2.0 Hz), 7.37 (1H, d, *J*=8.4 Hz), 7.03 (2H, m), 6.90 (1H, m), 6.47 (1H, d, *J*=8.4 Hz), 6.02 (2H, s). ^{13}C NMR (75 MHz, $CDCl_3$): δ 160.72, 153.18, 148.38, 147.52, 143.44, 137.59, 133.70, 130.51, 125.69, 120.67, 119.01, 117.07, 108.77, 107.53, 101.35.

5.4.16. General Procedure for the Synthesis of Substituted Ethyl-4Hchromene-3-carboxylate Compounds (CXL025-CXL038).

Freshly cut sodium (0.096 mmol) was added to anhydrous ethanol (2 mL), followed by the addition of ethyl cyanoacetate (0.192 mmol). The reaction mixture was stirred at room temperature under an inert atmosphere for 30 min, followed by the addition of a solution of the corresponding coumarin (0.08 mmol) in anhydrous ethanol (1 mL). The resulting reaction mixture was stirred at room temperature. Upon

consumption of the coumarin, the reaction mass was concentrated, diluted with water (30 mL), and extracted using methylene chloride (3 x 20 mL). The organics were combined, dried ($MgSO_4$), and the solvent removed under vacuum to afford an oil. This crude oil was subjected to column chromatography to afford the pure product.

Compounds CXL025-CXL031, CXL035, 036 and 038 were synthesized by Dr. Balasubramanian srinivasan. Compounds CXL032-CXL034 and CXL037 were synthesized by Nicholas P. Bleeker.

5.4.17. Ethyl 2-amino-4-(2-ethoxy-2-oxoethyl)-6-(3-methoxyphenyl)-4H-chromene-3-carboxylate (CXL025)

Yield: 74 %. ^{1}H NMR ($CDCl_3$): δ 7.46 (1H, d, *J*=2.4 Hz), 7.40 (1H, dd, *J*=2.0 Hz, 8.4 Hz), 7.32 (1H, t, *J*=8.0 Hz), 7.11 (1H, d, *J*=8.0 Hz), 7.06 (1H, t, *J*=2.0 Hz), 7.00 (1H, d, *J*=8.4 Hz), 6.87 (1H, dd, *J*=2.0 Hz, 8.0 Hz), 6.34 (2H, bs), 4.35 (1H, m), 4.23 (2H, q, *J*=7.2 Hz), 4.02 (2H, q, *J*=7.2 Hz), 3.85 (3H, s), 2.59-2.71 (2H, m), 1.33 (3H, t, *J*=7.2 Hz), 1.13 (3H, t, *J*=7.2 Hz). ^{13}C NMR (75 MHz, $CDCl_3$): δ 171.73, 169.04, 161.49, 159.96, 149.54, 141.81, 137.32, 129.78, 127.07, 126.42, 125.89, 119.37, 116.10, 112.60, 112.59, 60.20, 59.54, 55.28, 43.67, 31.38, 14.59, 14.07. MS (ESI, positive) m/z 434.36. Calcd for $C_{23}H_{25}NO_6Na$: 434.17.

5.4.18. Ethyl 2-amino-4-(2-ethoxy-2-oxoethyl)-6-(4-methoxyphenyl)-4H-chromene-3-carboxylate (CXL026)

Yield: 79 %. ^{1}H NMR ($CDCl_3$): δ 7.44-7.47 (2H, m), 7.42 (1H, d, *J*=2.0 Hz), 7.35 (1H, dd, *J*=2.4 Hz, 8.4 Hz), 6.99 (1H, d, *J*=8.4 Hz), 6.95 (1H, d, *J*=8.8 Hz), 6.32 (2H, bs), 4.32-4.35 (1H, m), 4.23 (2H, q, *J*=7.2 Hz), 4.02 (2H, q, *J*=7.2 Hz), 3.84 (3H, s), 2.58-2.70

(2H, m), 1.33 (3H, t, *J*=7.2 Hz), 1.12 (3H, t, *J*=7.2 Hz). ^{13}C NMR (75 MHz, $CDCl_3$): δ 171.76, 169.06, 161.52, 159.05, 149.00, 137.12, 132.88, 127.85, 126.54, 125.92, 125.84, 116.05, 114.21, 60.19, 59.51, 55.34, 43.70, 31.38, 14.58, 14.07. MS (ESI, positive) m/z 434.35. Calcd for $C_{23}H_{25}NO_6Na$: 434.17.

5.4.19. Ethyl 2-amino-4-(2-ethoxy-2-oxoethyl)-6-(2-methoxyphenyl)-4H-chromene-3-carboxylate (CXL027)

Yield: %. ^{1}H NMR ($CDCl_3$): δ 7.40 (1H, d, *J*=2.0 Hz), 7.36 (1H, dd, *J*=2.4 Hz, 8.4 Hz), 7.26-7.32 (2H, m), 6.96-7.03 (3H, m), 6.35 (2H, bs), 4.32-4.35 (1H, m), 4.23 (2H, q, *J*=7.2 Hz), 4.02 (2H, q, *J*=7.2 Hz), 3.83 (3H, s), 2.58-2.69 (2H, m), 1.33 (3H, t, *J*=7.2 Hz), 1.12 (3H, t, *J*=7.2 Hz). ^{13}C NMR (75 MHz, $CDCl_3$): δ 171.75, 169.13, 161.56, 156.37, 148.93, 134.71, 130.68, 129.76, 129.48, 128.90, 128.60, 125.08, 120.84, 115.32, 111.21, 60.13, 59.49, 55.53, 43.75, 31.34, 14.59, 14.04. MS (ESI, positive) m/z 434.36. Calcd for $C_{23}H_{25}NO_6Na$: 434.17.

5.4.20. Ethyl 2-amino-6-(3,4-dimethoxyphenyl)-4-(2-ethoxy-2-oxoethyl)-4H-chromene-3-carboxylate (CXL028)

Yield: 71 %. ^{1}H NMR ($CDCl_3$): δ 7.42 (1H, d, *J*=2.0 Hz), 7.36 (1H, dd, *J*=2.0 Hz, 8.4 Hz), 7.07 (1H, dd, *J*=2.0 Hz, 8.0 Hz), 7.04 (1H, d, *J*=2.0 Hz), 7.00 (1H, d, *J*=8.4 Hz), 6.92 (1H, d, *J*=8.0 Hz), 6.34 (2H, bs), 4.35 (1H, m), 4.23 (2H, q, *J*=7.2 Hz), 4.02 (2H, q, *J*=7.2 Hz), 3.94 (3H, s), 3.92 (3H, s), 2.58-2.67 (2H, m), 1.33 (3H, t, *J*=7.2 Hz), 1.13 (3H, t, *J*=7.2 Hz). ^{13}C NMR (75 MHz, $CDCl_3$): δ 171.76, 169.05, 161.50, 149.15, 149.11, 148.54, 137.33, 133.36, 126.67, 126.06, 125.88, 119.12, 116.06, 111.48, 110.17, 60.18,

59.53, 55.98, 55.93, 43.72, 31.37, 14.58, 14.09. MS (ESI, positive) m/z 464.68. Calcd for $C_{24}H_{27}NO_7Na$: 464.18.

5.4.21. Ethyl 2-amino-4-(2-ethoxy-2-oxoethyl)-6-(m-tolyl)-4H-chromene-3-carboxylate (CXL029)

Yield: 69 %. ^{1}H NMR ($CDCl_3$): δ 7.46 (1H, d, *J*=2.4 Hz), 7.40 (1H, dd, *J*=2.4 Hz, 8.4 Hz), 7.28-7.34 (3H, m), 7.15 (1H, d, *J*=6.4 Hz), 7.01 (1H, d, *J*=8.4 Hz), 6.33 (2H, bs), 4.35 (1H, m), 4.23 (2H, q, *J*=6.8 Hz), 4.02 (2H, q, *J*=7.2 Hz), 2.63 (2H, m), 2.41 (3H, m), 1.33 (3H, t, *J*=6.8 Hz), 1.13 (3H, t, *J*=7.2 Hz). ^{13}C NMR (75 MHz, $CDCl_3$): δ 171.74, 169.07, 161.50, 149.38, 140.27, 138.35, 137.60, 128.68, 127.91, 127.66, 127.01, 126.37, 125.84, 123.95, 116.05, 60.20, 59.53, 43.68, 31.38, 21.52, 14.58, 14.06. MS (ESI, positive) m/z 418.28. Calcd for $C_{23}H_{25}NO_5Na$: 418.17. HPLC purity: 93%

5.4.22. Ethyl 2-amino-6-(3,5-dimethylphenyl)-4-(2-ethoxy-2-oxoethyl)-4H-chromene-3-carboxylate (CXL030)

Yield: 61 %. ^{1}H NMR ($CDCl_3$): δ 7.45 (1H, d, *J*=2.0 Hz), 7.39 (1H, dd, *J*=2.4 Hz, 8.4 Hz), 7.14 (2H, d, *J*=2.0 Hz), 7.00 (1H, d, *J*=8.4 Hz), 6.97 (1H, s), 6.32 (2H, bs), 4.35 (1H, m), 4.23 (2H, q, *J*=7.2 Hz), 4.02 (2H, q, *J*=7.2 Hz), 2.66 (2H, m), 2.37 (6H, m), 1.33 (3H, t, *J*=7.2 Hz), 1.13 (3H, t, *J*=7.2 Hz). ^{13}C NMR (75 MHz, $CDCl_3$): δ 171.74, 169.08, 161.51, 149.32, 104.28, 138.27, 137.71, 128.80, 126.98, 126.36, 125.77, 124.79, 115.98, 60.20, 59.52, 43.68, 31.38, 24.74, 21.39, 14.57, 14.06. MS (ESI, positive) m/z 432.38. Calcd for $C_{24}H_{27}NO_5Na$: 432.19. HPLC purity: 92.2%

5.4.23. Ethyl 2-amino-6-(benzo[d][1,3]dioxol-5-yl)-4-(2-ethoxy-2-oxoethyl)-4H-chromene-3-carboxylate (CXL031)

Yield: 52 %. ^{1}H NMR ($CDCl_3$): δ 7.26-7.48 (2H, m), 6.93-7.01 (2H, m), 6.80-6.89 (2H, m), 5.98 (2H, s), 4.06-4.18 (5H, m), 2.89-3.13 (2H, m), 1.14-1.22 (6H, m).^{13}C NMR (75 MHz, $CDCl_3$): δ 171.71, 166.04, 165.17, 152.80, 148.09, 146.77, 134.81, 134.10, 127.62, 127.18, 124.82, 120.10, 117.00, 108.58, 107.29, 101.12, 63.00, 61.24, 41.79, 36.31, 34.99, 14.00, 13.79. MS (ESI, positive) m/z 448.42. Calcd for $C_{23}H_{23}NO_7Na$: 448.15.

5.4.24. Propyl 2-amino-6-(3,5-dimethoxyphenyl)-4-(2-oxo-2-propoxyethyl)-4H-chromene-3-carboxylate (CXL032)

Yield: 58 %. ^{1}H NMR (400 MHz, $CDCl_3$) δ 7.45 (d, *J* = 2.26 Hz, 1H), 7.40 (dd, *J* = 2.13, 8.41 Hz, 1H), 7.02 (d, *J* = 8.28 Hz, 1H), 6.67 (d, *J* = 2.26 Hz, 2H), 6.46 (t, *J* = 2.26 Hz, 1H), 6.34 (br. s., 2H), 4.37 (dd, *J* = 4.02, 7.78 Hz, 1H), 4.15 (t, *J* = 6.65 Hz, 2H), 3.94 (dt, *J* = 2.38, 6.71 Hz, 2H), 3.85 (s, 6H), 2.58 - 2.75 (m, 2H), 1.75 (sxt, *J* = 7.08 Hz, 2H), 1.53 (qd, *J* = 7.19, 14.31 Hz, 2H), 1.03 (t, *J* = 7.40 Hz, 3H), 0.81 (t, *J* = 7.40 Hz, 3H). ^{13}C NMR (101 MHz, $CDCl_3$) δ 171.74, 169.10, 161.43, 161.05, 149.56, 142.53, 137.44, 127.05, 126.45, 125.79, 116.08, 105.19, 99.21, 65.89, 65.25, 55.40, 43.67, 31.42, 29.69, 22.31, 21.84, 10.66, 10.28. MS (ESI, positive) m/z calcd for $C_{26}H_{31}NO_7$ (M + H), 470.22; found, 470.20.

5.4.25. Butyl 2-amino-4-(2-butoxy-2-oxoethyl)-6-(3,5-dimethoxyphenyl)-4H-chromene-3-carboxylate (CXL033)

Yield: 63 %. ^{1}H NMR (400 MHz, $CDCl_3$) δ 7.45 (d, *J* = 2.26 Hz, 1H), 7.40 (dd, *J* = 2.26, 8.28 Hz, 1H), 7.02 (d, *J* = 8.28 Hz, 1H), 6.68 (d, *J* = 2.26 Hz, 2H), 6.46 (t, *J* = 2.26 Hz, 1H), 6.34 (br. s., 2H), 4.35 (dd, *J* = 4.02, 7.53 Hz, 1H), 4.19 (t, *J* = 6.15 Hz, 2H),

3.98 (t, *J* = 7.53 Hz, 2H), 3.85 (s, 6H), 2.56 - 2.74 (m, 2H), 1.65 - 1.76 (m, 2H), 1.41 - 1.55 (m, 4H), 1.24 (qd, *J* = 7.38, 15.00 Hz, 2H), 0.98 (t, *J* = 7.40 Hz, 3H), 0.84 (t, *J* = 7.40 Hz, 3H). ^{13}C NMR (101 MHz, $CDCl_3$) δ 171.74, 169.10, 161.41, 161.04, 149.53, 142.50, 137.42, 127.05, 126.43, 125.76, 116.06, 105.19, 99.17, 64.18, 63.45, 55.38, 43.66, 31.39, 31.01, 30.53, 19.33, 19.03, 13.78, 13.62. MS (ESI, positive) m/z calcd for $C_{28}H_{35}NO_7$ (M + H), 498.25; found, 498.21.

5.4.26. Allyl 4-(2-(allyloxy)-2-oxoethyl)-2-amino-6-(3,5-dimethoxyphenyl)-4H-chromene-3-carboxylate (CXL034)

Yield: 47 %. ^{1}H NMR (400 MHz, $CDCl_3$) δ 7.46 (d, *J* = 2.01 Hz, 1H), 7.40 (dd, *J* = 2.13, 8.41 Hz, 1H), 7.02 (d, *J* = 8.53 Hz, 1H), 6.67 (d, *J* = 2.26 Hz, 2H), 6.46 (t, *J* = 2.13 Hz, 1H), 6.38 (br. s., 2H), 5.95 - 6.08 (m, 1H), 5.73 - 5.85 (m, 1H), 5.39 (d, *J* = 17.32 Hz, 1H), 5.07 - 5.28 (m, 3H), 4.70 (d, *J* = 5.27 Hz, 2H), 4.48 (d, *J* = 5.77 Hz, 2H), 4.41 (dd, *J* = 4.27, 7.28 Hz, 1H), 3.85 (s, 6H), 2.62 - 2.79 (m, 2H). ^{13}C NMR (101 MHz, $CDCl_3$) δ 171.23, 168.54, 161.75, 161.05, 149.53, 142.44, 137.54, 133.00, 132.02, 127.06, 126.52, 125.66, 118.18, 117.18, 116.11, 105.21, 99.21, 65.01, 64.25, 55.39, 43.58, 31.35. MS (ESI, positive) m/z calcd for $C_{26}H_{27}NO_7$ (M + H), 466.19; found, 466.21.

5.4.27. Prop-2-yn-1-yl 2-amino-6-(3,5-dimethoxyphenyl)-4-(2-oxo-2-(prop-2-yn-1-yloxy)ethyl)-4H-chromene-3-carboxylate (CXL035)

Yield: 43 %. ^{1}H NMR ($CDCl_3$): δ 7.46 (1H, d, *J*=2.0 Hz), 7.40 (1H, dd, *J*=2.0 Hz, 8.4 Hz), 7.02 (1H, d, *J*=8.4 Hz), 6.66 (2H, d, *J*=2.0 Hz), 6.44 (1H, t, *J*=2.0 Hz), 6.39 (2H, br. s), 4.78-4.79 (2H, m), 4.54-4.64 (2H, m), 4.39 (1H, dd, *J*=4.8 Hz, 8.4 Hz), 3.84

(6H, s), 2.66-2.77 (2H, m), 2.47 (3H, t, *J*=2.4 Hz), 2.31 (3H, t, *J*=2.4 Hz). ^{13}C NMR (75 MHz, $CDCl_3$): δ 170.64, 167.88, 162.20, 161.05, 149.45, 142.40, 137.78, 127.09, 126.70, 125.39, 116.19, 105.31, 99.24, 78.68, 75.86, 74.89, 74.28, 55.43, 51.81, 51.16, 43.33, 31.12. MS (ESI, positive) m/z 484.46. Calcd for $C_{26}H_{23}NO_7Na$: 484.15.

5.4.28. Ethyl 2-amino-6-(3,5-dimethoxyphenyl)-4-(2-oxo-2-(prop-2-yn-1-yloxy)ethyl)-4H-chromene-3-carboxylate (CXL036)

Yield: 22 %. ^{1}H NMR ($CDCl_3$): δ 7.46 (1H, d, *J*=2.4 Hz), 7.39 (1H, dd, *J*=2.4 Hz, 8.4 Hz), 7.01 (1H, d, *J*=8.8 Hz), 6.67 (2H, d, *J*=2.0 Hz), 6.44 (1H, t, *J*=2.0 Hz), 6.32 (2H, br. s), 4.53-4.62 (2H, m), 4.38 (1H, q, *J*=7.2 Hz), 4.23 (2H, dd, *J*=4.8 Hz, 8.4 Hz), 3.84 (6H, s), 2.62-2.75 (2H, m), 2.30 (3H, t, *J*=2.4 Hz), 1.33 (3H, t, *J*=7.2 Hz). ^{13}C NMR (75 MHz, $CDCl_3$): δ 170.80, 168.92, 161.50, 161.03, 149.56, 142.49, 137.58, 127.09, 126.61, 125.57, 116.16, 105.32, 99.18, 77.58, 74.87, 59.60, 55.43, 51.73, 43.35, 31.29, 14.59. MS (ESI, positive) m/z 474.15. Calcd for $C_{25}H_{25}NO_7Na$: 474.16. HPLC purity: 88%

5.4.29. Cyclopropylmethyl 2-amino-4-(2-(cyclopropylmethoxy)-2-oxoethyl)-6-(3,5-dimethoxyphenyl)-4H-chromene-3-carboxylate (CXL037)

Yield: 46 %. ^{1}H NMR (400 MHz, CDCl3) δ 7.48 (d, *J* = 2.26 Hz, 1H), 7.40 (dd, *J* = 2.26, 8.28 Hz, 1H), 7.02 (d, *J* = 8.53 Hz, 1H), 6.67 (d, *J* = 2.26 Hz, 2H), 6.45 (t, *J* = 2.26 Hz, 1H), 6.00 - 6.42 (br. s, 2H), 4.40 (dd, *J* = 4.27, 7.28 Hz, 1H), 3.98 - 4.08 (m, 2H), 3.85 (s, 6H), 3.80 (dd, *J* = 1.25, 7.28 Hz, 2H), 2.65 - 2.79 (m, 2H), 1.27 (s, 2H), 0.56 - 0.62 (m, 2H), 0.42 - 0.48 (m, 2H), 0.31 - 0.37 (m, 2H), 0.13 - 0.18 (m, 2H). ^{13}C NMR (101 MHz, $CDCl_3$) δ 170.8, 168.1, 160.4, 160.0, 148.6, 141.5, 136.4, 126.1, 125.4, 124.8,

115.1, 104.2, 98.2, 76.3, 76.0, 75.7, 68.0, 67.1, 54.4, 42.5, 30.4, 28.7, 9.1, 8.7, 2.2, 2.1, 2.1, 2.1. MS (ESI, positive) m/z calcd for $C_{28}H_{31}NO_7$ (M + H), 494.22; found, 494.40. . HPLC purity: 90%

5.4.30. Ethyl 6-(3,5-dimethoxyphenyl)-4-(2-ethoxy-2-oxoethyl)-2-methyl-4H-chromene-3-carboxylate(CXL038)

Yield: 82 %. ^{1}H NMR ($CDCl_3$): δ 7.43 (1H, d, *J*=2.0 Hz), 7.40 (1H, dd, *J*=2.4 Hz, 8.4 Hz), 7.03 (1H, d, *J*=8.4 Hz), 6.66 (2H, d, *J*=2.4 Hz), 6.44 (1H, t, *J*=2.0 Hz), 4.24 (1H, m), 4.05 (2H, q, *J*=7.2 Hz), 4.03 (2H, q, *J*=7.2 Hz), 3.83 (6H, s), 2.68 (1H, dd, *J*=4.4 Hz, 14.8 Hz), 2.56 (1H, dd, *J*= 8.0 Hz, 15.2 Hz), 2.45 (3H, s), 1.34 (3H, t, *J*=6.8 Hz), 2.45 (3H, s), 1.13 (3H, t, *J*=6.8 Hz). ^{13}C NMR (75 MHz, $CDCl_3$): δ 171.32, 166.90, 162.52, 161.07, 150.30, 142.57, 137.47, 126.87, 126.59, 124.49, 116.27, 105.14, 104.72, 99.18, 60.36, 60.35, 55.40, 43.59, 32.4.

5.4.31. (E)-Ethyl 3-(4-hydroxy-3',5'-dimethoxy-[1,1'-biphenyl]-3-yl)acrylate (11)

Yield: 72 %. ^{1}H NMR ($CDCl_3$): δ 8.06 (1H, d, *J*=16 Hz), 7.67 (1H, d, *J*=2.4 Hz), 7.45 (1H, dd, *J*=2.4 Hz, 8.4 Hz), 6.91 (1H, d, *J*=8.4 Hz), 6.73 (1H, d, *J*=16 Hz), 6.67 (2H, d, *J*=2 Hz), 6.50 (1H, s), 6.44 (1H, t, *J*=2.0 Hz), 4.30 (2H, q, *J*= 6.8 Hz), 3.85 (6H, s), 1.36 (3H, t, *J*= 5.4 Hz). ^{13}C NMR (75 MHz, $CDCl_3$): δ 168.23, 161.11, 154.90, 142.44, 140.30, 134.01, 130.11, 127.84, 121.88, 119.04, 116.75, 105.05, 99.00, 60.74, 55.45, 14.33.

5.4.32. Cell cultures

HL60 and HL60/MX2 cells were purchased from ATCC. HL60 cell line was grown in IMDM glutamax media supplemented with 20% FBS. All other cell lines were grown in RPMI 1640 purchased from ATCC supplemented with 10% FBS. All cell lines were incubated at 37 ºC with 5% CO_2 in air atmosphere.

5.4.33. Cell viability measurement

The *in vitro* cytotoxicity of these small molecules were assayed by determining their ability to inhibit the growth of the tumor cells. In brief, the tumor cells were plated in a 96 - well plate (the density of 1 x 10^4 cells/well). The cells were treated with a series of dilutions of the test compounds of varied concentrations with 1 % DMSO in the final cell medium (cells treated with medium containing 1 % DMSO served as a control). After a 48 h treatment, the relative cell viability in each well was determined by using Cell Titer-Blue Cell Viability Assay kit. The IC_{50} of each candidate was determined by fitting the relative viability of the cells to the drug concentration by using a dose-response model in Prism program from GraphPad Software, Inc. (San Diego, CA).

5.4.34. Statistical analysis

The *in vitro* cytotoxicity assay was performed at least twice with triplicates in each experiment. Data are presented as means ± S.D., and comparisons were made using Student's *t* test. The synergism assay was performed as a single replicate with triplicates in each experiment. We performed the Bonferroni multiple comparison analysis for determining significant selectivity ratio's in comparison to no selectivity with a ratio of 1. A probability of 0.05 or less was considered statistically significant.

6. References

1. Gatti, L.; Beretta, G. L.; Cossa, G.; Zunino, F.; Perego, P. ABC transporters as potential targets for modulation of drug resistance. *Mini Rev Med Chem* **2009,** 9, 1102-12.

2. Wu, C.-P.; Hsieh, C.-H.; Wu, Y.-S. The Emergence of Drug Transporter-Mediated Multidrug Resistance to Cancer Chemotherapy. *Mol. Pharmaceutics* **2011,** doi: 10.1021/mp200261n.

3. Li, Y.; Yuan, H.; Yang, K.; Xu, W.; Tang, W.; Li, X. The structure and functions of P-glycoprotein. *Curr Med Chem* **2010,** 17, 786-800.

4. Cotter, T. G. Apoptosis and cancer: the genesis of a research field. *Nat Rev Cancer* **2009,** 9, 501-7.

5. Vaux, D. L.; Strasser, A. The molecular biology of apoptosis. *Proc Natl Acad Sci U S A* **1996,** 93, 2239-44.

6. Degterev, A.; Yuan, J. Expansion and evolution of cell death programmes. *Nat Rev Mol Cell Biol* **2008,** 9, 378-90.

7. Adams, J. M. Ways of dying: multiple pathways to apoptosis. *Genes Dev* **2003,** 17, 2481-95.

8. Kang, M. H.; Reynolds, C. P. Bcl-2 Inhibitors: Targeting Mitochondrial Apoptotic Pathways in Cancer Therapy. *Clin Cancer Res* **2009,** 15, 1126-1132.

9. Ashkenazi, A. Targeting the extrinsic apoptosis pathway in cancer. *Cytokine Growth Factor Rev* **2008,** 19, 325-31.

10. Ashkenazi, A.; Dixit, V. M. Apoptosis control by death and decoy receptors. *Curr Opin Cell Biol* **1999,** 11, 255-60.

11. Ashkenazi, A. Targeting death and decoy receptors of the tumour-necrosis factor superfamily. *Nat Rev Cancer* **2002,** 2, 420-30.

12. Tsujimoto, Y.; Gorham, J.; Cossman, J.; Jaffe, E.; Croce, C. M. The t(14;18) chromosome translocations involved in B-cell neoplasms result from mistakes in VDJ joining. *Science* **1985,** 229, 1390-3.

13. Slavov, N.; Dawson, K. A. Correlation signature of the macroscopic states of the gene regulatory network in cancer. *Proc Natl Acad Sci U S A* **2009,** 106, 4079-84.

14. Korsmeyer, S. J. Programmed cell death: Bcl-2. *Important Adv Oncol* **1993**, 19-28.

15. Youle, R. J.; Strasser, A. The BCL-2 protein family: opposing activities that mediate cell death. *Nat Rev Mol Cell Biol* **2008,** 9, 47-59.

16. Reed, J. C. Bcl-2 family proteins. *Oncogene* **1998,** 17, 3225-36.

17. Reed, J. C. Bcl-2 family proteins: regulators of chemoresistance in cancer. *Toxicol Lett* **1995,** 82-83, 155-8.

18. Reed, J. C. Bcl-2-family proteins and hematologic malignancies: history and future prospects. *Blood* **2008,** 111, 3322-30.

19. Letai, A. Pharmacological manipulation of Bcl-2 family members to control cell death. *J Clin Invest* **2005,** 115, 2648-55.

20. Leber, B.; Lin, J.; Andrews, D. Embedded together: The life and death consequences of interaction of the Bcl-2 family with membranes. *Apoptosis* **2007,** 12, 897-911.

21. Rong, Y.; Distelhorst, C. W. Bcl-2 Protein Family Members: Versatile Regulators of Calcium Signaling in Cell Survival and Apoptosis. *Annu. Rev. Physiol.* **2008,** 70, 73-91.

22. Scorrano, L.; Oakes, S. A.; Opferman, J. T.; Cheng, E. H.; Sorcinelli, M. D.; Pozzan, T.; Korsmeyer, S. J. BAX and BAK regulation of endoplasmic reticulum Ca2+: a control point for apoptosis. *Science* **2003,** 300, 135-9.

23. Hanson, C. J.; Bootman, M. D.; Distelhorst, C. W.; Wojcikiewicz, R. J.; Roderick, H. L. Bcl-2 suppresses Ca(2+) release through inositol 1,4,5-trisphosphate receptors and inhibits Ca(2+) uptake by mitochondria without affecting ER calcium store content. *Cell Calcium* **2008,** 44, 324-38.

24. Pinton, P.; Rizzuto, R. Bcl-2 and Ca2+ homeostasis in the endoplasmic reticulum. *Cell death and differentiation* **2006,** 13, 1409-18.

25. Chen, R.; Valencia, I.; Zhong, F.; McColl, K. S.; Roderick, H. L.; Bootman, M. D.; Berridge, M. J.; Conway, S. J.; Holmes, A. B.; Mignery, G. A.; Velez, P.; Distelhorst, C. W. Bcl-2 functionally interacts with inositol 1,4,5-trisphosphate receptors to regulate calcium release from the ER in response to inositol 1,4,5-trisphosphate. *J Cell Biol* **2004,** 166, 193-203.

26. Hanson, C. J.; Bootman, M. D.; Distelhorst, C. W.; Wojcikiewicz, R. J.; Roderick, H. L. Bcl-2 suppresses Ca2+ release through inositol 1,4,5-trisphosphate

receptors and inhibits Ca2+ uptake by mitochondria without affecting ER calcium store content. *Cell Calcium* **2008,** 44, 324-38.

27. Kuo, T. H.; Kim, H. R.; Zhu, L.; Yu, Y.; Lin, H. M.; Tsang, W. Modulation of endoplasmic reticulum calcium pump by Bcl-2. *Oncogene* **1998,** 17, 1903-10.

28. Dremina, E. S.; Sharov, V. S.; Kumar, K.; Zaidi, A.; Michaelis, E. K.; Schoneich, C. Anti-apoptotic protein Bcl-2 interacts with and destabilizes the sarcoplasmic/endoplasmic reticulum Ca2+-ATPase (SERCA). *Biochem J* **2004,** 383, 361-70.

29. Dremina, E. S.; Sharov, V. S.; Schoneich, C. Displacement of SERCA from SR lipid caveolae-related domains by Bcl-2: a possible mechanism for SERCA inactivation. *Biochemistry* **2006,** 45, 175-84.

30. Yin, D.; Kondo, S.; Takeuchi, J.; Morimura, T.; Vaux, D. Bcl-2 gene prevents apoptosis in murine acth-secreting adenoma cells induced by bromocriptine. *Int J Oncol* **1994,** 4, 187-91.

31. McDonnell, T. J.; Deane, N.; Platt, F. M.; Nunez, G.; Jaeger, U.; McKearn, J. P.; Korsmeyer, S. J. bcl-2-immunoglobulin transgenic mice demonstrate extended B cell survival and follicular lymphoproliferation. *Cell* **1989,** 57, 79-88.

32. Reed, J. C.; Kitada, S.; Takayama, S.; Miyashita, T. Regulation of chemoresistance by the bcl-2 oncoprotein in non-Hodgkin's lymphoma and lymphocytic leukemia cell lines. *Ann Oncol* **1994,** 5 Suppl 1, 61-5.

33. Tsujimoto, Y.; Cossman, J.; Jaffe, E.; Croce, C. M. Involvement of the bcl-2 gene in human follicular lymphoma. *Science* **1985,** 228, 1440-3.

34. Byrd, J. C.; Kitada, S.; Flinn, I. W.; Aron, J. L.; Pearson, M.; Lucas, D.; Reed, J. C. The mechanism of tumor cell clearance by rituximab in vivo in patients with B-cell chronic lymphocytic leukemia: evidence of caspase activation and apoptosis induction. *Blood* **2002,** 99, 1038-43.

35. Wilson, N. S.; Yang, B.; Yang, A.; Loeser, S.; Marsters, S.; Lawrence, D.; Li, Y.; Pitti, R.; Totpal, K.; Yee, S.; Ross, S.; Vernes, J. M.; Lu, Y.; Adams, C.; Offringa, R.; Kelley, B.; Hymowitz, S.; Daniel, D.; Meng, G.; Ashkenazi, A. An Fcgamma receptor-dependent mechanism drives antibody-mediated target-receptor signaling in cancer cells. *Cancer Cell* **2011,** 19, 101-13.

36. Letai, A. A new face of BCL-2 inhibition in CLL. *Blood* **2011,** 117, 2750-1.

37. Buggins, A. G. S.; Pepper, C. J. The role of Bcl-2 family proteins in chronic lymphocytic leukaemia. *Leukemia Research* **2010,** 34, 837-842.

38. Perego, P.; Righetti, S.; Supino, R.; Delia, D.; Caserini, C.; Carenini, N.; Bedogné, B.; Broome, E.; Krajewski, S.; Reed, J.; Zunino, F. Role of apoptosis and apoptosis-related proteins in the cisplatin-resistant phenotype of human tumor cell lines. *Apoptosis* **1997,** 2, 540-548.

39. Tome, M. E.; Lutz, N. W.; Briehl, M. M. Overexpression of catalase or Bcl-2 alters glucose and energy metabolism concomitant with dexamethasone resistance. *Biochim Biophys Acta* **2004,** 1693, 57-72.

40. Hoetelmans, R. W.; Vahrmeijer, A. L.; Mulder, G. J.; van de Velde, C. J.; Nagelkerke, J. F.; van Dierendonck, J. H. Bcl-2 overexpression does not prevent but

retards adriamycin toxicity in CC531 colon carcinoma cells. *Chemotherapy* **2003,** 49, 309-15.

41. Miyake, H.; Hara, S.; Arakawa, S.; Kamidono, S.; Hara, I. Overexpression of Bcl-2 regulates sodium butyrate- and/or docetaxel-induced apoptosis in human bladder cancer cells both in vitro and in vivo. *Int J Cancer* **2001,** 93, 26-32.

42. Allouche, M.; Bettaieb, A.; Vindis, C.; Rousse, A.; Grignon, C.; Laurent, G. Influence of Bcl-2 overexpression on the ceramide pathway in daunorubicin-induced apoptosis of leukemic cells. *Oncogene* **1997,** 14, 1837-45.

43. Williams, S. S.; French, J. N.; Gilbert, M.; Rangaswami, A. A.; Walleczek, J.; Knox, S. J. Bcl-2 overexpression results in enhanced capacitative calcium entry and resistance to SKF-96365-induced apoptosis. *Cancer Res* **2000,** 60, 4358-61.

44. Dai, Y.; Rahmani, M.; Corey, S. J.; Dent, P.; Grant, S. A Bcr/Abl-independent, Lyn-dependent form of imatinib mesylate (STI-571) resistance is associated with altered expression of Bcl-2. *J Biol Chem* **2004,** 279, 34227-39.

45. Kitada, S.; Reed, J. C. MCL-1 promoter insertions dial-up aggressiveness of chronic leukemia. *J Natl Cancer Inst* **2004,** 96, 642-3.

46. Pepper, C.; Lin, T. T.; Pratt, G.; Hewamana, S.; Brennan, P.; Hiller, L.; Hills, R.; Ward, R.; Starczynski, J.; Austen, B.; Hooper, L.; Stankovic, T.; Fegan, C. Mcl-1 expression has in vitro and in vivo significance in chronic lymphocytic leukemia and is associated with other poor prognostic markers. *Blood* **2008,** 112, 3807-17.

47. Kaufmann, S. H.; Karp, J. E.; Svingen, P. A.; Krajewski, S.; Burke, P. J.; Gore, S. D.; Reed, J. C. Elevated expression of the apoptotic regulator Mcl-1 at the time of leukemic relapse. *Blood* **1998,** 91, 991-1000.

48. Chen, S.; Dai, Y.; Harada, H.; Dent, P.; Grant, S. Mcl-1 down-regulation potentiates ABT-737 lethality by cooperatively inducing Bak activation and Bax translocation. *Cancer Res* **2007,** 67, 782-91.

49. Martin, A. P.; Miller, A.; Emad, L.; Rahmani, M.; Walker, T.; Mitchell, C.; Hagan, M. P.; Park, M. A.; Yacoub, A.; Fisher, P. B.; Grant, S.; Dent, P. Lapatinib resistance in HCT116 cells is mediated by elevated MCL-1 expression and decreased BAK activation and not by ERBB receptor kinase mutation. *Mol Pharmacol* **2008,** 74, 807-22.

50. Fontana, J. A.; Sun, R. J.; Rishi, A. K.; Dawson, M. I.; Ordonez, J. V.; Zhang, Y.; Tschang, S. H.; Bhalla, K.; Han, Z.; Wyche, J.; Poirer, G.; Sheikh, M. S.; Shroot, B.; Reichert, U. Overexpression of bcl-2 or bcl-XL fails to inhibit apoptosis mediated by a novel retinoid. *Oncol Res* **1998,** 10, 313-24.

51. Ibrado, A. M.; Huang, Y.; Fang, G.; Liu, L.; Bhalla, K. Overexpression of Bcl-2 or Bcl-xL inhibits Ara-C-induced CPP32/Yama protease activity and apoptosis of human acute myelogenous leukemia HL-60 cells. *Cancer Res* **1996,** 56, 4743-8.

52. Blanco-Colio, L. M.; Justo, P.; Daehn, I.; Lorz, C.; Ortiz, A.; Egido, J. Bcl-xL overexpression protects from apoptosis induced by HMG-CoA reductase inhibitors in murine tubular cells. *Kidney Int* **2003,** 64, 181-91.

53. Datta, R.; Manome, Y.; Taneja, N.; Boise, L. H.; Weichselbaum, R.; Thompson, C. B.; Slapak, C. A.; Kufe, D. Overexpression of Bcl-XL by cytotoxic drug exposure confers resistance to ionizing radiation-induced internucleosomal DNA fragmentation. *Cell Growth Differ* **1995,** 6, 363-70.

54. Su, Y.; Zhang, X.; Sinko, P. J. Exploitation of drug-induced Bcl-2 overexpression for restoring normal apoptosis function: a promising new approach to the treatment of multidrug resistant cancer. *Cancer Lett* **2007,** 253, 115-23.

55. Adams, J. M.; Cory, S. The Bcl-2 apoptotic switch in cancer development and therapy. *Oncogene* **2007,** 26, 1324-37.

56. Patel, M. P.; Masood, A.; Patel, P. S.; Chanan-Khan, A. A. Targeting the Bcl-2. *Current Opinion in Oncology* **2009,** 21, 516-523 10.1097/CCO.0b013e328331a7a4.

57. Storey, S. Targeting apoptosis: selected anticancer strategies. *Nat Rev Drug Discov* **2008,** 7, 971-2.

58. Leber, B.; Geng, F.; Kale, J.; Andrews, D. W. Drugs targeting Bcl-2 family members as an emerging strategy in cancer. *Expert Rev Mol Med* **2010,** 12, e28.

59. Adams, J. M.; Cory, S. Bcl-2-regulated apoptosis: mechanism and therapeutic potential. *Curr Opin Immunol* **2007,** 19, 488-96.

60. Reed, J. C.; Stein, C.; Subasinghe, C.; Haldar, S.; Croce, C. M.; Yum, S.; Cohen, J. Antisense-mediated inhibition of BCL2 protooncogene expression and leukemic cell growth and survival: comparisons of phosphodiester and phosphorothioate oligodeoxynucleotides. *Cancer Res* **1990,** 50, 6565-70.

61. Reed, J. C.; Cuddy, M.; Haldar, S.; Croce, C.; Nowell, P.; Makover, D.; Bradley, K. BCL2-mediated tumorigenicity of a human T-lymphoid cell line: synergy with MYC and inhibition by BCL2 antisense. *Proc Natl Acad Sci U S A* **1990,** 87, 3660-4.

62. Sentman, C. L.; Shutter, J. R.; Hockenbery, D.; Kanagawa, O.; Korsmeyer, S. J. bcl-2 inhibits multiple forms of apoptosis but not negative selection in thymocytes. *Cell* **1991,** 67, 879-88.

63. Kitada, S.; Miyashita, T.; Tanaka, S.; Reed, J. C. Investigations of antisense oligonucleotides targeted against bcl-2 RNAs. *Antisense Res Dev* **1993,** 3, 157-69.

64. Banerjee, D. Genasense (Genta Inc). *Curr Opin Investig Drugs* **2001,** 2, 574-80.

65. Klasa, R. J.; Gillum, A. M.; Klem, R. E.; Frankel, S. R. Oblimersen Bcl-2 antisense: facilitating apoptosis in anticancer treatment. *Antisense Nucleic Acid Drug Dev* **2002,** 12, 193-213.

66. Pro, B.; Leber, B.; Smith, M.; Fayad, L.; Romaguera, J.; Hagemeister, F.; Rodriguez, A.; McLaughlin, P.; Samaniego, F.; Zwiebel, J.; Lopez, A.; Kwak, L.; Younes, A. Phase II multicenter study of oblimersen sodium, a Bcl-2 antisense oligonucleotide, in combination with rituximab in patients with recurrent B-cell non-Hodgkin lymphoma. *Br J Haematol* **2008,** 143, 355-60.

67. O'Brien, S. M.; Cunningham, C. C.; Golenkov, A. K.; Turkina, A. G.; Novick, S. C.; Rai, K. R. Phase I to II multicenter study of oblimersen sodium, a Bcl-2 antisense oligonucleotide, in patients with advanced chronic lymphocytic leukemia. *J Clin Oncol* **2005,** 23, 7697-702.

68. O'Brien, S.; Moore, J. O.; Boyd, T. E.; Larratt, L. M.; Skotnicki, A. B.; Koziner, B.; Chanan-Khan, A. A.; Seymour, J. F.; Gribben, J.; Itri, L. M.; Rai, K. R. 5-year survival in patients with relapsed or refractory chronic lymphocytic leukemia in a randomized, phase III trial of fludarabine plus cyclophosphamide with or without oblimersen. *J Clin Oncol* **2009,** 27, 5208-12.

69. G 3139. Augmerosen, Bcl-2 antisense oligonucleotide--Genta, GC 3139, Genasense. *Drugs R D* **2002,** 3, 44-9.

70. Piche, A.; Grim, J.; Rancourt, C.; Gomez-Navarro, J.; Reed, J. C.; Curiel, D. T. Modulation of Bcl-2 protein levels by an intracellular anti-Bcl-2 single-chain antibody increases drug-induced cytotoxicity in the breast cancer cell line MCF-7. *Cancer Res* **1998,** 58, 2134-40.

71. Dorai, T.; Olsson, C. A.; Katz, A. E.; Buttyan, R. Development of a hammerhead ribozyme against bcl-2. I. Preliminary evaluation of a potential gene therapeutic agent for hormone-refractory human prostate cancer. *The Prostate* **1997,** 32, 246-58.

72. Muchmore, S. W.; Sattler, M.; Liang, H.; Meadows, R. P.; Harlan, J. E.; Yoon, H. S.; Nettesheim, D.; Chang, B. S.; Thompson, C. B.; Wong, S.-L.; Ng, S.-C.; Fesik, S. W. X-ray and NMR structure of human Bcl-xL, an inhibitor of programmed cell death. *Nature* **1996,** 381, 335-41.

73. Sattler, M.; Liang, H.; Nettesheim, D.; Meadows, R. P.; Harlan, J. E.; Eberstadt, M.; Yoon, H. S.; Shuker, S. B.; Chang, B. S.; Minn, A. J.; Thompson, C. B.; Fesik, S. W. Structure of Bcl-xL-Bak Peptide Complex: Recognition Between Regulators of Apoptosis. *Science* **1997,** 275, 983-86.

74. Holinger, E. P.; Chittenden, T.; Lutz, R. J. Bak BH3 peptides antagonize Bcl-xL function and induce apoptosis through cytochrome c-independent activation of caspases. *J Biol Chem* **1999,** 274, 13298-304.

75. Wang, J. L.; Zhang, Z. J.; Choksi, S.; Shan, S.; Lu, Z.; Croce, C. M.; Alnemri, E. S.; Korngold, R.; Huang, Z. Cell permeable Bcl-2 binding peptides: a chemical approach to apoptosis induction in tumor cells. *Cancer Res* **2000,** 60, 1498-502.

76. Oh, K. J.; Barbuto, S.; Pitter, K.; Morash, J.; Walensky, L. D.; Korsmeyer, S. J. A membrane-targeted BID BCL-2 homology 3 peptide is sufficient for high potency activation of BAX in vitro. *J Biol Chem* **2006,** 281, 36999-7008.

77. Walensky, L. D.; Pitter, K.; Morash, J.; Oh, K. J.; Barbuto, S.; Fisher, J.; Smith, E.; Verdine, G. L.; Korsmeyer, S. J. A stapled BID BH3 helix directly binds and activates BAX. *Mol Cell* **2006,** 24, 199-210.

78. Sadowsky, J. D.; Fairlie, W. D.; Hadley, E. B.; Lee, H. S.; Umezawa, N.; Nikolovska-Coleska, Z.; Wang, S.; Huang, D. C. S.; Tomita, Y.; Gellman, S. H. (alpha/beta+alpha)-peptide antagonists of BH3 domain/Bcl-x(L) recognition: toward general strategies for foldamer-based inhibition of protein-protein interactions. *J. Am. Chem. Soc.* **2007,** 129, 139-54.

79. Stewart, M. L.; Fire, E.; Keating, A. E.; Walensky, L. D. The MCL-1 BH3 helix is an exclusive MCL-1 inhibitor and apoptosis sensitizer. *Nat Chem Biol* 6, 595-601.

80. Yin, H.; Lee, G. I.; Sedey, K. A.; Kutzki, O.; Park, H. S.; Orner, B. P.; Ernst, J. T.; Wang, H. G.; Sebti, S. M.; Hamilton, A. D. Terphenyl-Based Bak BH3 alpha-helical

proteomimetics as low-molecular-weight antagonists of Bcl-xL. *J Am Chem Soc* **2005,** 127, 10191-6.

81. Degterev, A.; Lugovskoy, A.; Cardone, M.; Mulley, B.; Wagner, G.; Mitchison, T.; Yuan, J. Identification of small-molecule inhibitors of interaction between the BH3 domain and Bcl-xL. *Nat Cell Biol* **2001,** 3, 173-82.

82. Kitada, S.; Leone, M.; Sareth, S.; Zhai, D.; Reed, J. C.; Pellecchia, M. Discovery, characterization, and structure-activity relationships studies of proapoptotic polyphenols targeting B-cell lymphocyte/leukemia-2 proteins. *J Med Chem* **2003,** 46, 4259-64.

83. Benz, C. C.; Keniry, M. A.; Ford, J. M.; Townsend, A. J.; Cox, F. W.; Palayoor, S.; Matlin, S. A.; Hait, W. N.; Cowan, K. H. Biochemical correlates of the antitumor and antimitochondrial properties of gossypol enantiomers. *Mol Pharmacol* **1990,** 37, 840-7.

84. Qiu, J.; Levin, L. R.; Buck, J.; Reidenberg, M. M. Different pathways of cell killing by gossypol enantiomers. *Exp Biol Med (Maywood)* **2002,** 227, 398-401.

85. Ready, N.; Karaseva, N. A.; Orlov, S. V.; Luft, A. V.; Popovych, O.; Holmlund, J. T.; Wood, B. A.; Leopold, L. Double-blind, placebo-controlled, randomized phase 2 study of the proapoptotic agent AT-101 plus docetaxel, in second-line non-small cell lung cancer. *J Thorac Oncol* **2011,** 6, 781-5.

86. Heist, R. S.; Fain, J.; Chinnasami, B.; Khan, W.; Molina, J. R.; Sequist, L. V.; Temel, J. S.; Fidias, P.; Brainerd, V.; Leopold, L.; Lynch, T. J. Phase I/II study of AT-101 with topotecan in relapsed and refractory small cell lung cancer. *J Thorac Oncol* **2010,** 5, 1637-43.

87. McGregor, N.; Patel, L.; Craig, M.; Weidner, S.; Wang, S.; Pienta, K. J. AT-101 (R-(-)-gossypol acetic acid) enhances the effectiveness of androgen deprivation therapy in the VCaP prostate cancer model. *J Cell Biochem* **2010,** 110, 1187-94.

88. Moretti, L.; Li, B.; Kim, K. W.; Chen, H.; Lu, B. AT-101, a pan-Bcl-2 inhibitor, leads to radiosensitization of non-small cell lung cancer. *J Thorac Oncol* **2010,** 5, 680-7.

89. Loberg, R. D.; McGregor, N.; Ying, C.; Sargent, E.; Pienta, K. J. In vivo evaluation of AT-101 (R-(-)-gossypol acetic acid) in androgen-independent growth of VCaP prostate cancer cells in combination with surgical castration. *Neoplasia* **2007,** 9, 1030-7.

90. Kline, M. P.; Rajkumar, S. V.; Timm, M. M.; Kimlinger, T. K.; Haug, J. L.; Lust, J. A.; Greipp, P. R.; Kumar, S. R-(-)-gossypol (AT-101) activates programmed cell death in multiple myeloma cells. *Exp Hematol* **2008,** 36, 568-76.

91. Paoluzzi, L.; Gonen, M.; Gardner, J. R.; Mastrella, J.; Yang, D.; Holmlund, J.; Sorensen, M.; Leopold, L.; Manova, K.; Marcucci, G.; Heaney, M. L.; O'Connor, O. A. Targeting Bcl-2 family members with the BH3 mimetic AT-101 markedly enhances the therapeutic effects of chemotherapeutic agents in in vitro and in vivo models of B-cell lymphoma. *Blood* **2008,** 111, 5350-8.

92. Balakrishnan, K.; Burger, J. A.; Wierda, W. G.; Gandhi, V. AT-101 induces apoptosis in CLL B cells and overcomes stromal cell-mediated Mcl-1 induction and drug resistance. *Blood* **2009,** 113, 149-53.

93. Varol, U.; Karaca, B.; Tunali, D.; Degirmenci, M.; Cirak, Y.; Purcu, D. U.; Uzunoglu, S.; Sezgin, C.; Karabulut, B.; Sanli, U. A.; Uslu, R. The effect of racemic

gossypol and at-101 on angiogenic profile of ovcar-3 cells: a preliminary molecular framework for gossypol enantiomers. *Exp Oncol* **2009,** 31, 220-5.

94. Liu, G.; Kelly, W. K.; Wilding, G.; Leopold, L.; Brill, K.; Somer, B. An open-label, multicenter, phase I/II study of single-agent AT-101 in men with castrate-resistant prostate cancer. *Clin Cancer Res* **2009,** 15, 3172-6.

95. Wang, G.; Nikolovska-Coleska, Z.; Yang, C. Y.; Wang, R.; Tang, G.; Guo, J.; Shangary, S.; Qiu, S.; Gao, W.; Yang, D.; Meagher, J.; Stuckey, J.; Krajewski, K.; Jiang, S.; Roller, P. P.; Abaan, H. O.; Tomita, Y.; Wang, S. Structure-based design of potent small-molecule inhibitors of anti-apoptotic Bcl-2 proteins. *J Med Chem* **2006,** 49, 6139-42.

96. Mohammad, R. M.; Goustin, A. S.; Aboukameel, A.; Chen, B.; Banerjee, S.; Wang, G.; Nikolovska-Coleska, Z.; Wang, S.; Al-Katib, A. Preclinical studies of TW-37, a new nonpeptidic small-molecule inhibitor of Bcl-2, in diffuse large cell lymphoma xenograft model reveal drug action on both Bcl-2 and Mcl-1. *Clin Cancer Res* **2007,** 13, 2226-35.

97. Zeitlin, B. D.; Spalding, A. C.; Campos, M. S.; Ashimori, N.; Dong, Z.; Wang, S.; Lawrence, T. S.; Nor, J. E. Metronomic small molecule inhibitor of Bcl-2 (TW-37) is antiangiogenic and potentiates the antitumor effect of ionizing radiation. *Int J Radiat Oncol Biol Phys* **2010,** 78, 879-87.

98. Al-Katib, A. M.; Sun, Y.; Goustin, A. S.; Azmi, A. S.; Chen, B.; Aboukameel, A.; Mohammad, R. M. SMI of Bcl-2 TW-37 is active across a spectrum of B-cell tumors irrespective of their proliferative and differentiation status. *J Hematol Oncol* **2009,** 2, 8.

99. Wang, Z.; Song, W.; Aboukameel, A.; Mohammad, M.; Wang, G.; Banerjee, S.; Kong, D.; Wang, S.; Sarkar, F. H.; Mohammad, R. M. TW-37, a small-molecule inhibitor of Bcl-2, inhibits cell growth and invasion in pancreatic cancer. *Int J Cancer* **2008,** 123, 958-66.

100. Ashimori, N.; Zeitlin, B. D.; Zhang, Z.; Warner, K.; Turkienicz, I. M.; Spalding, A. C.; Teknos, T. N.; Wang, S.; Nor, J. E. TW-37, a small-molecule inhibitor of Bcl-2, mediates S-phase cell cycle arrest and suppresses head and neck tumor angiogenesis. *Mol Cancer Ther* **2009,** 8, 893-903.

101. Sun, Y.; Wu, J.; Aboukameel, A.; Banerjee, S.; Arnold, A. A.; Chen, J.; Nikolovska-Coleska, Z.; Lin, Y.; Ling, X.; Yang, D.; Wang, S.; Al-Katib, A.; Mohammad, R. M. Apogossypolone, a nonpeptidic small molecule inhibitor targeting Bcl-2 family proteins, effectively inhibits growth of diffuse large cell lymphoma cells in vitro and in vivo. *Cancer Biol Ther* **2008,** 7, 1418-26.

102. Wei, J.; Kitada, S.; Stebbins, J. L.; Placzek, W.; Zhai, D.; Wu, B.; Rega, M. F.; Zhang, Z.; Cellitti, J.; Yang, L.; Dahl, R.; Reed, J. C.; Pellecchia, M. Synthesis and biological evaluation of Apogossypolone derivatives as pan-active inhibitors of antiapoptotic B-cell lymphoma/leukemia-2 (Bcl-2) family proteins. *J Med Chem* **2010,** 53, 8000-11.

103. Banerjee, S.; Choi, M.; Aboukameel, A.; Wang, Z.; Mohammad, M.; Chen, J.; Yang, D.; Sarkar, F. H.; Mohammad, R. M. Preclinical studies of apogossypolone, a novel pan inhibitor of bcl-2 and mcl-1, synergistically potentiates cytotoxic effect of gemcitabine in pancreatic cancer cells. *Pancreas* **2009,** 39, 323-31.

104. Arnold, A. A.; Aboukameel, A.; Chen, J.; Yang, D.; Wang, S.; Al-Katib, A.; Mohammad, R. M. Preclinical studies of Apogossypolone: a new nonpeptidic pan small-molecule inhibitor of Bcl-2, Bcl-XL and Mcl-1 proteins in Follicular Small Cleaved Cell Lymphoma model. *Mol Cancer* **2008,** 7, 20.

105. Wei, J.; Stebbins, J. L.; Kitada, S.; Dash, R.; Placzek, W.; Rega, M. F.; Wu, B.; Cellitti, J.; Zhai, D.; Yang, L.; Dahl, R.; Fisher, P. B.; Reed, J. C.; Pellecchia, M. BI-97C1, an optically pure Apogossypol derivative as pan-active inhibitor of antiapoptotic B-cell lymphoma/leukemia-2 (Bcl-2) family proteins. *J Med Chem* **2010,** 53, 4166-76.

106. Dash, R.; Azab, B.; Quinn, B. A.; Shen, X.; Wang, X. Y.; Das, S. K.; Rahmani, M.; Wei, J.; Hedvat, M.; Dent, P.; Dmitriev, I. P.; Curiel, D. T.; Grant, S.; Wu, B.; Stebbins, J. L.; Pellecchia, M.; Reed, J. C.; Sarkar, D.; Fisher, P. B. Apogossypol derivative BI-97C1 (Sabutoclax) targeting Mcl-1 sensitizes prostate cancer cells to mda-7/IL-24-mediated toxicity. *Proc Natl Acad Sci U S A* **2011,** 108, 8785-90.

107. Azab, B.; Dash, R.; Das, S. K.; Bhutia, S. K.; Shen, X. N.; Quinn, B. A.; Sarkar, S.; Wang, X. Y.; Hedvat, M.; Dmitriev, I. P.; Curiel, D. T.; Grant, S.; Dent, P.; Reed, J. C.; Pellecchia, M.; Sarkar, D.; Fisher, P. B. Enhanced delivery of mda-7/IL-24 using a serotype chimeric adenovirus (Ad.5/3) in combination with the Apogossypol derivative BI-97C1 (Sabutoclax) improves therapeutic efficacy in low CAR colorectal cancer cells. *J Cell Physiol* **2011,** Jul 21. doi: 10.1002/jcp.22947. [Epub ahead of print].

108. Oltersdorf, T.; Elmore, S. W.; Shoemaker, A. R.; Armstrong, R. C.; Augeri, D. J.; Belli, B. A.; Bruncko, M.; Deckwerth, T. L.; Dinges, J.; Hajduk, P. J.; Joseph, M. K.; Kitada, S.; Korsmeyer, S. J.; Kunzer, A. R.; Letai, A.; Li, C.; Mitten, M. J.; Nettesheim,

D. G.; Ng, S.; Nimmer, P. M.; O'Connor, J. M.; Oleksijew, A.; Petros, A. M.; Reed, J. C.; Shen, W.; Tahir, S. K.; Thompson, C. B.; Tomaselli, K. J.; Wang, B.; Wendt, M. D.; Zhang, H.; Fesik, S. W.; Rosenberg, S. H. An inhibitor of Bcl-2 family proteins induces regression of solid tumours. *Nature* **2005,** 435, 677-81.

109. Chauhan, D.; Velankar, M.; Brahmandam, M.; Hideshima, T.; Podar, K.; Richardson, P.; Schlossman, R.; Ghobrial, I.; Raje, N.; Munshi, N.; Anderson, K. C. A novel Bcl-2//Bcl-XL//Bcl-w inhibitor ABT-737 as therapy in multiple myeloma. *Oncogene* **2006,** 26, 2374-80.

110. Del Gaizo Moore, V.; Schlis, K. D.; Sallan, S. E.; Armstrong, S. A.; Letai, A. BCL-2 dependence and ABT-737 sensitivity in acute lymphoblastic leukemia. *Blood* **2008,** 111, 2300-09.

111. Kuroda, J.; Kimura, S.; Andreeff, M.; Ashihara, E.; Kamitsuji, Y.; Yokota, A.; Kawata, E.; Takeuchi, M.; Tanaka, R.; Murotani, Y.; Matsumoto, Y.; Tanaka, H.; Strasser, A.; Taniwaki, M.; Maekawa, T. ABT-737 is a useful component of combinatory chemotherapies for chronic myeloid leukaemias with diverse drug-resistance mechanisms. *British Journal of Haematology* **2008,** 140, 181-90.

112. Xu, H.; Krystal, G. W. Actinomycin D decreases Mcl-1 expression and acts synergistically with ABT-737 against small cell lung cancer cell lines. *Clin Cancer Res* **2010,** 16, 4392-400.

113. Konopleva, M.; Contractor, R.; Tsao, T.; Samudio, I.; Ruvolo, P. P.; Kitada, S.; Deng, X.; Zhai, D.; Shi, Y.-X.; Sneed, T.; Verhaegen, M.; Soengas, M.; Ruvolo, V. R.; McQueen, T.; Schober, W. D.; Watt, J. C.; Jiffar, T.; Ling, X.; Marini, F. C.; Harris, D.;

Dietrich, M.; Estrov, Z.; McCubrey, J.; May, W. S.; Reed, J. C.; Andreeff, M. Mechanisms of apoptosis sensitivity and resistance to the BH3 mimetic ABT-737 in acute myeloid leukemia. *Cancer Cell* **2006,** 10, 375-88.

114. Keuling, A. M.; Felton, K. E.; Parker, A. A.; Akbari, M.; Andrew, S. E.; Tron, V. A. RNA silencing of Mcl-1 enhances ABT-737-mediated apoptosis in melanoma: role for a caspase-8-dependent pathway. *PLoS One* **2009,** 4, e6651.

115. Yecies, D.; Carlson, N. E.; Deng, J.; Letai, A. Acquired resistance to ABT-737 in lymphoma cells that up-regulate MCL-1 and BFL-1. *Blood* 115, 3304-13.

116. Tse, C.; Shoemaker, A. R.; Adickes, J.; Anderson, M. G.; Chen, J.; Jin, S.; Johnson, E. F.; Marsh, K. C.; Mitten, M. J.; Nimmer, P.; Roberts, L.; Tahir, S. K.; Xiao, Y.; Yang, X.; Zhang, H.; Fesik, S.; Rosenberg, S. H.; Elmore, S. W. ABT-263: a potent and orally bioavailable Bcl-2 family inhibitor. *Cancer Res* **2008,** 68, 3421-8.

117. Gandhi, L.; Camidge, D. R.; Ribeiro de Oliveira, M.; Bonomi, P.; Gandara, D.; Khaira, D.; Hann, C. L.; McKeegan, E. M.; Litvinovich, E.; Hemken, P. M.; Dive, C.; Enschede, S. H.; Nolan, C.; Chiu, Y. L.; Busman, T.; Xiong, H.; Krivoshik, A. P.; Humerickhouse, R.; Shapiro, G. I.; Rudin, C. M. Phase I study of Navitoclax (ABT-263), a novel Bcl-2 family inhibitor, in patients with small-cell lung cancer and other solid tumors. *J Clin Oncol* **2011,** 29, 909-16.

118. Wilson, W. H.; O'Connor, O. A.; Czuczman, M. S.; LaCasce, A. S.; Gerecitano, J. F.; Leonard, J. P.; Tulpule, A.; Dunleavy, K.; Xiong, H.; Chiu, Y.-L.; Cui, Y.; Busman, T.; Elmore, S. W.; Rosenberg, S. H.; Krivoshik, A. P.; Enschede, S. H.; Humerickhouse, R. A. Navitoclax, a targeted high-affinity inhibitor of BCL-2, in lymphoid malignancies:

a phase 1 dose-escalation study of safety, pharmacokinetics, pharmacodynamics, and antitumour activity. *The Lancet Oncology* **2010,** 11, 1149-1159.

119. Tang, H.; Shao, H.; Yu, C.; Hou, J. Mcl-1 downregulation by YM155 contributes to its synergistic anti-tumor activities with ABT-263. *Biochem Pharmacol* **2011,** doi: 10.1016/j.bcp.2011.07.064.

120. Nguyen, M.; Marcellus, R. C.; Roulston, A.; Watson, M.; Serfass, L.; Murthy Madiraju, S. R.; Goulet, D.; Viallet, J.; Bélec, L.; Billot, X.; Acoca, S.; Purisima, E.; Wiegmans, A.; Cluse, L.; Johnstone, R. W.; Beauparlant, P.; Shore, G. C. Small molecule obatoclax (GX15-070) antagonizes MCL-1 and overcomes MCL-1-mediated resistance to apoptosis. *Proc Natl Acad Sci U S A* **2007,** 104, 19512-517.

121. O'Brien, S. M.; Claxton, D. F.; Crump, M.; Faderl, S.; Kipps, T.; Keating, M. J.; Viallet, J.; Cheson, B. D. Phase I study of obatoclax mesylate (GX15-070), a small molecule pan-Bcl-2 family antagonist, in patients with advanced chronic lymphocytic leukemia. *Blood* **2009,** 113, 299-305.

122. Schimmer, A. D.; O'Brien, S.; Kantarjian, H.; Brandwein, J.; Cheson, B. D.; Minden, M. D.; Yee, K.; Ravandi, F.; Giles, F.; Schuh, A.; Gupta, V.; Andreeff, M.; Koller, C.; Chang, H.; Kamel-Reid, S.; Berger, M.; Viallet, J.; Borthakur, G. A Phase I Study of the Pan Bcl-2 Family Inhibitor Obatoclax Mesylate in Patients with Advanced Hematologic Malignancies. *Clin Cancer Res* **2008,** 14, 8295-301.

123. Trudel, S.; Li, Z. H.; Rauw, J.; Tiedemann, R. E.; Wen, X. Y.; Stewart, A. K. Preclinical studies of the pan-Bcl inhibitor obatoclax (GX015-070) in multiple myeloma. *Blood* **2007,** 109, 5430-38.

124. Wang, J. L.; Liu, D.; Zhang, Z. J.; Shan, S.; Han, X.; Srinivasula, S. M.; Croce, C. M.; Alnemri, E. S.; Huang, Z. Structure-based discovery of an organic compound that binds Bcl-2 protein and induces apoptosis of tumor cells. *Proc Natl Acad Sci U S A* **2000,** 97, 7124-9.

125. Oliver, L.; Mahe, B.; Gree, R.; Vallette, F. M.; Juin, P. HA14-1, a small molecule inhibitor of Bcl-2, bypasses chemoresistance in leukaemia cells. *Leuk Res* **2007,** 31, 859-63.

126. Lickliter, J. D.; Wood, N. J.; Johnson, L.; McHugh, G.; Tan, J.; Wood, F.; Cox, J.; Wickham, N. W. HA14-1 selectively induces apoptosis in Bcl-2-overexpressing leukemia/lymphoma cells, and enhances cytarabine-induced cell death. *Leukemia* **2003,** 17, 2074-80.

127. Manero, F.; Gautier, F.; Gallenne, T.; Cauquil, N.; Gree, D.; Cartron, P.-F.; Geneste, O.; Gree, R.; Vallette, F. M.; Juin, P. The Small Organic Compound HA14-1 Prevents Bcl-2 Interaction with Bax to Sensitize Malignant Glioma Cells to Induction of Cell Death. *Cancer Res* **2006,** 66, 2757-64.

128. Skommer, J.; Wlodkowic, D.; Matto, M.; Eray, M.; Pelkonen, J. HA14-1, a small molecule Bcl-2 antagonist, induces apoptosis and modulates action of selected anticancer drugs in follicular lymphoma B cells. *Leuk Res* **2006,** 30, 322-31.

129. Wlodkowic, D.; Skommer, J.; Pelkonen, J. Brefeldin A triggers apoptosis associated with mitochondrial breach and enhances HA14-1- and anti-Fas-mediated cell killing in follicular lymphoma cells. *Leuk Res* **2007,** 31, 1687-700.

130. Srimatkandada, P.; Loomis, R.; Carbone, R.; Srimatkandada, S.; Lacy, J. Combined proteasome and Bcl-2 inhibition stimulates apoptosis and inhibits growth in EBV-transformed lymphocytes: a potential therapeutic approach to EBV-associated lymphoproliferative diseases. *Eur J Haematol* **2008,** 80, 407-18.

131. Jin, C. Y.; Park, C.; Lee, J. H.; Chung, K. T.; Kwon, T. K.; Kim, G. Y.; Choi, B. T.; Choi, Y. H. Naringenin-induced apoptosis is attenuated by Bcl-2 but restored by the small molecule Bcl-2 inhibitor, HA 14-1, in human leukemia U937 cells. *Toxicol In Vitro* **2009,** 23, 259-65.

132. Pei, X. Y.; Dai, Y.; Grant, S. The proteasome inhibitor bortezomib promotes mitochondrial injury and apoptosis induced by the small molecule Bcl-2 inhibitor HA14-1 in multiple myeloma cells. *Leukemia* **2003,** 17, 2036-45.

133. Pei, X. Y.; Dai, Y.; Grant, S. The small-molecule Bcl-2 inhibitor HA14-1 interacts synergistically with flavopiridol to induce mitochondrial injury and apoptosis in human myeloma cells through a free radical-dependent and Jun NH2-terminal kinase-dependent mechanism. *Mol Cancer Ther* **2004,** 3, 1513-24.

134. Arisan, E. D.; Kutuk, O.; Tezil, T.; Bodur, C.; Telci, D.; Basaga, H. Small inhibitor of Bcl-2, HA14-1, selectively enhanced the apoptotic effect of cisplatin by modulating Bcl-2 family members in MDA-MB-231 breast cancer cells. *Breast Cancer Res Treat* **2009,** 119, 271-81.

135. Milella, M.; Estrov, Z.; Kornblau, S. M.; Carter, B. Z.; Konopleva, M.; Tari, A.; Schober, W. D.; Harris, D.; Leysath, C. E.; Lopez-Berestein, G.; Huang, Z.; Andreeff, M.

Synergistic induction of apoptosis by simultaneous disruption of the Bcl-2 and MEK/MAPK pathways in acute myelogenous leukemia. *Blood* **2002,** 99, 3461-4.

136. Witters, L. M.; Witkoski, A.; Planas-Silva, M. D.; Berger, M.; Viallet, J.; Lipton, A. Synergistic inhibition of breast cancer cell lines with a dual inhibitor of EGFR-HER-2/neu and a Bcl-2 inhibitor. *Oncol Rep* **2007,** 17, 465-9.

137. Doshi, J. M.; Tian, D.; Xing, C. Ethyl-2-amino-6-bromo-4-(1-cyano-2-ethoxy-2-oxoethyl)-4H- chromene-3-carboxylate (HA 14-1), a prototype small-molecule antagonist against antiapoptotic Bcl-2 proteins, decomposes to generate reactive oxygen species that induce apoptosis. *Mol Pharm* **2007,** 4, 919-28.

138. An, J.; Chervin, A. S.; Nie, A.; Ducoff, H. S.; Huang, Z. Overcoming the radioresistance of prostate cancer cells with a novel Bcl-2 inhibitor. *Oncogene* **2007,** 26, 652-61.

139. Doshi, J. M.; Tian, D.; Xing, C. Structure-activity relationship studies of ethyl 2-amino-6-bromo-4-(1-cyano-2-ethoxy-2-oxoethyl)-4H-chromene-3-carboxylate (HA 14-1), an antagonist for antiapoptotic Bcl-2 proteins to overcome drug resistance in cancer. *J Med Chem* **2006,** 49, 7731-9.

140. Das, S. G.; Doshi, J. M.; Tian, D.; Addo, S. N.; Srinivasan, B.; Hermanson, D. L.; Xing, C. Structure-activity relationship and molecular mechanisms of ethyl 2-amino-4-(2-ethoxy-2-oxoethyl)-6-phenyl-4h-chromene-3-carboxylate (sha 14-1) and its analogues. *J Med Chem* **2009,** 52, 5937-49.

141. Tian, D.; Das, S. G.; Doshi, J. M.; Peng, J.; Lin, J.; Xing, C. sHA 14-1, a stable and ROS-free antagonist against anti-apoptotic Bcl-2 proteins, bypasses drug resistances and synergizes cancer therapies in human leukemia cell. *Cancer Lett* **2008,** 259, 198-208.

142. Hofslokken, N. U.; Skattebol, L. Convenient method for the ortho-formylation of phenols. *Anglais* **1999,** 53, 258-32.

143. Hurwitz, R.; Hozier, J.; LeBien, T.; Minowada, J.; Gajl-Peczalska, K.; Kubonishi, I.; Kersey, J. Characterization of a leukemic cell line of the pre-B phenotype. *Int J Cancer* **1979,** 23, 174-80.

144. Chou, T. C.; Talalay, P. Quantitative analysis of dose-effect relationships: the combined effects of multiple drugs or enzyme inhibitors. *Adv Enzyme Regul* **1984,** 22, 27-55.

145. Hermanson, D.; Addo, S. N.; Bajer, A. A.; Marchant, J. S.; Das, S. G.; Srinivasan, B.; Al-Mousa, F.; Michelangeli, F.; Thomas, D. D.; Lebien, T. W.; Xing, C. Dual mechanisms of sHA 14-1 in inducing cell death through endoplasmic reticulum and mitochondria. *Mol Pharmacol* **2009,** 76, 667-78.

146. Shoemaker, R. H. The NCI60 human tumour cell line anticancer drug screen. *Nat Rev Cancer* **2006,** 6, 813-23.

147. Naasani, I.; Seimiya, H.; Yamori, T.; Tsuruo, T. FJ5002: a potent telomerase inhibitor identified by exploiting the disease-oriented screening program with COMPARE analysis. *Cancer Res* **1999,** 59, 4004-11.

148. Yamori, T.; Matsunaga, A.; Sato, S.; Yamazaki, K.; Komi, A.; Ishizu, K.; Mita, I.; Edatsugi, H.; Matsuba, Y.; Takezawa, K.; Nakanishi, O.; Kohno, H.; Nakajima, Y.;

Komatsu, H.; Andoh, T.; Tsuruo, T. Potent antitumor activity of MS-247, a novel DNA minor groove binder, evaluated by an in vitro and in vivo human cancer cell line panel. *Cancer Res* **1999,** 59, 4042-9.

149. Das, S. G.; Srinivasan, B.; Hermanson, D. L.; Bleeker, N. P.; Doshi, J. M.; Tang, R.; Beck, W. T.; Xing, C. Structure-Activity Relationship and Molecular Mechanisms of Ethyl 2-Amino-6-(3,5-dimethoxyphenyl)-4-(2-ethoxy-2-oxoethyl)-4H-chromene-3-carboxylate (CXL017) and Its Analogues. *Journal of Medicinal Chemistry* **2011,** 54, 5937-5948.

150. Harker, W. G.; Slade, D. L.; Dalton, W. S.; Meltzer, P. S.; Trent, J. M. Multidrug resistance in mitoxantrone-selected HL-60 leukemia cells in the absence of P-glycoprotein overexpression. *Cancer Res* **1989,** 49, 4542-9.

151. Warr, M. R.; Shore, G. C. Unique biology of Mcl-1: therapeutic opportunities in cancer. *Curr Mol Med* **2008,** 8, 138-47.

152. Wei, S. H.; Dong, K.; Lin, F.; Wang, X.; Li, B.; Shen, J. J.; Zhang, Q.; Wang, R.; Zhang, H. Z. Inducing apoptosis and enhancing chemosensitivity to gemcitabine via RNA interference targeting Mcl-1 gene in pancreatic carcinoma cell. *Cancer Chemother Pharmacol* **2008,** 62, 1055-64.

153. van Delft, M. F.; Wei, A. H.; Mason, K. D.; Vandenberg, C. J.; Chen, L.; Czabotar, P. E.; Willis, S. N.; Scott, C. L.; Day, C. L.; Cory, S.; Adams, J. M.; Roberts, A. W.; Huang, D. C. The BH3 mimetic ABT-737 targets selective Bcl-2 proteins and efficiently induces apoptosis via Bak/Bax if Mcl-1 is neutralized. *Cancer Cell* **2006,** 10, 389-99.

154. Schulze-Bergkamen, H.; Fleischer, B.; Schuchmann, M.; Weber, A.; Weinmann, A.; Krammer, P. H.; Galle, P. R. Suppression of Mcl-1 via RNA interference sensitizes human hepatocellular carcinoma cells towards apoptosis induction. *BMC Cancer* **2006,** 6, 232.

155. Willis, S. N.; Adams, J. M. Life in the balance: how BH3-only proteins induce apoptosis. *Curr Opin Cell Biol* **2005,** 17, 617-25.

156. Scorrano, L.; Oakes, S. A.; Opferman, J. T.; Cheng, E. H.; Sorcinelli, M. D.; Pozzan, T.; Korsmeyer, S. J. BAX and BAK Regulation of Endoplasmic Reticulum Ca2+: A Control Point for Apoptosis. *Science* **2003,** 300, 135-39.

157. Oakes, S. A.; Scorrano, L.; Opferman, J. T.; Bassik, M. C.; Nishino, M.; Pozzan, T.; Korsmeyer, S. J. Proapoptotic BAX and BAK regulate the type 1 inositol trisphosphate receptor and calcium leak from the endoplasmic reticulum. *Proc Natl Acad Sci U S A* **2005,** 102, 105-10.

158. Oltersdorf, T.; Elmore, S. W.; Shoemaker, A. R.; Armstrong, R. C.; Augeri, D. J.; Belli, B. A.; Bruncko, M.; Deckwerth, T. L.; Dinges, J.; Hajduk, P. J.; Joseph, M. K.; Kitada, S.; Korsmeyer, S. J.; Kunzer, A. R.; Letai, A.; Li, C.; Mitten, M. J.; Nettesheim, D. G.; Ng, S.; Nimmer, P. M.; O'Connor, J. M.; Oleksijew, A.; Petros, A. M.; Reed, J. C.; Shen, W.; Tahir, S. K.; Thompson, C. B.; Tomaselli, K. J.; Wang, B.; Wendt, M. D.; Zhang, H.; Fesik, S. W.; Rosenberg, S. H. An inhibitor of Bcl-2 family proteins induces regression of solid tumours. *Nature* **2005,** 435, 677-81.

159. Dai, L. Z.; Shi, Y. L.; Zhao, G. L.; Shi, M. A facile synthetic route to 2 H-chromenes: reconsideration of the mechanism of the DBU-catalyzed reaction between salicylic aldehydes and ethyl 2-methylbuta-2,3-dienoate. *Chemistry* **2007,** 13, 3701-6.